SYNTHESIS, CHARACTERIZATION, AND REACTIVITY OF ACTINIDE COMPLEXES BEARING An-E BONDS (An = Th, U; E = P, As)

A Dissertation presented to the Faculty of the Graduate School at the University of Missouri-Columbia

---

In Partial Fulfillment of the Requirements for the Degree of Doctor of Philosophy

---

By

MICHAEL LLOYD TARLTON

Dr. Justin R. Walensky, Dissertation Supervisor

May 2021

The undersigned, appointed by the dean of the Graduate School, have examined the dissertation entitled

SYNTHESIS, CHARACTERIZATION, AND REACTIVITY OF ACTINIDE COMPLEXES BEARING An-E BONDS (An = Th, U; E = P, As)

presented by Michael Lloyd Tarlton, a candidate for the degree of Doctor of Philosophy and hereby certify that, in their opinion, it is worthy of acceptance.

Professor Justin R. Walensky

Professor Silvia Jurisson

Professor Wesley Bernskoetter

Professor Bret Ulery

ACKNOWLEDGMENTS

I would like to thank my PhD advisor, Dr. Justin R. Walensky, not only for his guidance and support, but for his endless patience.

Thanks to Dr. Laurent Maron, Dr. Andrew Kerridge and Dr. Iker Del Rosal for the contribution of computational analysis.

Thanks to Dr. Matthew Shores and Tom Malcomson for their magnetism measurements and helpful discussion.

Special thanks to Dr. Steven P. Kelley for assistance with the X-ray crystallography, and his several years of mentorship in my effort to learn the technique.

Additional thanks to my research group members: Alexander Myers, Alexander Gremillion, Robert Ward, O. Jonathan Fajen, Xhensila Xhani, and Jason Ross.

Finally, thanks to my loving and supportive parents, Douglas and Sandra Tarlton, and my sister, Amber Tarlton.

TABLE OF CONTENTS

Table of Figures

Table of Tables

SYNTHESIS, CHARACTERIZATION, AND REACTIVITY OF ACTINIDE COMPLEXES BEARING An-E BONDS (An = Th, U; E = P, As)

Michael Lloyd Tarlton

Dr. Justin R. Walensky, Dissertation Supervisor

ABSTRACT OF DISSERTATION

Organoactinide complexes bearing An-E (An = Th, U; E = P, As) bonds were synthesized and reactivity studies were performed with various unsaturated and industrially/environmentally relevant small molecules in an effort to elucidate further information regarding their functionalization, and to expand the currently limited knowledge on actinide phosphido/arsenido chemistry.

Reaction of isostructural, primary pnictido complexes of the form $(C_5Me_5)_2An[P(H)Mes]_2$ exhibited insertion-type reactivity with ^{t}BuCN, ^{t}BuNC, CO_2 and CO. The products with CO_2 and ^{t}BuNC were isostructural between Th, and U, resulting in the bis(phosphinocarboxylato), and phosphaazaallene complexes, $(C_5Me_5)_2An[\kappa_2\text{-}(O,O)\text{-}O_2CP(H)Mes]_2$, and $(C_5Me_5)_2An[(CN^tBu)(\eta^2\text{-}(C,N)\text{-}^t BuNC{=}PMes)]_2$, respectively. Divergent reactivity was observed with ^{t}BuCN, and CO, producing the U(IV) bis(ketimido) complex **(**$C_5Me_5)_2U[\kappa_2\text{-}(N,N)\text{-}(N{=}C^tBu)_2(PMes)]_2$, formed via elimination of free H_2PMes, and $(C_5Me_5)_2U[(\kappa_2\text{-}(O,O)\text{-}O_2C(PMes)C(H)P(H)Mes]$, for which mechanistic analysis (DFT) attributed the difference to lower the acidity of the U-center to that of Th.

Reaction of $(C_5Me_5)_2Th[P(H)Mes]_2$ with $MN(SiMe_3)_2$ (M = Na, K, Rb, Cs) leads to deprotonation of the P-H proton, leading to formation of alkali-metal phosphinidiide complexes of the form $\{(C_5Me_5)_2Th[\mu_2\text{-}P(Mes)][\mu_2\text{-}P(H)Mes]M(L)_n\}_2$ (L = THF, Et_2O), where computational (DFT) analysis and ^{31}P NMR spectroscopy suggests significant Th-

P multiple bond character. Reaction of $(C_5Me_5)_2Th[P(H)Mes]_2$ with CuMes in a 2:3 molar ratio leads to the formation of the bimetallic cluster, $(C_5Me_5)_2Th[(\mu_2\text{-}PH(Mes)P(Mes)]Cu\}_2Cu[\mu_2\text{-}PH(Mes)]$.

Reaction of $(C_5Me_5)_2ThMe_2$ with H_2PMes in a 2:1 molar ratio leads to the formation of the T-shaped, bridging Th-phosphinidiide, $[(C_5Me_5)_2Th]_2(P\text{-}2,6\text{-}CH_2C_6H_2\text{-}4\text{-}CH_3)$ as a result of C-H bond activation at the *o*-CH_3 groups on the mesityl ring. Computational analysis (DFT) of the mechanism reveals that it progresses a different mechanism than that of the previously published and analogous reaction with H_2PTipp (Tipp = 2,4,6-triisopropylphenyl), yielding $[(C_5Me_5)_2Th]_2(\mu_2\text{-}P[(2,6\text{-}CH_2CHCH_3)_2\text{-}4\text{-}^{i}PrC_6H_2]$.

A comparative study was carried out in which isostructural Th and U complexes bearing bonds to P and As was conducted, yielding primary bis(pnictido) complexes of the form $(C_5Me_5)_2An[E(H)Mes]_2$, dipnictido complexes of the form $(C_5Me_5)_2Th(\eta^2\text{-}E_2Mes_2)$, bridging bis(pnictinidiide) complexes of the form $[(C_5Me_5)_2U]_2(\mu_2\text{-}AsMes)_2$ (with the exception of An = Th, E = P, which underwent C-H bond activation to form $\{(C_5Me_5)_2Th[\mu_2\text{-}P(H)(2,4\text{-}Me_2C_6H_2\text{-}6\text{-}CH_2)]\}_2$), and the terminal, U-phosphinidene complex, $(C_5Me_5)_2U(=PMes)OPPh_3$. Attempts were made to generate terminal arsinidene complexes from the bridging bis(arsinidiide) complexes by reaction with 2 molar equivalents of $OPPh_3$, but the oxo group was abstracted in the case of the Th-arsinidiide with concomitant elimination of 0.5 Mes-As=As-Mes, resulting in the bridging oxo complex $[(C_5Me_5)_2Th]_2(\mu_2\text{-}AsMes)(\mu_2\text{-}O)$. The analogous reaction between $[(C_5Me\text{-}_5)_2U]_2(\mu_2\text{-}AsMes)_2$ and $OPPh_3$ results in reduction of the U(IV/IV) centers and concomitant

coupling of the arsinidiide ligands to form the U(III/III) diarsenido/$OPPh_3$ adduct ion pair, $[(C_5Me_5)_2U(\eta^2\text{-}As_2Mes_2)][(C_5Me_5)_2U(OPPh_3)_2]$.

Following this study, the An-diarsenido complexes were reacted with CO and isoelectronic analog, ^{t}BuNC, forming the adducts $(C_5Me_5)_2An(\eta^2\text{-}As_2Mes_2)(CN^tBu)$ and $(C_5Me_5)_2An(\eta^2\text{-}As_2Mes_2)(CO)$. The latter complexes represent very rare examples of characterizable carbonyl compounds of f elements.

INTRODUCTION

The lanthanides and actinides exhibit many similar properties including bonding that is primarily electrostatic in nature, oxophilic, with high coordination numbers. Their chemical behavior is nearly identical as a result, making differentiation between them extremely difficult, which presents a major obstacle to economic recovery of such elements from mining operations where many minerals contain significant amounts of both, but most importantly from spent nuclear fuel, where both trivalent lanthanides and minor actinides (Np, Pu, Am) are present.[1-4] Initially, Ln(III)/An(III) differentiation was thought to be unfeasible, however an affinity on the part of actinides over lanthanides for softer donor atoms such as N and S has been the subject of study for some time, which presented a viable basis for separations methods.[5-9] The most prominent modern example of this being Cyanex 301, in which differentiation is accomplished with the use of dialkyldithiophosphonates ($S_2PR_2^-$).[10]

The origin of this slight selectivity is thought to be the result of a greater degree of covalency in the bond between the actinide (An)and soft donor atoms over the analogous interaction with lanthanides (Ln), a consequence of the energy-degeneracy driven covalency principle which describes the trend in covalent character of the actinides across the series, where the energy of the 5f orbital manifold gradually becomes closer to that of the ligand orbitals until they are approximately degenerate, an opposite trend in comparison with the degree of orbital overlap between the two, which decreases as the f-orbital manifold decreases in energy, becoming more core-like.[11-15]

Our group seeks to explore this phenomenon by studying such systems bearing An-soft donor bonds within organoactinide chemistry, using spectroscopic, crystallographic,

and computational analysis. Our efforts focus mainly upon the chemistry phosphido- and arsenido-complexes of Th(IV) and U(IV) using the bis(pentamethylcyclopentadienyl) $[(C_5Me_5)]_2^{2-}$ ancillary ligand framework. This moiety serve as steric protection for the central metal ion, and impose restriction on the chemistry that force it to occur at the meridian, enabling a greater degree of control and predictability. The methyl substitution on the inner ring carbons also inhibit most reactivity, namely by energetically difficult C-H bond activation.

The ligands of primary interest in the subsequent studies primarily consists of mesityl (Mes)-substituted (Mes = 2,4,6-$Me_3C_6H_2$) primary (M-E(H)Mes) (E = P, As), and secondary (M_nEMes, n = 1-2), where reactivity can take the form of insertion, proton-migration, E-E oxidative coupling, and protonolysis due to the basic nature of the ligands, Fig 1, and both pnictides have potential to undergo redox chemistry with the (III/V) redox couple. The high-abundance, I = ½ NMR-active nucleus, ^{31}P is also invaluable in the tracking of reaction progress and the study of structural characteristics. Phosphido- and arsenido-chemistry with actinides has experienced a great increase in number of publications over recent years,[16-27] with the former being far more common in the literature. This dissertation seeks to expand upon both areas in actinide chemistry, with emphasis on arsenido chemistry, and to provide a wealth of direct comparisons between analogous Th/U and P/As containing complexes.

Herein, the synthesis and reactivity of An-phosphido and arsenido complexes of the form in Eq. 1 with a variety of substrates is described.

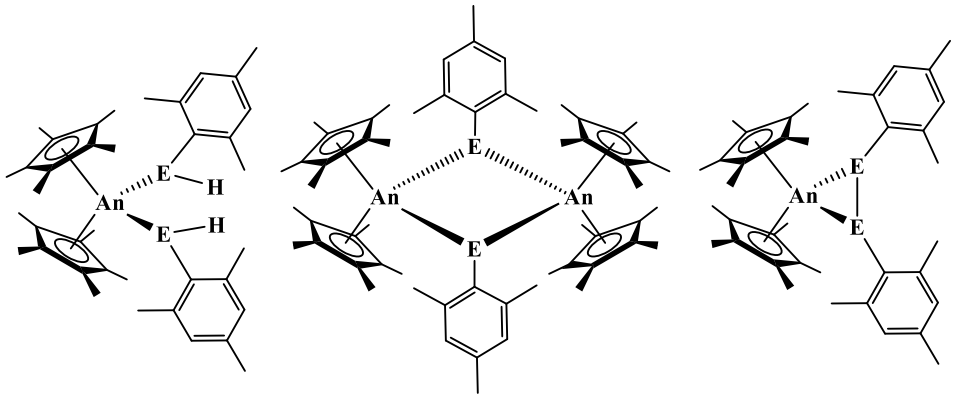

An = Th, U
E = P, As

(1)

Chapter 1 details the insertion-type chemistry of the $(C_5Me_5)_2An[P(H)Mes]_2$ system (An = Th, U) with the industrially and environmentally relevant small molecules, CO, CO_2, ^{t}BuCN and ^{t}BuNC, building upon previously reported work and providing a direct and useful comparison between the bonding characteristics of Th and U with P.

Chapter 2 covers the deprotonation-type reactivity of the above mentioned $(C_5Me_5)_2Th[P(H)Mes]_2$ with alkali-metal amides of the form $MN(SiMe_3)_2$, in an attempt to generate phosphinidiide (M_2PR) or phosphinidene (M=P-R) complexes exhibiting Th-P multiple bonding character, giving insight into the degree of covalency in the Th-P bonding interaction.

Chapter 3 focuses upon the synthesis, and insertion-type reactivity of the T-shaped Th-phosphinidiide complex, $[(C_5Me_5)_2Th]_2$(*P*-2,6-$CH_2C_6H_2$-4-CH_3), complexes prepared via protonolysis of H_2PMes with $(C_5Me_5)_2ThMe_2$ in a 1:2 molar ratio, similar to that of the triisopropyl analog, $[(C_5Me_5)_2Th]_2(\mu_2$-P[(2,6-$CH_2CHCH_3)_2$-4-^{i}PrC_6H_2].

Chapter 4 focuses upon a comparative study between isostructural phosphido- and arsenido-complexes with tetravalent Th and U centers. The structural characteristics and reactivity are examined experimentally and computationally (DFT) in an effort to further

explore energy-driven covalency, and to attempt the preparation of thermally stable complexes bearing An-P/As multiple bonds.

Chapter 5 details a set of reactivity studies with complexes of the form $(C_5Me_5)_2Th(\eta^2\text{-}As_2Mes_2)$ with small, unsaturated substrates, specifically synthesis of the corresponding An-CO complexes and its isoelectronic analog, ^{t}BuNC. Stable carbonyl complexes of f-elements are extremely rare due to their limited ability to backbond, leading to labile and short-lived interactions. The combination of steric saturation of the metal center in each complex and the electronic deficiency facilitated coordination of CO. Insight into the structure and reactivity of complexes containing An-P and An-As bonds paints broader picture of the An-soft donor interaction phenomenon. Our expansion of this knowledge base to phosphorus and arsenic is pertinent, as the majority of research conducted upon An-soft donor complexes has been undergone with N and S, which are close of the pnictides on the periodic table, and share similar physical, and bonding characteristics. These efforts yield important information that will likely in turn be used in the design of further fundamental research and applied in the design of advanced separations methods.

REFERENCES.

1. Lewis, F. W.; Hudson, M. J.; Harwood, L. M., Development of Highly Selective Ligands for Separations of Actinides from Lanthanides in the Nuclear Fuel Cycle. *Synlett* **2011**, *2011*, 2609-2632.

2. Kolarik, Z., Complexation and Separation of Lanthanides(III) and Actinides(III) by Heterocyclic N-Donors in Solutions. *Chemical Reviews* **2008**, *108*, 4208-4252.

3. Hudson, M. J.; Harwood, L. M.; Laventine, D. M.; Lewis, F. W., Use of Soft Heterocyclic N-Donor Ligands To Separate Actinides and Lanthanides. *Inorg. Chem.* **2013**, *52*, 3414-3428.

4. Bessen, N. P.; Jackson, J. A.; Jensen, M. P.; Shafer, J. C., Sulfur donating extractants for the separation of trivalent actinides and lanthanides. *Coord. Chem. Rev.* **2020,** *421*, 213446.

5. Chandrasekar, A.; Ghanty, T. K., Uncovering Heavy Actinide Covalency: Implications for Minor Actinide Partitioning. *Inorganic Chemistry* **2019**, *58*, 3744-3753.

6. Xu, L.; Pu, N.; Li, Y.; Wei, P.; Sun, T.; Xiao, C.; Chen, J.; Xu, C., Selective Separation and Complexation of Trivalent Actinide and Lanthanide by a Tetradentate Soft–Hard Donor Ligand: Solvent Extraction, Spectroscopy, and DFT Calculations. *Inorg. Chem.* **2019**, *58*, 4420-4430.

7. Lehman-Andino, I.; Su, J.; Papathanasiou, K. E.; Eaton, T. M.; Jian, J.; Dan, D.; Albrecht-Schmitt, T. E.; Dares, C. J.; Batista, E. R.; Yang, P.; Gibson, J. K.; Kavallieratos, K., Soft-donor dipicolinamide derivatives for selective actinide(III)/lanthanide(III) separation: the role of S- vs. O-donor sites. *Chem. Commun.* **2019**, *55*, 2441-2444.

8. Grimes, T. S.; Heathman, C. R.; Jansone-Popova, S.; Ivanov, A. S.; Bryantsev, V. S.; Zalupski, P. R., Exploring Soft Donor Character of the N-2-Pyrazinylmethyl Group by Coordinating Trivalent Actinides and Lanthanides Using Aminopolycarboxylates. *Inorg. Chem.* **2019**, 59, 138-150.

9. Behrle, A. C.; Barnes, C. L.; Kaltsoyannis, N.; Walensky, J. R., Systematic Investigation of Thorium(IV)– and Uranium(IV)–Ligand Bonding in Dithiophosphonate, Thioselenophosphinate, and Diselenophosphonate Complexes. *Inorg. Chem.* **2013**, *52*, 10623-10631.

10. Bhattacharyya, A.; Mohapatra, P. K.; Manchanda, V. K., Separation of trivalent actinides and lanthanides using a flat sheet supported liquid membrane containing Cyanex-301 as the carrier. *Sep. Purif. Technol.* **2006**, *50*, 278-281.

11. Su, J.; Batista, E. R.; Boland, K. S.; Bone, S. E.; Bradley, J. A.; Cary, S. K.; Clark, D. L.; Conradson, S. D.; Ditter, A. S.; Kaltsoyannis, N.; Keith, J. M.; Kerridge, A.; Kozimor, S. A.; Löble, M. W.; Martin, R. L.; Minasian, S. G.; Mocko, V.; La Pierre, H. S.; Seidler, G. T.; Shuh, D. K.; Wilkerson, M. P.; Wolfsberg, L. E.; Yang, P., Energy-Degeneracy-Driven Covalency in Actinide Bonding. *J. Am. Chem. Soc.* **2018**, *140*, 17977-17984.

12. Walensky, J. R.; Martin, R. L.; Ziller, J. W.; Evans, W. J., Importance of Energy Level Matching for Bonding in Th3+-Am3+ Actinide Metallocene Amidinates, $(C_5Me_5)_2[^iPrNC(Me)N^iPr]An$. *Inorg. Chem.* **2010**, *49*, 10007-10012.

13. Kelley, M. P.; Su, J.; Urban, M.; Luckey, M.; Batista, E. R.; Yang, P.; Shafer, J. C., On the Origin of Covalent Bonding in Heavy Actinides. *J. Am. Chem. Soc.* **2017**, *139*, 9901-9908.

14. Kerridge, A., Quantification of f-element covalency through analysis of the electron density: insights from simulation. *Chem. Commun.* **2017**, *53*, 6685-6695.

15. Vitova, T.; Pidchenko, I.; Fellhauer, D.; Bagus, P. S.; Joly, Y.; Pruessmann, T.; Bahl, S.; Gonzalez-Robles, E.; Rothe, J.; Altmaier, M.; Denecke, M. A.; Geckeis, H., The role of the 5 f valence orbitals of early actinides in chemical bonding. *Nat. Commun.* **2017**, *8*, 16053.

16. Actinides: Pnictogen Complexes. In *Encyclopedia of Inorganic and Bioinorganic Chemistry*, pp 1-17.

17. Wildman, E. P.; Balázs, G.; Wooles, A. J.; Scheer, M.; Liddle, S. T., Triamidoamine thorium-arsenic complexes with parent arsenide, arsinidiide and arsenido structural motifs. *Nat. Commun.* **2017**, *8*, 14769.

18. Vilanova, S. P.; Alayoglu, P.; Heidarian, M.; Huang, P.; Walensky, J. R., Metal–Ligand Multiple Bonding in Thorium Phosphorus and Thorium Arsenic Complexes. *Chem. Eur. J.* **2017**, *23*, 16748-16752.

19. Behrle, A. C.; Walensky, J. R., Insertion of tBuNC into thorium–phosphorus and thorium–arsenic bonds: phosphaazaallene and arsaazaallene moieties in f element chemistry. *Dalton Trans.* **2016**, *45*, 10042-10049.

20. Rookes, T. M.; Wildman, E. P.; Balázs, G.; Gardner, B. M.; Wooles, A. J.; Gregson, M.; Tuna, F.; Scheer, M.; Liddle, S. T., Actinide–Pnictide (An−Pn) Bonds Spanning Non-Metal, Metalloid, and Metal Combinations (An=U, Th; Pn=P, As, Sb, Bi). *Angew. Chem. Int. Ed. Engl.* **2018**, *57*, 1332-1336.

21. Scherer, O. J.; Schulze, J.; Wolmershäuser, G., Bicyclisches As6 als komplexligand. *J. Organomet. Chem.* **1994**, *484*, c5-c7.

22. Gardner, B. M.; Balázs, G.; Scheer, M.; Wooles, A. J.; Tuna, F.; McInnes, E. J. L.; McMaster, J.; Lewis, W.; Blake, A. J.; Liddle, S. T., Isolation of Elusive HAsAsH in a Crystalline Diuranium(IV) Complex. *Angew. Chem. Int. Ed. Engl.* **2015**, *54*, 15250-15254.

23. Gardner, B. M.; Balázs, G.; Scheer, M.; Tuna, F.; McInnes, E. J. L.; McMaster, J.; Lewis, W.; Blake, A. J.; Liddle, S. T., Triamidoamine uranium(IV)–arsenic complexes containing one-, two- and threefold U–As bonding interactions. *Nat. Chem.* **2015**, *7*, 582.

24. Hoerger, C. J.; Heinemann, F. W.; Louyriac, E.; Rigo, M.; Maron, L.; Grützmacher, H.; Driess, M.; Meyer, K., Cyaarside (CAs−) and 1,3-Diarsaallendiide ($AsCAs^{2-}$) Ligands Coordinated to Uranium and Generated via Activation of the Arsaethynolate Ligand ($OCAs^{-}$). *Angew. Chem. Int. Ed. Engl.* **2019**, *58*, 1679-1683.

25. Rozenel, S. S.; Edwards, P. G.; Petrie, M. A.; Andersen, R. A., Eight coordinate 1,2-bis(dimethylarsino) and 1,2-bis(dimethylphosphino)-benzene complexes of uranium tetrachloride, $UCl_4[(1,2\text{-}Me_2E)_2C_6H_4]_2$ where E is As or P. *Polyhedron* **2016**, *116*, 122-126.

26. Zhang, C.; Hou, G.; Zi, G.; Walter, M. D., A base-free terminal thorium phosphinidene metallocene and its reactivity toward selected organic molecules. *Dalton Trans.* **2019**, *48*, 2377-2387.

27. Arney, D. S. J.; Schnabel, R. C.; Scott, B. C.; Burns, C. J., Preparation of Actinide Phosphinidene Complexes: Steric Control of Reactivity. *J. Am. Chem. Soc.* **1996**, *118*, 6780-6781.

Chapter 1: Comparative Insertion Reactivity of CO, CO_2, ^{t}BuCN, and ^{t}BuNC into Thorium- and Uranium-Phosphorus Bonds

Michael L. Tarlton,[1] Iker Del Rosal,[2] Sean P. Vilanova,[1] Steven P. Kelley,[1] Laurent Maron,[2] Justin R. Walensky[1]*

[1] Department of Chemistry, University of Missouri, 601 S. College Avenue, Columbia, MO 65211, United States

[2]Universite de Toulouse, 135 Avenuede Rangueil, 31077 Toulouse (France)

ABSTRACT.

A study of the comparative reactivity of CO, CO_2, ^{t}BuCN and ^{t}BuNC with $(C_5Me_5)_2An[PH(Mes)]_2$ (An = Th, U) has been undertaken. While CO_2 ^{t}BuNC form identical products with both metals, namely $(C_5Me_5)_2An[\kappa^2\text{-}(O,O)\text{-}O_2CPH(Mes)]_2$ and $(C_5Me_5)_2An[\eta^2\text{-}(^tBuNC{=}PMes](CN^tBu)$, respectively, differing results are obtained with CO and ^{t}BuCN. The reaction of *tert*-butylnitrile with $(C_5Me_5)_2U[P(H)Mes]_2$ in a 2:1 ratio leads to double insertion into the U-P bonds and elimination of H_2PMes forming the diketimido complex $(C_5Me_5)_2U[\kappa^2\text{-}(N,N)\text{-}(N{=}C^tBu)_2P(Mes)]$. This is another case in which the analogous reaction with $(C_5Me_5)_2Th[P(H)Mes]_2$ affords a different product, $(C_5Me_5)_2Th[PH(Mes)][\kappa^2\text{-}(P,N)\text{-}N(H)C(CMe_3)P(Mes)]$. The reaction of 1 atm of CO with $(C_5Me_5)_2U[P(H)Mes]_2$ results in the double insertion with proton migration from one phosphido ligand to one of the CO carbons to form $(C_5Me_5)U[(\kappa^2\text{-}(O,O)\text{-}OC(PMes)\text{-}C(H)P(H)MesO]$. This is in contrast to the previously published result of the reaction between $(C_5Me_5)_2Th[P(H)Mes]_2$ and CO, in which the product is similar, but both protons from the phosphido ligands migrate to one carbon atom, resulting in $(C_5Me_5)_2Th[\kappa^2\text{-}(O,O)\text{-}$

OC=P(Mes)P(Mes)C(H)$_2$O]. Density functional theory calculations were carried out to show why this difference occurs.

INTRODUCTION.

Metal complexes play an important role in the activation of small-molecules, particularly of environmentally, biologically, and industrially relevant C_1 feedstocks such as CO and CO_2. The conversion of these substrates into commodity chemicals is desirable but such activation can be challenging. The use of metals like the actinides is thus an attractive prospect for this application, due to their high electropositive nature as well as and limited orbital participation, which leads to highly reactive centers. Insertion-type small-molecule reactivity is one of the most common reaction pathways for these substrates, especially with weak metal-ligand bonds. While the activation of CO,[1-7] CO_2,[8-20] isocyanates,[21-25] and nitriles[26-29] with f-element complexes that contain bonds to harder-donors like carbon, nitrogen, and hydrogen is well stablished, that of complexes containing soft-donors such as phosphorus. In this case, the weak interaction of the hard metal and soft donor ligand has been shown to lead to new reactivity patterns with respect to small molecule activation.

The analogous reactions of the latter are attractive targets, as they can be investigated to provide further insight into the potentially significant role that actinide-pnictido complexes can fill in the broader-context of C_1 manipulation. The slight differences in ionic radius and electronic structure among the actinides (e.g. Th vs. U) may additionally lead to divergent reactivity that may be exploited to optimize the strategies for which these complexes would be industrially employed. An extensive literature search reveals only a

small number of reactions involving CO and nitriles with metal-phosphorus bonds, and no such reactions with CO_2.

Herein, we describe the synthesis of a U(IV)-bis(phosphido) complex, $(C_5Me_5)_2U[P(H)Mes]_2$, and its reactivity with CO, CO_2, *tert*-butylnitrile, ^tBuCN, *tert*-butylisocyanide, ^tBuNC, in comparison to the products of the previously published[30-31] analogous set of reactions with $(C_5Me_5)_2Th[P(H)Mes]_2$. The novel reactivity of $(C_5Me_5)_2An[P(H)Mes]_2$ (An = Th, U) with CO_2 is also explored. Accompanying the synthetic details is a computational analysis of the mechanism for the reaction of $(C_5Me_5)_2U[P(H)Mes]_2$ with CO.

EXPERIMENTAL.

General Considerations. All syntheses were performed under an atmosphere of dry nitrogen either on a Schlenk-line or in a glovebox. All reagent-grade gasses were used as received and all solvents were dried over columns of activated alumina and molecular sieves in a solvent purification system by MBRAUN, USA. Tetrahydrofuran was freshly distilled over sodium/benzophenone. The compounds $(C_5Me_5)_2UMe_2$[32] and $(C_5Me_5)_2Th[P(H)Mes]_2$ (**1**)[31] were prepared according to literature procedures. KP(H)Mes, Mes = 2,4,6-$Me_3C_6H_2$, was prepared by addition of $KN(SiMe_3)_2$ to a room temperature, stirring solution of H_2PMes in toluene, followed by filtration over a medium-porosity glass frit to collect the product which was washed with 2 x 3 mL portions of toluene, and one portion of 5 mL pentane then stripped of volatiles under vacuum. The NMR spectra for **2** - **7** were recorded on either a 300 MHz or 600 MHz Bruker NMR spectrometer, with spectra being referenced to residual solvent. The IR spectra were recorded as KBr plates, on a Nicolet Summit PRO FTIR Spectrometer. The elemental analyses were conducted by

the University of California Berkeley Microanalytical Facility, Berkeley, CA, United States.

$(C_5Me_5)_2U[P(H)Mes]_2$, 2. A dark-orange pentane solution (5 mL) of $(C_5Me_5)_2UMe_2$ (503 mg, 0.934 mmol) was added dropwise to a stirring, colorless 5 mL pentane solution of H_2P-Mes (298 mg, 1.96 mmol) that had been pre-cooled to -30 ^oC in a glovebox freezer. The mixture was allowed to warm to room temperature, and had become dark-brown/black by 1 h stirring. The stirring was continued for 4 h without further color change, and a fine black, microcrystalline solid had precipitated over the time period. The mixture was cooled to -30 ^oC, and the solid was collected by suction filtration over a medium-porosity fritted glass funnel, then washed with 2 x 5 mL pentane and stripped of volatiles under vacuum, 598 mg, 78%. Crystals suitable for X-ray diffraction were grown from a concentrated pentane solution at -30 ^oC. ^1H NMR (600 MHz, C_6D_6, 25 ^oC): δ 10.04 (s, 30H, C_5Me_5), 5.86 (s, 6H, *p*-CH_3), 5.42 (s, 4H, *m*-H_{aryl}), -14.81 (s, br, 12H, *o*-CH_3), -122.9 (s, br, 2H, As-H). IR (cm^{-1}): 2950 (s), 2897 (s), 2855 (s), 2723 (w), 2298 (w), 1604 (w), 1459 (s), 1374 (s), 1261 (m), 1160 (w), 1065 (m), 1057 (s), 1024 (s), 955 (w), 882 (w), 846 (m), 803 (w), 696 (w), 603 (w). Elemental Analysis calculated for $C_{38}H_{54}P_2U$ (893.83 g/mol): C, 56.29%; H, 6.71%. Found: C, 55.98%; 6.52%.

$(C_5Me_5)_2U[\kappa^2$-(*O,O*)-$O_2CP(H)Mes]_2$, 3. A 50 mL Schlenk-flask containing a dark brown/black toluene solution (15 mL) of **2** (140 mg, 0.174 mmol) was cycled onto a high-vacuum Schlenk-line, and frozen by submersion in a bath of liquid nitrogen. The atmosphere was replaced with 1 atm CO_2, then the flask was allowed to thaw to room-temperature with stirring. A red solid immediately precipitated, and the suspension was stirred at room temperature for 1 h. After removal of the volatiles under vacuum, the flask

containing the red-solid residue was brought into a glovebox, and suspended in 10 mL THF, briefly stirred, and filtered over a medium-porosity fritted glass funnel, collecting a microcrystalline red solid which was washed with 10 mL more pentane, then stripped of volatiles under vacuum again, 115 mg, 77%. Due to the insolubility of this complex as well as the presence of two isomers, the ^{1}H NMR spectrum could not be satisfactorily obtained. ^{31}P{^{1}H} NMR (300 MHz, THF-d_8, 25 ^{o}C): δ -78.81 (s, Isomer 1), -83.47 (s, Isomer 2). ^{31}P NMR (300 MHz, THF-d_8, 25 ^{o}C): δ -78.81 (d, $^{1}J_{P\text{-}H}$ = 245 Hz, Isomer 1), -83.47 (d, $^{1}J_{P\text{-}H}$ = 245 Hz, Isomer 2). KBr (cm^{-1}): 2967 (m), 2927 (m), 2904 (s), 2857 (m), 2726 (w), 2372 (w), 1603 (m), 1488 (m), 1469 (m), 1438 (m), 1378 (m), 1346 (s), 1063 (w), 1031 (m), 947 (w), 843 (w), 833 (s), 639 (w), 611 (w). Elemental analysis calculated for $C_{40}H_{54}P_2O_2U$ (893.83 g/mol): C, 53.45%; H, 6.06%. Found: C, 53.37%; 5.98%.

(C$_5$Me$_5$)$_2$Th[κ^2-(*O*,*O*)-O$_2$CP(H)Mes]$_2$, 4. A 100 mL Schlenk-flask containing a toluene solution (13 mL) of **1** (65 mg, 0.081 mmol), was cycled onto a high-vacuum Schlenk-line, then frozen by submersion in a bath of liquid nitrogen. The atmosphere was evacuated and replaced by 1 atm CO_2, then the mixture was allowed to warm to room temperature with stirring. The reaction mixture quickly became a white suspension, and was allowed to stir for 30 min. After removing the solvent under reduced pressure, the resulting white solid was extracted in THF (15 mL), and filtered through Celite®. The filtrate was then concentrated which causing immediate precipitation of a white solid. The solution was placed in a freezer at -30 ^{o}C overnight to facilitate completion of crystallization. The white, crystalline product was isolated and volatiles removed under vacuum, 42 mg, 63%. Due to the insolubility of this complex as well as the presence of two isomers, the ^{1}H NMR spectrum could not be satisfactorily obtained. ^{31}P{^{1}H} NMR (300 MHz, THF-d_8, 25 ^{o}C):

δ -75.33 (s, Isomer 1), -75.43 (s, Isomer 2). ^{31}P NMR (300 MHz, THF-d_8, 25 ^{o}C): δ 75.33 (d, $^{1}J_{P\text{-}H}$ = 245 Hz, Isomer 1), 75.45 (d, $^{1}J_{P\text{-}H}$ = 243 Hz, Isomer 2). IR (cm^{-1}): 2968 (m), 2929 (m), 2902 (s), 2857 (m), 2729 (w), 2371 (m), 1603 (m), 1491 (m), 1469 (m), 1438 (m), 1379 (m), 1344 (s), 1032 (m), 946 (w), 880 (w), 855 (m), 835 (s), 790 (w), 641 (w), 611 (w), 550 (w), 473 (m). Despite several attempts, a satisfactory elemental analysis for **4** could not be obtained.

(C$_5$Me$_5$)$_2$U[(CN^{t}Bu)(η^2-(*C*,*N*)-^{t}BuNC=PMes)]$_2$, 5. A 2 mL toluene solution of ^{t}BuNC (20 mg, 0.247 mmol) was added dropwise to a stirring, dark brown-black toluene solution (6 mL) of **2** (75 mg, 0.0925 mmol mmol) that had been pre-cooled to – 30 ^{o}C in a glovebox freezer. The mixture was stirred at room temperature for 1h, and then stripped of volatiles under vacuum, leaving a slightly sticky dark-brown solid. The residue was extracted in 2 x 4 mL Et$_2$O, filtered through Celite®, and concentrated to 2 mL under vacuum, by which point a significant amount of a black crystalline solid had grown. The solution was cooled to –30 ^{o}C in a glovebox freezer to facilitate completion of crystallization. The crystals were isolated and triturated in 2 mL pentane, then isolated again and dried under vacuum, 54 mg, 71%. Variable-temperature ^{1}H and ^{31}P NMR experiments were performed (70 to -40 ^{o}C), but yielded inconclusive results. Resonances spanned -20 to 40 ppm in the ^{1}H spectra, and indicated possibility of a mixture of isomers. No ^{31}P resonances were observable, aside from residual free H$_2$PMes. IR (cm^{-1}): 2965 (s), 2905 (s), 2855 (s), 2721 (w), 2299 (w), 2165 (s), 1604 (w), 1447 (s), 1371 (s), 1192 (m), 1083 (m), 1021 (m), 911 (w), 849 (w), 803 (w), 716 (w), 642 (w). Elemental analysis calculated for C$_{39}$H$_{59}$N$_2$PU (812.89 g/mol): C, 56.15%; H, 7.32%; N, 3.45%; Found: C, 56.24 %; H 7.06 %, N 3.57%.

$(C_5Me_5)_2U[\kappa^2\text{-}(N,N)\text{-}(N{=}C^tBu)_2(PMes)]_2$, 6. A 2 mL Et_2O solution of ^{t}BuCN (30 mg, 0.361 mmol) was added dropwise to a stirring, 6 mL, black solution of **2** (102 mg, 0.126 mmol) that had been pre-cooled to – 30 ^{o}C in a glovebox freezer. The mixture was allowed to warm to room temperature, and stir for 2 h. After filtration through Celite®, the mixture was concentrated to 1.5 mL under vacuum, by which point a black, crystalline solid had begun to grow. The solution was cooled to – 30 ^{o}C in a glovebox freezer to facilitate completion of crystallization. The crystals were isolated, triturated in 3 mL pentane, then isolated again and dried under vacuum, 60 mg, 57%. ^{1}H NMR (C_6D_6, 25 ^{o}C): δ 15.13 (s, br, 6H, *o*-CH_3), 13.20 (s, br, 2H, *m*-H) 7.85 (s, br, 18H, ^{t}Bu) 6.33 (s, 3H, *p*-CH_3), -4.67 (s, br, 30H, C_5Me_5). ^{31}P{^{1}H} NMR (C_6D_6, 25 ^{o}C): δ 98.74 (s, br). IR (cm^{-1}): 2962 (s), 2902 (s), 2858 (s), 2724 (w), 2234 (w), 1577 (s), 1458 (m), 1385 (m), 1375 (w), 1324 (w), 1211 (w), 1025 (w), 1047 (w), 877 (w), 850 (w), 795 (w), 686 (w). Elemental analysis calculated for $C_{39}H_{59}N_2PU$ (812.89 g/mol): C, 56.15%; H, 7.32%; N, 3.45%; Found: C, 56.86%; H 7.21%, N 3.46%.

$(C_5Me_5)_2U[(\kappa^2\text{-}(O,O)\text{-}O_2C(PMes)C(H)P(H)Mes]$, **7.** A 50 mL Schlenk-flask was charged with a 20 mL toluene solution of **2** (105 mg, 0.130 mmol), cycled onto a high-vacuum Schlenk-line and frozen in a liquid-nitrogen bath. The atmosphere in the flask was evacuated, then replaced with 1 atm CO, and the flask was allowed to warm to room-temperature with stirring. The color changed from dark-brown/black to dark red, and after stirring for 5 h, the volatiles were removed under vacuum. The remaining red solid was extracted into pentane (2 x 5 mL), filtered through Celite®, and concentrated to ~4 mL, then cooled to -30 ^{o}C whereby a dark-red, microcrystalline solid had precipitated. The crystals were isolated, triturated in ~3 mL cold pentane, isolated again and dried under

vacuum, 65 mg, 62%. Crystals suitable for X-ray diffraction were obtained from a concentrated, 4:1 methylcyclohexane:pentane solution at -30 °C. ^{1}H NMR (C_6D_6, 25 °C): δ 56.19 (s, 1H, P-C(H)-C), 12.49 (d, 1H, $^{1}J_{P-H}$ = 113 Hz, -P(H)Mes), 5.88 (s, 2H, *m*-H), 1.88 (s, 3H, *p*-CH_3), 1.31 (s, 15H, C_5Me_5), 0.655 (s, 15H, C_5Me_5), -1.09 (s, 6H, *o*-CH_3), -3.29 (s, 3H, *p*-CH_3). ^{31}P{^{1}H} NMR (300 MHz, C_6D_6, 25 °C): δ 124.34 (d, $^{3}J_{P-P}$ = 58 Hz, C=P(Mes)), 21.09 (d, $^{3}J_{P-P}$ = 58 Hz, C(H)-P(H)Mes). ^{31}P NMR (300 MHz, C_6D_6, 25 °C): δ 124.32 (dd, $^{3}J_{P-P}$ = 59 Hz, $^{3}J_{P-H}$ = 12 Hz, (C=P(Mes)), 21.15 (dd, $^{1}J_{P-H}$ = 225 Hz, $^{3}J_{P-P}$ = 58 Hz, C(H)-P(H)Mes). IR (cm^{-1}): 3008 (w), 2954 (s), 2911 (s), 2856 (s), 2725 (w), 2333 (w), 1603 (m), 1563 (m), 1442 (m), 1377 (m), 1245 (s), 1173 (m), 1084 (m), 1024 (w), 984 (m), 882 (w), 848 (m), 728 (w), 700 (w), 620 (m), 507 (w). Elemental Analysis calculated for $C_{40}H_{54}O_2P_2U$ (812.89 g/mol): C, 55.42%; H, 6.28%; N; Found: C, 56.68%; H 6.92% (consistent with cocrystallization of 0.5 molar equivalents of pentane).

Crystallographic Data Collection and Structure Determination. The selected single crystal was coated with viscous hydrocarbon oil inside the glove box before being mounted on a nylon cryoloop using Parabar® hydrocarbon oil. The X-ray data were collected on a Bruker CCD diffractometer with monochromated Mo-Kα radiation (λ = 0.71073 Å). The data collection and processing utilized Bruker Apex3 suite of programs. The structures were solved using direct methods and refined by full-matrix least-squares methods on F2 using Bruker SHELX-2014/7 program.[33] All non-hydrogen atoms were refined with anisotropic displacement parameters, aside from those bound to P atoms in **2** and **7** where Q-peaks in chemically reasonable positions were modeled as H atoms and allowed to freely refine. All other hydrogen atoms were placed at calculated positions and

included in the refinement using a riding model. Thermal ellipsoid plots were prepared by using Olex2[34] with 50% of probability displacements for non-hydrogen atoms.

Table 1-1. Summary of crystallographic information for complexes **2-7**.

	2	**4**	**5**	**6**	**7**
CCDC Deposition Number	1990082	1990362	1990388	1990456	1989186
Molecular formula	$C_{38}H_{54}P_2U$	$C_{40}H_{54}O_4P_2Th$	$C_{39}H_{59}PN_2U$	$C_{39}H_{59}N_2PU$	$C_{40}H_{54}O_2P_2U$
Formula weight (g/mol)	810.78	892.81	831.93	824.88	866.83
Crystal habit/color	Black Prism	Colorless prism	Black Prism	Black Prism	Red/Orange Prism
Temperature of data collection (K)	100	100	100	100	100
Space group	*Pbcn*	*C2/c*	$P2_12_12_1$	$P2_1$	$P2_1/c$
Crystal system	Orthorhombic	Monoclinic	Orthorhombic	Monoclinic	Monoclinic
Volume (Å)	3546.0(7)	3789.6(5)	7449.1(6)	2187.5(2)	4427.2(2)
a (Å)	10.9864(12)	21.6224(17)	18.9349(8)	10.8294(6)	19.8895(6)
b (Å)	15.3674(17)	8.5000(6)	19.6755(8)	17.4552(10)	11.9242(3)
c (Å)	21.003(2)	21.0850(14)	19.9948(9)	12.2922(7)	18.7206(6)
α (º)	90	90	90	90	90
β (º)	90	102.065(3)	90	109.7047(17)	94.3400(10)
γ (º)	90	90	90	90	90
Z	4	4	8	2	4
Calculated density (g/**c**m^3)	1.519	1.565	1.471	1.252	1.448

Absorption coefficient (mm^{-1})	4.692	4.058	4.428	3.770	3.774
Final *R* indices [$I > 2\sigma(I)$]	$R = 0.0267$ $R_w = 0.0495$	$R = 0.0270$ $R_w = 0.0536$	$R = 0.0239$ $R_w = 0.0460$	$R = 0.0517$ $R_w = 0.1503$	$R = 0.0298$ $R_w = 0.0635$

RESULTS AND DISCUSSION.

Addition of $(C_5Me_5)_2UMe_2$ to a pentane solution of H_2PMes results in the formation of $(C_5Me_5)_2U[P(H)Mes]_2$, **2**, in good yield (79%) after workup (Equation 1). The ^1H NMR spectrum of **2** shows the resonances for the (C_5Me_5), *p*-CH_3, and *m*-H groups at 10.03, 5.86, and 5.42 ppm, respectively. The *o*-CH_3 resonance appears at -14.89 ppm as a broadened singlet, and that for the P-H protons appears as another broadened singlet at -122.9 ppm. No coupling was observed for the P-H signals, likely a consequence of the paramagnetic character of the U(IV) center which also precludes detection of a signal in the ^{31}P NMR spectrum as the P is bound directly to the U. The IR spectrum indicates a characteristic P-H stretch at 2298 cm^{-1}.

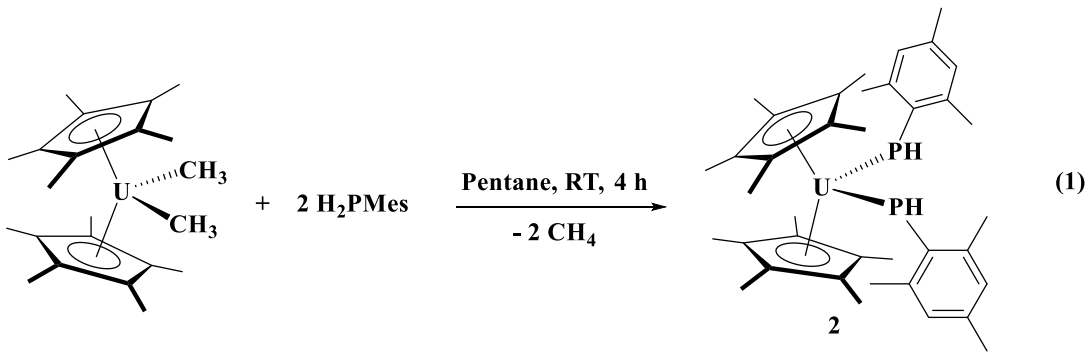

(1)

The solid-state structure of **2** was determined by X-ray crystallography analysis, Figure 1. Complex **2** is isostructural with the previously published thorium analog,[31] $(C_5Me_5)_2Th[P(H)Mes]_2$, **1**. The U-P bond distance at 2.7768(12) Å is shorter by approximately 0.095 Å than that of the Th-P bond, 2.872(5) Å, in **1**. Complex **2** is the first

bis(primary phosphido) complex of U to be isolated. The U-P bond in **2** is shorter by ~0.042 Å than the bridging-phodphido complexes of the Liddle group, [{U(Tren^{TIPS})}$_2$(μ-PH)],[35] and the Marks-group, [(C_5Me_5)$_2$U(OCH_3)]$_2$PH[36]. The difference in distance between **2** and [{U(Tren^{TIPS})}$_2$(μ-PH)] is likely due to the steric bulk of the flanking triisopropyl groups, and the dimeric nature of the complex, but the P-H stretching frequency is similar, with that of [{U(Tren^{TIPS})}$_2$(μ-PH)] appearing at 2169 cm^{-1}. Mark's [(C_5Me_5)$_2$U(OCH_3)]$_2$PH exhibits a P-H stretching frequency at 2193 cm^{-1}.

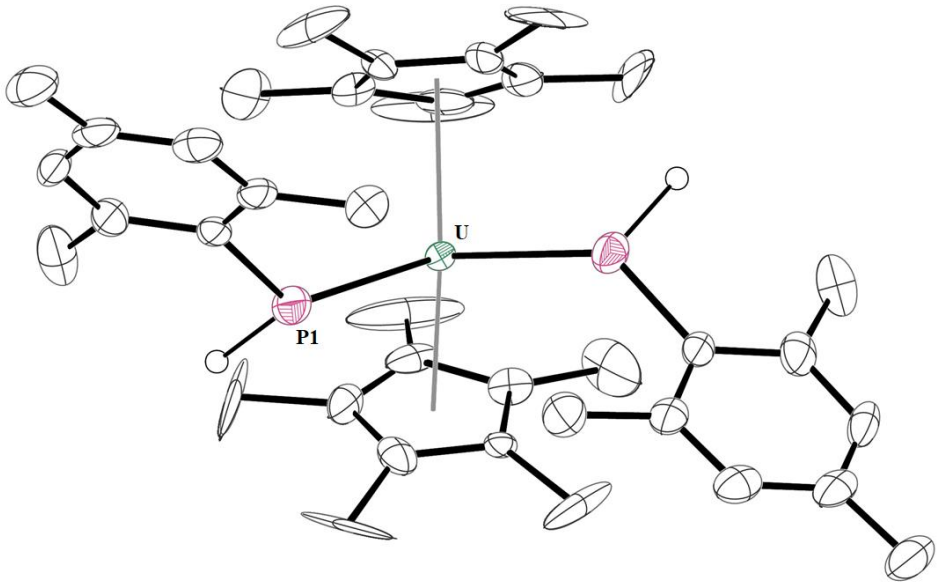

Figure 1-1. Thermal ellipsoid plots of **2** shown at the 50%-probability level. Hydrogen atoms have been omitted for clarity, with the exception of those bound to the phosphorus atoms. Pertinent structural information is as follows: U-P, 2.7768(12) Å; P-U-P, 102.42(6) ^{o}.

The reactivity of **2** with substrates previously explored with **1** were conducted. CO_2 (excess, 1 atm) was added to toluene solutions of **1** and **2**, resulting in fast and quantitative

conversion to **3** and **4** (Equation 2). The products in each case precipitate from the reaction mixture and are only sparingly soluble in organic solvents. Pure samples are only obtained by collection of the initial precipitate, or by exhaustively extracting the products in polar organic solvents such as THF followed by filtration through Celite®, and precipitation by concentration and cooling. The presence of P-H bonds is indicated by pairs of doublet resonances in the ^{31}P-NMR spectra collected in THF-d_8 of **3** at -78.81 ($^1J_{H\text{-}P}$ = 245 Hz) and -83.47 ppm ($^1J_{H\text{-}P}$ = 245 Hz), and **4** at -78.33 ($^1J_{P\text{-}H}$ = 245 Hz) and -75.43 ppm ($^1J_{P\text{-}H}$ = 243 Hz).

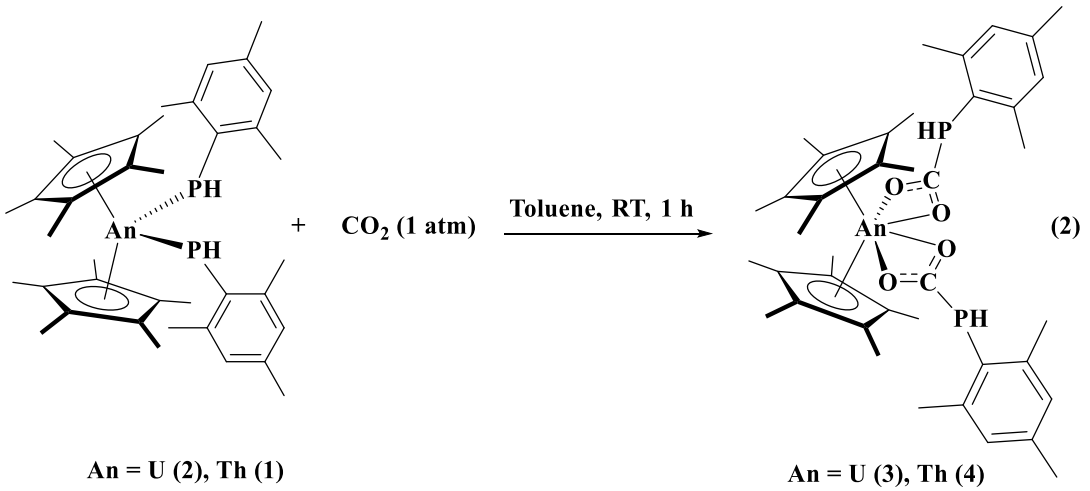

The pairs of unique doublets in the spectra indicate that the products form as mixtures of stereoisomers in an approximate 1:1 ratio, the origin of which is likely conformational isomerism where the orientations of the P-H bonds in the phosphine-moieties are either pointing in either the same or opposite directions. This phenomenon is also reflected in the ^{1}H NMR spectra, which show complicated sets of peaks corresponding to these mixtures. Variable-temperature NMR experiments were conducted, but yielded inconclusive results since cooling to -30 °C did not change the distribution in either case, whereas increasing the temperature led to thermal decomposition of **4**. Complex **3** was more thermally stable

at elevated temperatures, but no change in isomeric distribution was evident. Fortunately, the ^{1}H NMR spectra show P-H resonances with clear major/minor character that mirror what is seen in the ^{31}P NMR spectra, as well as clear and discreet pairs of Cp*-CH_3 resonances, further supporting the hypothesis that spectral quality suffers as a result of the products being isomeric mixtures.

While X-ray quality crystals of **3** were grown from THF at -30 ^{o}C, confirming the proposed structure, all attempts to grow X-ray quality crystals of **4** were not successful. The ^{31}P spectra, however, as well as the elemental analysis support the proposed structure. The IR spectra of **3** and **4** further support the proposed structures as well, with stretches at 2372 and 2373 cm^{-1}, within the typical range for P-H stretches. These species bear similarity to the complex obtained[37] from double-insertion of benzophenone into the Th-P bonds of $(C_5Me_5)_2Th[P(H)Mes]_2$ and $(C_5Me_5)_2Th(\mu_2\text{-}P_3Ph_3)$, although no such isomerization was observed in those cases. The Th-O bond lengths are similar to previously published Th-alkoxides[38] and aryloxides.[39]

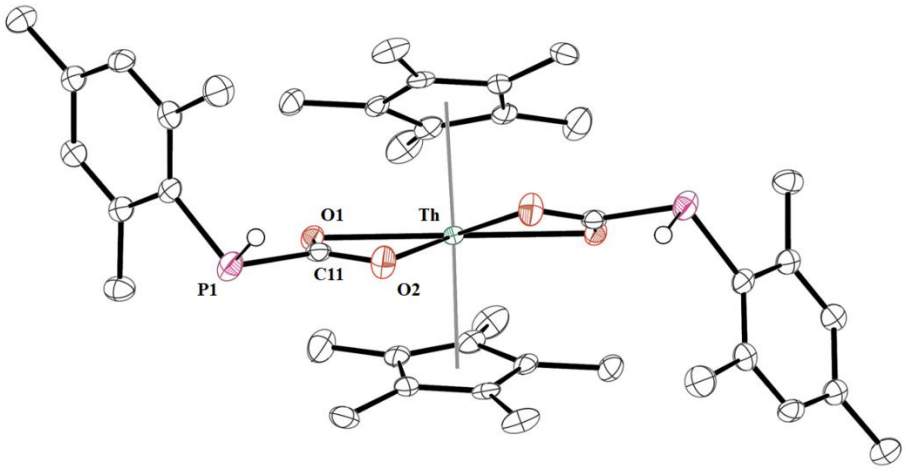

Figure 1-2. Thermal ellipsoid plot of **4**, shown at the 50% probability level. The hydrogen atoms have been omitted for clarity, except those bound to each phosphorus atom. Pertinent

structural information is as follows: Th-O1, 2.510(3) Å; Th-O2, 2.500(2) Å; O1-Th-O2, 52.18(8) °.

Previously, we reported the insertion of ^{t}BuNC into the An-P bonds of $(C_5Me_5)_2Th[P(H)Tipp]_2$,[31] Tipp = 2,4,6-$^{i}Pr_3C_6H_2$, $(C_5Me_5)_2Th[P(H)Mes]_2$,[31] and $(C_5Me_5)_2U(P(SiMe_3)Ph)_2$[40] to form the phosphaazaallenes, $[(C_5Me_5)_2An(CN^{t}Bu)(\eta^2\text{-N,C})$-(^{t}BuNC=PAr)], Ar = Ph, Mes, Tipp. The analogous product $(C_5Me_5)_2U(CN^{t}Bu)(\eta^2\text{-N,C})$-(^{t}BuNC=PMes), **5** (Equation 4, Figure 4), obtainable in moderate yield (57 %) by with elimination of free H_2PMes observed in the ^{31}P NMR spectrum. The ^{1}H NMR spectrum at room temperature was complicated, indicating another potential mixture of stereoisomers and no signal in the ^{31}P NMR spectrum was visible. Variable temperature NMR studies were conducted, but no spectrum collected at any temperature within the temperature range of -40 °C to 80 °C was reflective of the proposed structure, and no ^{31}P NMR resonance was observable within this range either.

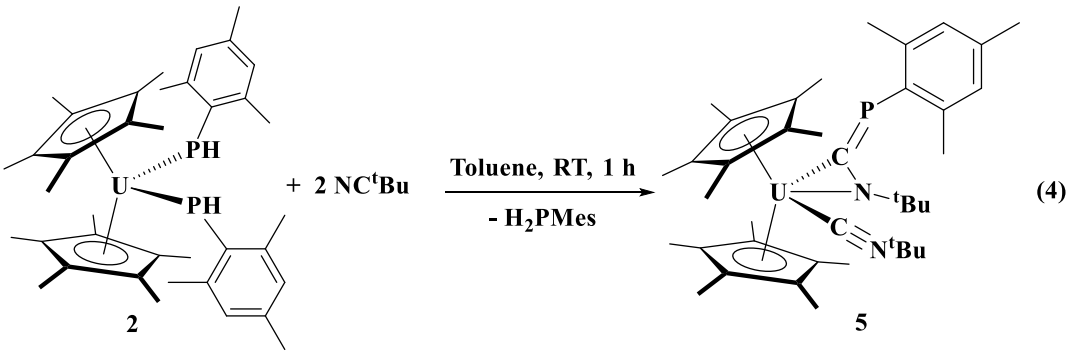

2 5 (4)

The U-C bond distances for the ^{t}BuNC ligands in **5** and $(C_5Me_5)_2U(CN^{t}Bu)[(\eta^2\text{-}N(^{t}Bu)C=PPh)]$ are nearly identical, at 2.555(8) Å and 2.568(3) Å. The U-C bond of the phosphaazaallene moiety in **5** at 2.373 (7) Å is slightly longer than the corresponding U-C

bond in $(C_5Me_5)_2U(CN^tBu)[(\eta^2\text{-}N(^tBu)C{=}PPh)]$, but the U-N bond in **5** (2.302(7) Å) is conversely, longer than that in $(C_5Me_5)_2U(CN^tBu)[(\eta^2\text{-}N(^tBu)C{=}PPh)]$ at 2.273(2) Å.

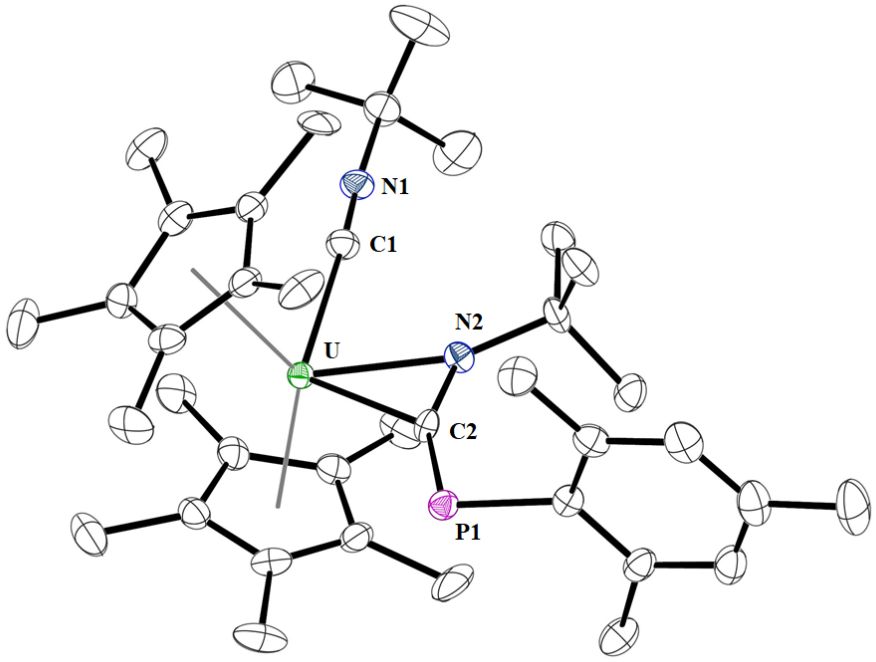

Figure 1-3. Thermal ellipsoid plot of **5** shown at the 50%-probability level. Hydrogen atoms have been omitted for clarity. Pertinent structural information is as follows: U-C2, 2.373(7) Å, U-N2, 2.302(7) Å, U-C1, 2.555(8) Å, C2-U-N2, 33.4(2)°.

Complex **2** reacts with an excess of ^{t}BuCN in toluene for 1 h, to form the $(C_5Me_5)_2U[\kappa^2\text{-}(N{=}C(C^tBu)_2)PMes]$, **6**, eq 4. This result is different from that of the analogous reaction performed with $(C_5Me_5)_2Th[P(H)Mes]_2$ which gave the phosphaamidinate-phosphido complex, $(C_5Me_5)_2Th[PH(Mes)][\kappa^2\text{-}(P,N)\text{-}N(H)C(CMe_3)P(Mes)]$.[30] The ^{1}H NMR spectrum shows the expected set of resonances at 6.33, 7.85, 13.20, and 15.13 ppm for the *p*-CH_3, ^{t}Bu, *m*-H, and *o*-CH_3 group, respectively, but a large shift and broadening of the resonance for the (C_5Me_5) peak to -4.67 ppm.

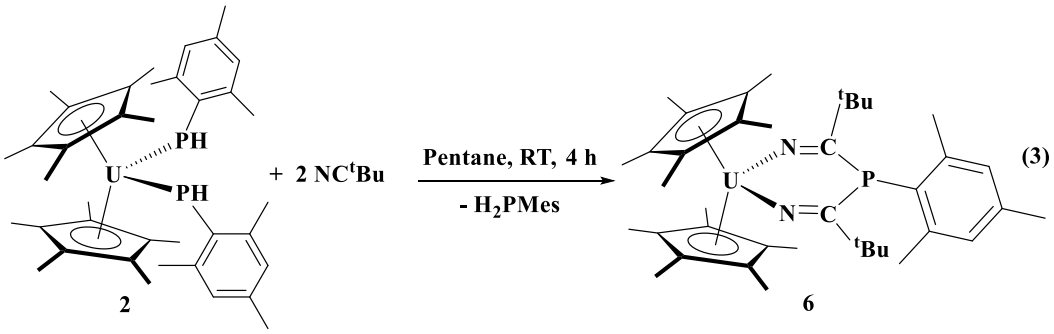

The solid-state structure of **6** was obtained by X-ray crystallography. The structural parameters for **6** are largely unremarkable and the U-N bond distances at 2.168(4) Å, and 2.173(4) Å are similar to those of previously reported An-ketimido complexes,[41-44] and nearly identical to those of $(C_5Me_5)_2U(N{=}CPh_2)$[45] at 2.179(6) Å and 2.185(5) Å.

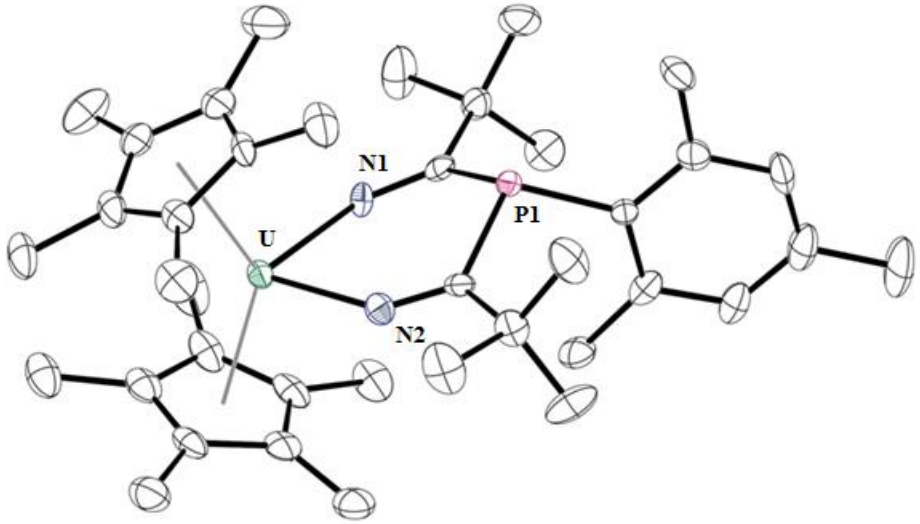

Figure 1-4. Thermal ellipsoid plot of **6** shown at the 50% probability level. Hydrogen atoms have been omitted for clarity. Pertinent structural information is as follows: U-N1, 2.168(4) Å; U-N2, 2.173(4) Å; N1-U-N2, 78.75(15) °.

Complex **2** reacts with an excess of CO to yield a dark red colored solution, **7** (Equation 5). The reaction proceeds to completion within ~1 hour at room-temperature in toluene, and isolated in moderate yield via crystallization from pentane. The IR spectrum shows

diagnostic P-H and C=P stretches at 2333, and 1603 cm^{-1}, respectively. The $^{31}P\{^{1}H\}$ spectrum exhibits two doublet resonances at 124.34, and 21.09 ppm with $^{3}J_{P\text{-}P}$ values of 58.3 and 58.6 Hz, respectively, indicating P-P coupling. The resonance at 21.09 ppm further splits into a doublet of doublets in the ^{31}P spectrum with a new $^{1}J_{P\text{-}H}$ value of ~225 Hz, well within the usual range for a P-H coupling constant. The resonances in the ^{1}H NMR spectrum are paramagnetically shifted, with a C-H resonance appearing at 56.19 ppm as a singlet, and a P-H resonance appearing as a doublet ($^{1}J_{P\text{-}H}$ = 225 Hz) at 12.45 ppm. The other resonances for the aryl- and $(C_5Me_5)^{1-}$ appear between ~5.9 to -3.29 ppm. Variable-temperature NMR studies were conducted at the same temperature range of -40 ^{o}C to 80 ^{o}C, but no satisfactory spectra were obtained, and decomposition appeared to occur above 70 ^{o}C, with the ^{31}P NMR resonances disappearing.

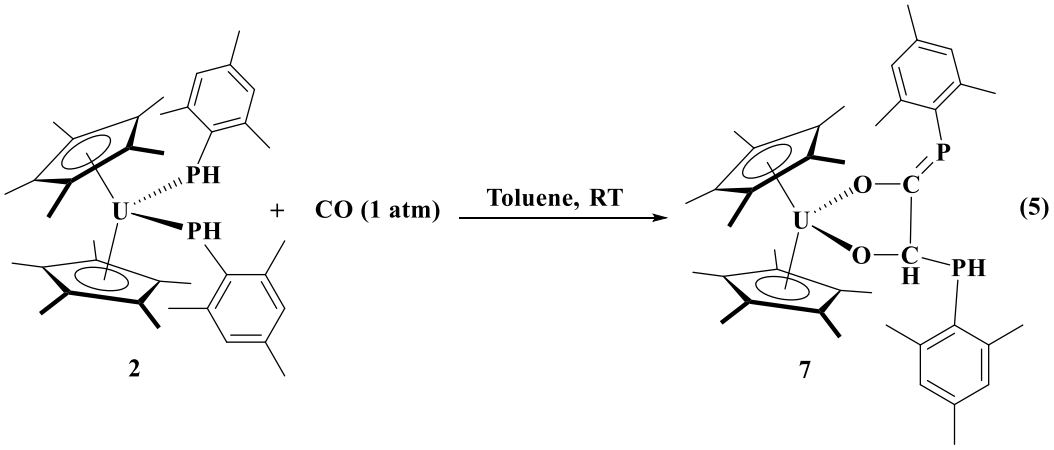

Crystals suitable for X-ray diffraction analysis were obtained from a saturated 4:1 methylcyclohexane:pentane solution at -25 °C. The structure of **7**, Figure 5, is a similar, but not the same product as obtained with thorium, $(C_5Me_5)_2Th(\kappa^2\text{-}(O,O)\text{-}OCH_2PMesC(O)PMes)$, **8**. The U-O distances in **7** (U-O1: 2.106(2) Å; U-O2: 2.212(2) Å) are slightly shorter than the Th-O bonds in **8**. The bond distance of the phosphalkene (P=C moiety) in **7** at 1.707(4) Å is the same as the P=C bond in **8** at 1.708(4) Å. The U-O bond

distances in **7** of 2.106(2) and 2.212(2) Å are within the typical range for U-O bonds in bis(pentamethylcyclopentadienyl) complexes such as $(C_5Me_5)_2U(OPh)_2$.[46]

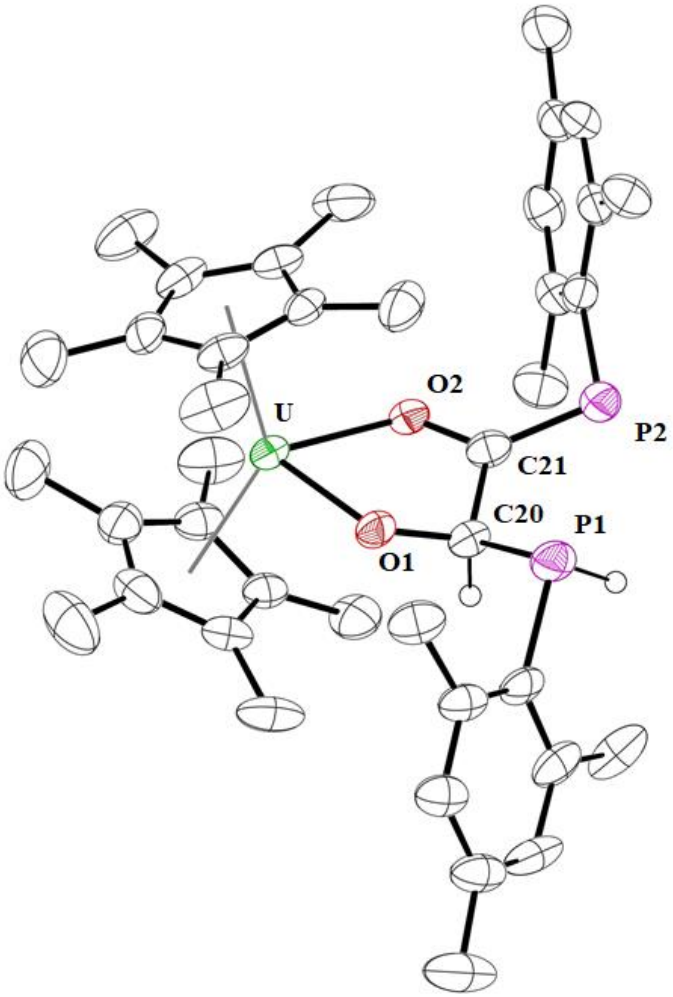

Figure 1-5. Thermal ellipsoid plot of **7** shown at the 50% probability level. Hydrogen atoms associated with $(C_5Me_5)^{1-}$ ligands have been omitted for clarity. Pertinent structural information is as follows: U-O1, 2.106(2) Å; U-O2, 2.212(2) Å; O1-U-O2, 71.71(9)°.

CONCLUSION. A U(IV)-bis(phosphido) complex, $(C_5Me_5)_2U[P(H)Mes]_2$, was synthesized and reacted with CO, CO_2, ^{t}BuCN, and ^{t}BuNC. The results are insertion reactions, sometimes involving proton migration and/or elimination of H_2PMes. The Th

analog, $(C_5Me_5)_2Th[P(H)Mes]_2$ was also reacted with CO_2, which combined with its previously reported reactivity, provides a complete set of results for comparison to those of uranium. The products of the reactions with CO_2 and ^tBuNC are identical, but those of $(C_5Me_5)_2U[P(H)Mes]_2$ with CO and ^tBuCN are different, reflecting that the reaction pathways are potentially affected by factors such as the increased covalent character of the U-P bond and smaller ionic radius relative to that of Th. Further studies of the comparative reactivity of $(C_5Me_5)_2An[P(H)Mes]_2$ are underway.

FUTURE WORK.

Deprotonation of $(C_5Me_5)_2An[P(H)Mes]_2$ with suitable bases such as alkali metal amides or hydrides, or alkyl/aryl-transition metal complexes may yield heterobimetallic complexes which could exhibit An-P multiple bond character, providing greater insight into the extent of orbital participation of the 5f manifold.

Reaction of the $(C_5Me_5)_2U[P(H)Mes]_2$ system with suitable oxidants such as ML salts (M = Cu, Ag; L = OTf, BPh_4, PF_6, SbF_6) may result in unprecedented U(V) bis(phosphido) complexes, which would enable comparison of the bonding characteristics with those of the U(IV) starting material. Reduction of the U(V) center by the phosphido ligands may be possible, but low-temperature reaction conditions may yield at least transient U(V) complexes that could be amenable to spectroscopic characterization. Similarly, oxidation of the phosphido ligands themselves may occur, which could yield ligand-based radical cations, which would be interesting from the perspective of analyzing the impact of the oxidation on the U-P bond.

REFERENCES.

1. Andrews, L.; Liang, B.; Li, J.; Bursten, B. E., Noble Gas−Actinide Complexes of the CUO Molecule with Multiple Ar, Kr, and Xe Atoms in Noble-Gas Matrices. *J. Am. Chem. Soc.* **2003**, *125*, 3126-3139.

2. Zhou, M.; Andrews, L.; Li, J.; Bursten, B. E., Reaction of Laser-Ablated Uranium Atoms with CO: Infrared Spectra of the CUO, CUO^-, OUCCO, $(\eta^2\text{-}C_2)UO_2$, and U(CO)x (x = 1−6) Molecules in Solid Neon. *J. Am. Chem. Soc.* **1999**, *121*, 9712-9721.

3. del Mar Conejo, M.; Parry, J. S.; Carmona, E.; Schultz, M.; Brennann, J. G.; Beshouri, S. M.; Andersen, R. A.; Rogers, R. D.; Coles, S.; Hursthouse, M. B., Carbon Monoxide and Isocyanide Complexes of Trivalent Uranium Metallocenes. *Chem. Eur. J.* **1999**, *5*, 3000-3009.

4. Evans, W. J.; Kozimor, S. A.; Nyce, G. W.; Ziller, J. W., Comparative Reactivity of Sterically Crowded nf^3 $(C_5Me_5)_3Nd$ and $(C_5Me_5)_3U$ Complexes with CO: Formation of a Nonclassical Carbonium Ion versus an f Element Metal Carbonyl Complex. *J. Am. Chem. Soc.* **2003**, *125*, 13831-13835.

5. Langeslay, R. R.; Chen, G. P.; Windorff, C. J.; Chan, A. K.; Ziller, J. W.; Furche, F.; Evans, W. J., Synthesis, Structure, and Reactivity of the Sterically Crowded Th3+ Complex (C5Me5)3Th Including Formation of the Thorium Carbonyl, $[(C_5Me_5)_3Th(CO)][BPh_4]$. *J. Am. Chem. Soc.* **2017**, *139*, 3387-3398.

6. Parry, J.; Carmona, E.; Coles, S.; Hursthouse, M., Synthesis and Single Crystal X-ray Diffraction Study on the First Isolable Carbonyl Complex of an Actinide, $(C_5Me_4H)_3U(CO)$. *J. Am. Chem. Soc.* **1995**, *117*, 2649-2650.

7. Li, J.; Bursten, B. E.; Zhou, M.; Andrews, L., A Combined Theoretical and Experimental Study of the Reaction Products of Laser-Ablated Thorium Atoms with CO: First Identification of the CThO, $CThO^-$, OThCCO, OTh(η^3-CCO), and $Th(CO)_n$ (n = 1−6) Molecules. *Inorg. Chem.* **2001**, *40*, 5448-5460.

8. Button, Z. E.; Higgins, J. A.; Suvova, M.; Cloke, F. G. N.; Roe, S. M., Mixed sandwich thorium complexes incorporating bis(tri-isopropylsilyl)cyclooctatetraenyl and pentamethylcyclopentadienyl ligands: synthesis, structure and reactivity. *Dalton Trans.* **2015**, *44*, 2588-2596.

9. Evans, W. J.; Miller, K. A.; Ziller, J. W., Synthesis of $(O_2CEPh)^{1-}$ Ligands (E = S, Se) by CO_2 Insertion into Lanthanide Chalcogen Bonds and Their Utility in Forming Crystallographically Characterizable Organoaluminum Complexes $[Me_2Al(\mu\text{-}O_2CEPh)]_2$. *Inorg. Chem.* **2006**, *45*, 424-429.

10. Evans, W. J.; Rego, D. B.; Ziller, J. W.; DiPasquale, A. G.; Rheingold, A. L., Facile Insertion of CO_2 into Tetra- and Pentamethylcyclopentadienyl Lanthanide Moieties To Form $(C_5Me_4RCO_2)^-$ Carboxylate Ligands (R = H, Me). *Organometallics* **2007**, *26*, 4737-4745.

11. Luo, L.; Huang, X.; Wang, N.; Wu, H.; Chen, W.; Feng, Z.; Zhu, H.; Peng, X.; Li, Y.; Huang, L.; Yue, S.; Liu, Y., Water molecule-enhanced CO_2 insertion in lanthanide coordination polymers. *J. Solid State Chem.* **2009**, *182*, 2213-2218.

12. Moloy, K. G.; Marks, T. J., The insertion of carbon dioxide into actinide alkyl and hydride bonds. *Inorg. Chim. Acta* **1985**, *110*, 127-131.

13. Mora, E.; Maria, L.; Biswas, B.; Camp, C.; Santos, I. C.; Pécaut, J.; Cruz, A.; Carretas, J. M.; Marçalo, J.; Mazzanti, M., Diamine Bis(phenolate) as Supporting Ligands

in Organoactinide(IV) Chemistry. Synthesis, Structural Characterization, and Reactivity of Stable Dialkyl Derivatives. *Organometallics* **2013**, *32*, 1409-1422.

14. Pagano, S.; Zeuner, M.; Baisch, U.; Schnick, W., Synthesis of Rare Earth (Oxo)nitridocarbonates by Employment of Supercritical Carbon Dioxide, Single-source Precursor, Solid-State, and Ion Exchange Reactions. *Z. Anorg. Allg. Chem.* **2010**, *636*, 2212-2221.

15. Qin, J.; Wang, P.; Li, Q.; Zhang, Y.; Yuan, D.; Yao, Y., Catalytic production of cyclic carbonates mediated by lanthanide phenolates under mild conditions. *Chem. Commun.* **2014**, *50*, 10952-10955.

16. Simler, T.; Feuerstein, T. J.; Yadav, R.; Gamer, M. T.; Roesky, P. W., Access to divalent lanthanide NHC complexes by redox-transmetallation from silver and CO_2 insertion reactions. *Chem. Commun.* **2019**, *55*, 222-225.

17. Steele, L. A. M.; Boyle, T. J.; Kemp, R. A.; Moore, C., The selective insertion of carbon dioxide into a lanthanide(III) 2,6-di-t-butyl-phenoxide bond. *Polyhedron* **2012**, *42*, 258-264.

18. Suvova, M.; O'Brien, K. T. P.; Farnaby, J. H.; Love, J. B.; Kaltsoyannis, N.; Arnold, P. L., Thorium(IV) and Uranium(IV) trans-Calix[2]benzene[2]pyrrolide Alkyl and Alkynyl Complexes: Synthesis, Reactivity, and Electronic Structure. *Organometallics* **2017**, *36*, 4669-4681.

19. Yin, C.-L.; Hu, Z.-B.; Long, Q.-Q.; Wang, H.-S.; Li, J.; Song, Y.; Zhang, Z.-C.; Zhang, Y.-Q.; Pan, Z.-Q., Single molecule magnet behaviors of Zn_4Ln_2 (Ln = Dy(III), Tb(III)) complexes with multidentate organic ligands formed by absorption of CO_2 in air through in situ reactions. *Dalton Trans.* **2019**, *48*, 512-522.

20. Zeuner, M.; Pagano, S.; Schnick, W., Precursor Approach to Lanthanide Dioxo Monocarbodiimides $Ln_2O_2CN_2$ (Ln=Y, Ho, Er, Yb) by Insertion of CO_2 into Organometallic Ln–N Compounds. *Chem. Eur. J.* **2008**, *14*, 1524-1531.

21. Karmel, I. S. R.; Tamm, M.; Eisen, M. S., Actinide-Mediated Catalytic Addition of E-H Bonds (E=N, P, S) to Carbodiimides, Isocyanates, and Isothiocyanates. *Angew. Chem. Int. Ed.* **2015**, *54*, 12422-12425.

22. Liu, H.; Fridman, N.; Tamm, M.; Eisen, M. S., Addition of E–H (E = N, P, C, O, S) Bonds to Heterocumulenes Catalyzed by Benzimidazolin-2-iminato Actinide Complexes. *Organometallics* **2017**, *36*, 3896-3903.

23. Lu, E.; Lewis, W.; Blake, A. J.; Liddle, S. T., The Ketimide Ligand is Not Just an Inert Spectator: Heteroallene Insertion Reactivity of an Actinide–Ketimide Linkage in a Thorium Carbene Amide Ketimide Complex. *Angew. Chem. Int. Ed.* **2014**, *53*, 9356-9359.

24. So, Y.-M.; Wang, G.-C.; Li, Y.; Sung, H. H.-Y.; Williams, I. D.; Lin, Z.; Leung, W.-H., A Tetravalent Cerium Complex Containing a Ce=O Bond. *Angew. Chem. Int. Ed.* **2014**, *53*, 1626-1629.

25. Zhu, X.; Fan, J.; Wu, Y.; Wang, S.; Zhang, L.; Yang, G.; Wei, Y.; Yin, C.; Zhu, H.; Wu, S.; Zhang, H., Synthesis, Characterization, Selective Catalytic Activity, and Reactivity of Rare Earth Metal Amides with Different Metal−Nitrogen Bonds. *Organometallics* **2009**, *28*, 3882-3888.

26. Avent, A. G.; Caro, C. F.; Hitchcock, P. B.; Lappert, M. F.; Li, Z.; Wei, X.-H., Synthetic and structural experiments on yttrium, cerium and magnesium trimethylsilylmethyls and their reaction products with nitriles; with a note on two cerium β-diketiminates. *Dalton Trans.* **2004**, 1567-1577.

27. Forsberg, J. H.; Spaziano, V. T.; Balasubramanian, T. M.; Liu, G. K.; Kinsley, S. A.; Duckworth, C. A.; Poteruca, J. J.; Brown, P. S.; Miller, J. L., Use of lanthanide(III) ions as catalysts for the reactions of amines with nitriles. *J. Org. Chem.* **1987**, *52*, 1017-1021.

28. Huang, S.; Shao, Y.; Zhang, L.; Zhou, X., Cycloamidination of Aminoalkenes with Nitriles: Synthesis of Substituted 2-Imidazolines and Tetrahydropyrimidines. *Angew. Chem. Int. Ed.* **2015**, *54*, 14452-14456.

29. Wang, C.; Xiang, L.; Leng, X.; Chen, Y., Rare-earth metal hydrides supported by silicon-bridged boratabenzene fluorenyl ligands: synthesis, structure and reactivity. *Dalton Trans.* **2017**, *46*, 1218-1227.

30. Vilanova, S. P.; del Rosal, I.; Tarlton, M. L.; Maron, L.; Walensky, J. R., Functionalization of Carbon Monoxide and tert-Butyl Nitrile by Intramolecular Proton Transfer in a Bis(Phosphido) Thorium Complex. *Angew. Chem. Int. Ed. Engl.* **2018**, *130*, 16990-16995.

31. Behrle, A. C.; Walensky, J. R., Insertion of tBuNC into thorium–phosphorus and thorium–arsenic bonds: phosphaazaallene and arsaazaallene moieties in f element chemistry. *Dalton Trans.* **2016**, *45*, 10042-10049.

32. Pagano, J. K.; Dorhout, J. M.; Waterman, R.; Czerwinski, K. R.; Kiplinger, J. L., Phenylsilane as a safe, versatile alternative to hydrogen for the synthesis of actinide hydrides. *Chem. Commun.* **2015**, *51*, 17379-17381.

33. Sheldrick, G., Crystal structure refinement with SHELXL. *Acta Crystallogr. C* **2015**, *71*, 3-8.

34. Dolomanov, O. V.; Bourhis, L. J.; Gildea, R. J.; Howard, J. A. K.; Puschmann, H., OLEX2: a complete structure solution, refinement and analysis program. *J. Appl. Crystallogr.* **2009**, *42*, 339-341.

35. Rookes, T. M.; Gardner, B. M.; Balázs, G.; Gregson, M.; Tuna, F.; Wooles, A. J.; Scheer, M.; Liddle, S. T., Crystalline Diuranium Phosphinidiide and μ-Phosphido Complexes with Symmetric and Asymmetric UPU Cores. *Angew. Chem. Int. Ed.* **2017**, *56*, 10495-10500.

36. Duttera, M. R.; Day, V. W.; Marks, T. J., Organoactinide phosphine/phosphite coordination chemistry. Facile hydride-induced dealkoxylation and the formation of actinide phosphinidene complexes. *J. Am. Chem. Soc.* **1984**, *106*, 2907-2912.

37. Vilanova, S. P.; Tarlton, M. L.; Barnes, C. L.; Walensky, J. R., Double insertion of benzophenone into thorium-phosphorus bonds. *J. Organomet. Chem.* **2018**, *857*, 159-163.

38. Clark, D. L.; Huffman, J. C.; Watkin, J. G., The first structurally characterised homoleptic thorium alkoxide: X-ray crystal structure of $[Th(OCH^iPr_2)_4]_2$, and NMR evidence for a monomer–dimer equilibrium. *J. Chem. Soc., Chem. Commun.* **1992**, 266-268.

39. Berg, J. M.; Clark, D. L.; Huffman, J. C.; Morris, D. E.; Sattelberger, A. P.; Streib, W. E.; Van der Sluys, W. G.; Watkin, J. G., Early actinide alkoxide chemistry. Synthesis, characterization, and molecular structures of thorium(IV) and uranium(IV) aryloxide complexes. *J. Am. Chem. Soc.* **1992**, *114*, 10811-10821.

40. Rungthanaphatsophon, P. F., O. J.; Kelley, S. P.; Walensky, J. R., Thorium(IV) and Uranium(IV) Phosphaazaallenes. *Inorganics* **2019**, *7*, 105.

41. Ayres, A. J.; Wooles, A. J.; Zegke, M.; Tuna, F.; Liddle, S. T., Preparation of Heterobimetallic Ketimido-Actinide-Molybdenum Complexes. *Inorg. Chem.* **2019**, *58*, 13077-13089.

42. Da Re, R. E.; Jantunen, K. C.; Golden, J. T.; Kiplinger, J. L.; Morris, D. E., Molecular Spectroscopy of Uranium(IV) Bis(ketimido) Complexes. Rare Observation of Resonance-Enhanced Raman Scattering from Organoactinide Complexes and Evidence for Broken-Symmetry Excited States. *J. Am. Chem. Soc.* **2005**, *127*, 682-689.

43. Jantunen, K. C.; Burns, C. J.; Castro-Rodriguez, I.; Da Re, R. E.; Golden, J. T.; Morris, D. E.; Scott, B. L.; Taw, F. L.; Kiplinger, J. L., Thorium(IV) and Uranium(IV) Ketimide Complexes Prepared by Nitrile Insertion into Actinide−Alkyl and −Aryl Bonds. *Organometallics* **2004**, *23*, 4682-4692.

44. Morris, D. E.; Da Re, R. E.; Jantunen, K. C.; Castro-Rodriguez, I.; Kiplinger, J. L., Trends in Electronic Structure and Redox Energetics for Early-Actinide Pentamethylcyclopentadienyl Complexes. *Organometallics* **2004**, *23*, 5142-5153.

45. Kiplinger, J. L.; Morris, D. E.; Scott, B. L.; Burns, C. J., The First f-Element Ketimido Complex: Synthesis and Characterization of $(C_5Me_5)_2U(=NCPh_2)_2$. *Organometallics* **2002**, *21*, 3073-3075.

46. Evans, W. J.; Miller, K. A.; DiPasquale, A. G.; Rheingold, A. L.; Stewart, T. J.; Bau, R., A Crystallizable f-Element Tuck-In Complex: The Tuck-in Tuck-over Uranium Metallocene $[(C_5Me_5)U\{\mu\text{-}\eta^5\text{:}\eta^1\text{:}\eta^1\text{-}C_5Me_3(CH_2)_2\}(\mu\text{-H})_2U(C_5Me_5)_2]$. *Angew. Chem. Int. Ed.* **2008**, *47*, 5075-5078.

Chapter 2: Investigating the Formation of a Thorium Phosphinidiide through a Combined Experimental and Computational Analysis

Michael L. Tarlton, Steven P. Kelley, Laurent Maron,* and Justin R. Walensky*
Department of Chemistry, University of Missouri, Columbia, MO 65211 USA

ABSTRACT. Investigation of the formation of a thorium phosphinidiide reveals that changing from the 2,4,6-$^{i}Pr_3C_6H_2$ (Trip) substituted phosphido ligand to the 2,4,6-$Me_3C_6H_2$ (Mes), forms a similar product, $[(C_5Me_5)_2Th]_2$(P-2,6-$CH_2C_6H_2$-4-CH_3), via a different sequence of bond activations. The resulting Th-P-Th bond was further probed through reaction with one and two equivalents of ^{t}BuCN. The decreasing Th-P-Th angle showed a decrease in the Th-P bond order with a corresponding upfield shift in the ^{31}P NMR sepctra.

INTRODUCTION.

Activation of P-H bonds[1-8] is an essential step in hydrophosphination[9-10] and hydrodecoupling[11-12] reactions, however, the mechanism by which metal complexes perform these P-H activations is poorly understood. Further mechanistic insight into these bond activations is important to afford strategies for functionalization of phosphines,[13-14] which are of interest for a wide array of applications. The reactivity of metal alkyl,[15] hydride, and amide complexes, especially with electropositive metals, help to facilitate these bond activations. There are limited examples of P-H bond activation with f elements.[16-30]

In 2015, our group showed that the reaction between two equivalents of $(C_5Me_5)_2ThMe_2$ and H_2P(Tipp), Tipp = 2,4,6-$^{i}Pr_3C_6H_2$, formed a bridging phosphinidene, more appropriately called a phosphinidiide, $[(C_5Me_5)_2Th]_2${P-2,6-$CH_2[C(H)CH_3]_2C_6H_2$-4-^{i}Pr}, 1, eq 1. In that reaction, two P-H and two C-H bond activations occurred from the

phosphine and two methyl groups, respectively. The mechanism by which this phosphinidiide formed was via P-H, C-H, C-H, and P-H bond activation, but no intermediates were isolated.

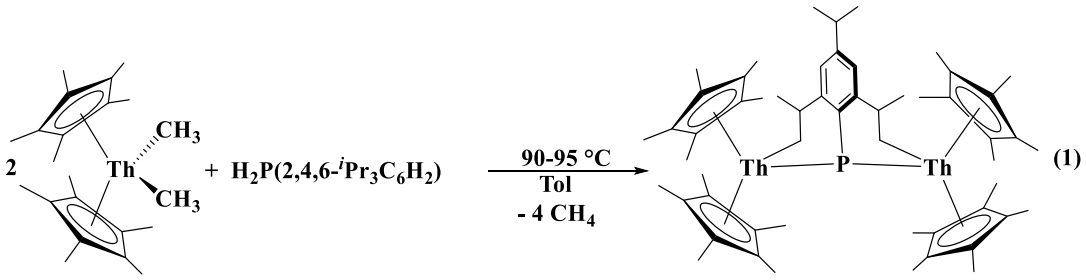

Recently, we reported the reaction of $(C_5Me_5)_2ThMe_2$ with the less sterically crowded phosphine, H_2PMes, Mes = 2,4,6-$Me_3C_6H_2$, in attempt to form the bridging phosphinidiide. However, the result was a phosphido with a C-H bond activation on one of the methyl groups of the mesityl, eq 2, along with another byproduct. This complex closely resembled the first step in the mechanism with formation of **1**, therefore we postulated that further heating and time could lead to the analogous phosphinidiide product.

Herein, we show that, indeed, the phosphinidiide can be isolated with mesityl, however, the mechanism by which the product forms is by P-H, C-H, P-H, and C-H bond activation due to the less sterically encumbering mesityl ligand. Reactivity with one and equivalents of ^{t}BuCN inserts into the Th-C bonds forming six-membered metallocycles with the Th-P-Th bond still intact. Computational analysis affords further evidence of the change in the sequence of bond activations as well as the bonding in the Th-P-Th moiety.

EXPERIMENTAL.

General consideration. All syntheses were carried out under an inert atmosphere of nitrogen using standard Schlenk and glovebox techniques. All solvents were purchased anhydrous, stored over activated 4 Å molecular sieves, and sparged with nitrogen prior to

use. All commercially available reactants were purchased from suppliers and used without further purification. $(C_5Me_5)_2ThMe_2$ and H_2PMes were synthesized as previously reported. Benzene-d_6 was dried over molecular sieves and degassed with three cycles of freeze-pump-thaw. All ^1H and ^{13}C NMR spectra were collected either on a Bruker Avance III 500 or 600 MHZ spectrometer. ^{31}P NMR spectra were collected on Bruker AVII+ 300MHz spectrometer. ^1H and ^{13}C NMR chemical shifts were referenced internally to the residue solvent peak at 7.16 ppm (C_6D_5H) and 128.06 ($^{13}C_6D_6$). ^{31}P NMR chemical shifts were referenced externally to H_3PO_4 at 0 ppm. Infrared spectra were recorded as a KBr pellets on Perkin-Elmer Spectrum One FT-IR spectrometer. Elemental analyses were performed by Microanalysis Facility, College of Chemistry, University of California, Berkeley.

Crystallographic Data Collection and Structure Determination. The selected single crystal of each complex was coated with viscous hydrocarbon oil inside a glove box before being mounted on a nylon cryoloop using Parabar® hydrocarbon oil. The X-ray data were collected on a Bruker Apex SMART diffractometer equipped with a Bruker APEX II area detector using Mo-Kα radiation (λ = 0.71073 Å) from a sealed Source Mo with TRIUMPH optics. The data collection and processing utilized Bruker Apex3 suite of programs. The structures were solved using an iterative dual space method as implemented in SHELXT and refined by full-matrix least-squares methods on F*2* using Bruker SHELX-2017/1 program. Full-occupancy non-hydrogen atoms were refined anisotropically. Disorder, when present, could be detected and modeled by locating all conformations from the difference map. Partial occupany atoms were refined at fixed occupancies, and in most cases the minor conformation could only be refined isotropically. Hydrogen atoms were placed at calculated positions and included in the refinement using a riding model

Table 2-1. Crystallographic Details for Complexes **2** to **4**.

Complex	**2**	**3**	**4**
Molecular Formula	$C_{49}H_{69}P_2Th_2$	$C54H78NPTh_2$	$C_{59}H_{87}N_2PTh_2$
Formula weight (g/mol)	1153.09	1236.22	1503.62
Crystal habit/color	Red Prism	Orange Prism	Orange Prism
Temperature (K)	150	150	150
Space group	*C2/c*	*P-1*	*C2/c*
Crystal system	Monoclinic	Triclinic	Monoclinic
Volume ($Å^3$)	4941.0(8)	2722.1(7)	6453.1(16)
a (Å)	19.3686(18)	11.0517(18)	19.523(3)
b (Å)	12.6400(12)	14.268(2)	22.997(16)
c (Å)	20.989(2)	18.641(3)	14.809(2)
α (^{o})	90	90	90
β (^{o})	105.936(2)	104.157(4)	103.937(3)
γ (^{o})	90	90	90
Z	4	2	4
Calculated density (g/cm^3)	1.550	1.508	1.548
Absorption coefficient (mm^{-1})	6.073	5.518	4.671
Final *R* indices [$I > 2\sigma(I)$]	R = 0.0300	R = 0.0431	R = 0.0469
	Rw = 0.0655	Rw = 0.0518	Rw = 0.0827

RESULTS AND DISCUSSION.

As previously reported, the reaction of $(C_5Me_5)_2ThMe_2$ with H_2PMes at 60 °C produces, $\{(C_5Me_5)_2Th[P(H)(2,4\text{-}Me_2C_6H_2\text{-}6\text{-}CH_2)]\}_2$, **1**, which has a $^{31}P\{^1H\}$ NMR resonance at -32 ppm. The other observed resonance is located at -62 ppm, which we attribute to the phosphide-methyl complex, $(C_5Me_5)_2Th(Me)[P(H)Mes]$. When two equivalents of $(C_5Me_5)_2ThMe_2$ is reacted with H_2PMes at 60 °C, the resonance at -62 ppm is observed, but far less, and **1** is still the major product. Increasing the heat to 95 °C, over the course of a few hours, the growth of a resonance at 201 ppm in the $^{31}P\{^1H\}$ NMR spectrum is observed. Finally, a chemical shift at 205 ppm is found for the product after prolonged heating overnight.

The ^1H NMR spectrum revealed an asymmetric molecule with two $(C_5Me_5)^{1-}$ resonances at 1.80 and 2.26 ppm. Two methylene protons are found at 0.53 and 3.10 ppm with $^3J_{P\text{-}H}$ = 10.71 Hz. The structure of this complex was structurally characterized using X-ray crystallography to reveal the anticipated phosphinidiide, $[(C_5Me_5)_2Th]_2(\mu_2\text{-}P\text{-}(2,6\text{-}(CH_2)_2\text{-}4\text{-}(CH_3)C_6H_2)$, **2**, Eq. 2, Fig. 1.

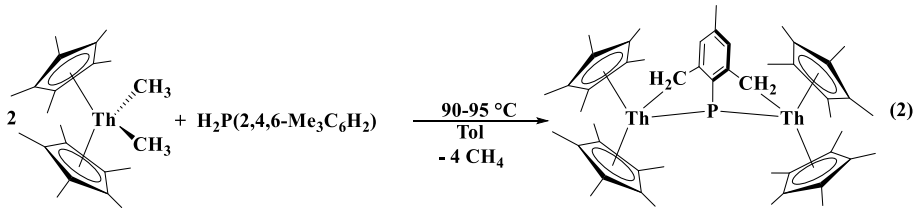

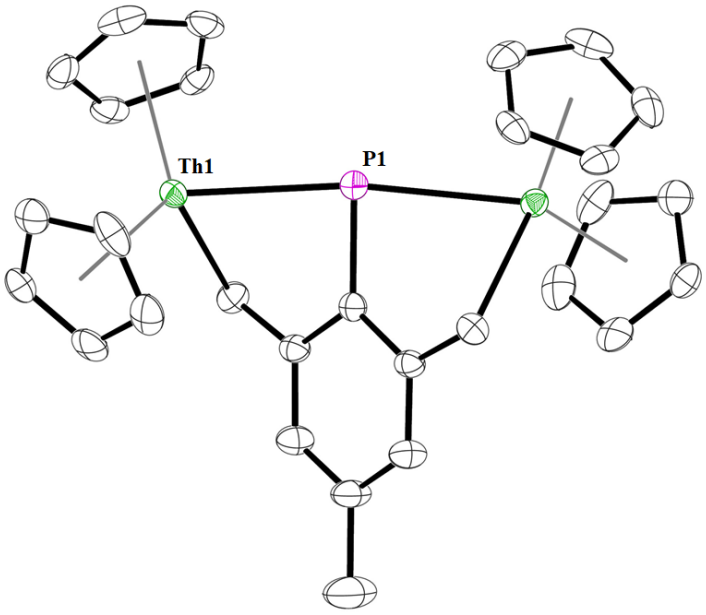

Figure 2-1. Thermal ellipsoid plot of 2 shown at the 50% probability level. Hydrogen atoms and the methyl groups on the C_5Me_5 groups have been omitted for clarity. Pertinent structural information is as follows: Th–P, 2.7552(3) Å; Th-C, 2.452(4) Å; P–Th–P, 171.73(6)°.

Complex **2** exhibits a ^{31}P resonance at 205 ppm, significantly more downfield than that of the $[(C_5Me_5)_2Th]_2\{$*P*-2,6-$CH_2[C(H)CH_3]_2C_6H_2$-4-^{i}Pr, **1** at 161.9 ppm. The Th-P and Th-C bond distances in **2** are somewhat shorter than those in **1** by ~0.05-6 Å, and ~0.02-3 Å, respectively, likely due to the lower degree of steric strain and smaller size of the metallacycle.

Addition of 1 molar equivalent of ^{t}BuCN to a stirring, toluene solution of **2** leads to insertion into the Th-C bond of one of the $(C_5Me_5)_2Th$ moieties, Eq. 3, Fig 2.

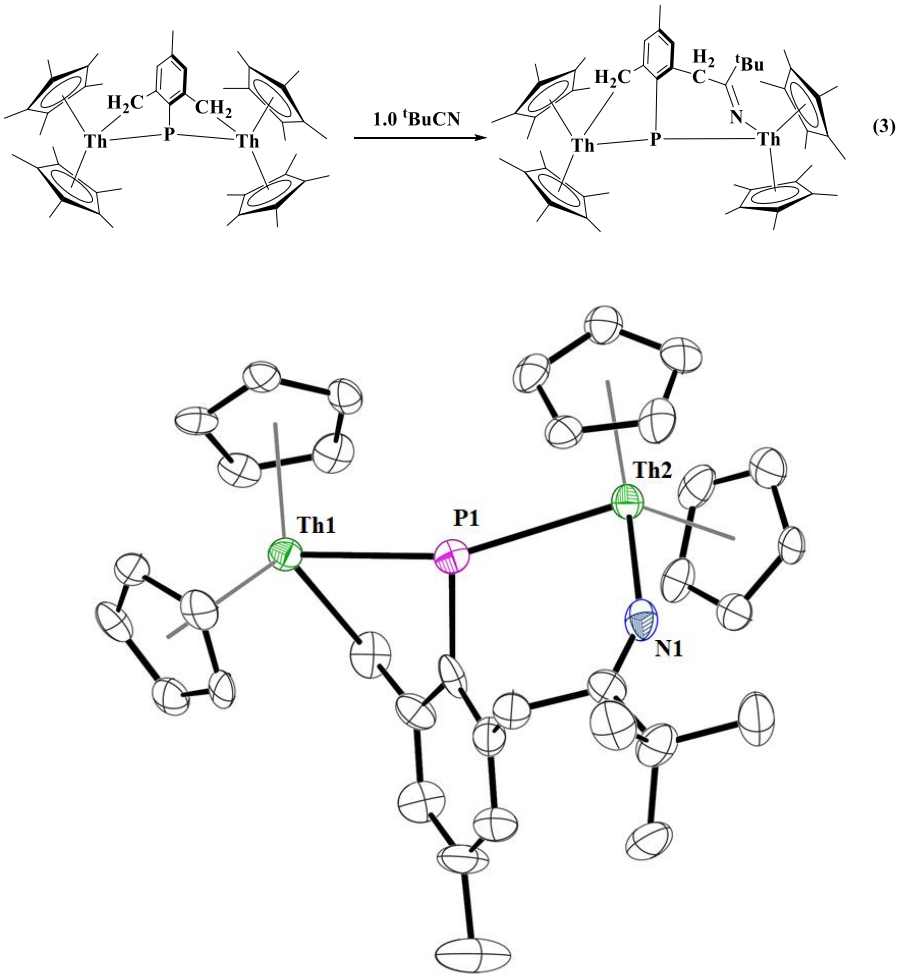

Figure 2-2. Thermal ellipsoid plot of **3** shown at the 50% probability level. Hydrogen atoms and the methyl groups on the C_5Me_5 groups have been omitted for clarity. Pertinent structural information is as follows: Th1–P1, 2.767(3) Å; Th1-C, 2.424(13) Å; Th1–P1–Th2, 157.69(14)°; Th2-N1, 2.176(11) Å.

The mono-insertion product, **3**, exhibits similar Th-P and Th-C distances to **1** and **2**, but a far more acute Th-P-Th angle compared to **2**, at 157.60(14)°, a consequence of the greater ring size of the phosphido/ketimido moiety in **3**. The ^{31}P NMR shift in **3** of 192 ppm is significantly low than that of **2**, approaching that of **1**, indicating that **3** is intermediate between **1** and **2** in electronic environment about the bridging P donor.

Complex **3** undergoes a similar, second insertion of ^{t}BuCN, resulting in a symmetric bridging Th-phosphinidiide, **4**, containing two seven membered-rings, Eq. 4, Fig 3.

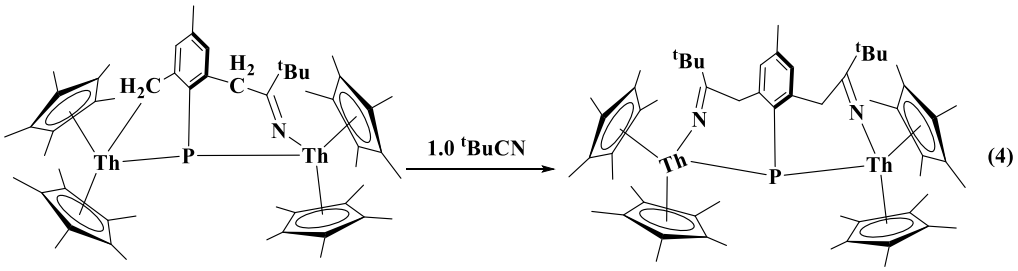

(4)

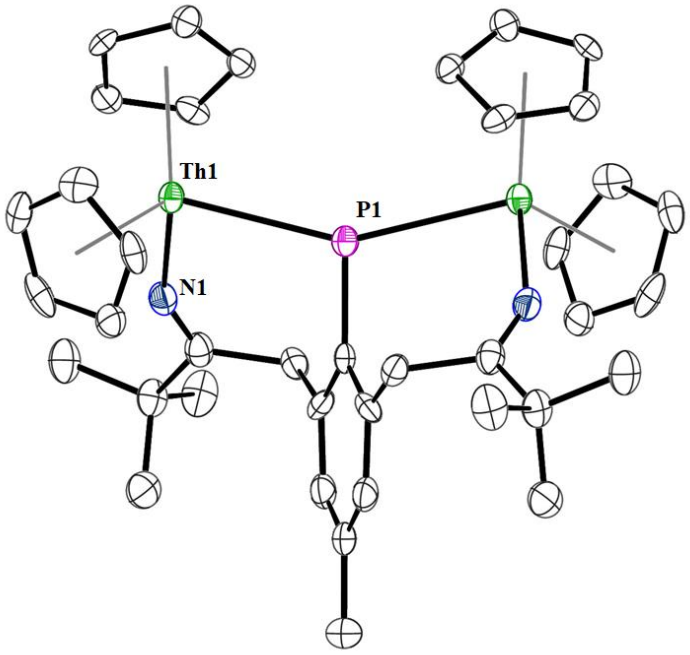

Figure 2-3. Thermal ellipsoid plot of **4** shown at the 50% probability level. Hydrogen atoms and the methyl groups on the C_5Me_5 groups have been omitted for clarity. Pertinent structural information is as follows: Th1–P1, 2.8579(8) Å; Th1-N, 2.194(6) Å; Th1–P1–Th2, 152.498 °.

The Th-P bond distance of 2.8579(8) Å in **4** is more similar to, but slightly longer than that in **1** at 2.8083(9) Å, possibly due to the steric strain of the C_5Me_5 moieties upon one another

as a consequence of shorter Th-N bonds at 2.194(6) Å compared to the analogous Th-C bonds in **1** at 2.482(3) Å and 2.472(3) Å. The ^{31}P NMR shift of the bridging phosphinidiide moiety in **4**, at 175 ppm is much closer to that of **1**, but slightly downfield.

The mechanism of formation of complexes **2**-**4** is currently underway.

CONCLUSION.

A bridging Th-phosphinidiide complex, **2**, has been synthesized by protonolysis of H_2PMes (Mes = 2,4,6-trimethylphenyl) with $(C_5Me_5)_2ThMe_2$. Sequential reactions of *tert*-butyl nitrile with **2** leads to insertion into the Th-C bonds, forming bridging Th-phosphinidiide compelxes **3** and **4**.

REFERENCES.

1. Weismann, J.; Scharf, L. T.; Gessner, V. H., Cooperative P–H Bond Activation with Ruthenium and Iridium Carbene Complexes. *Organometallics* **2016**, *35*, 2507-2515.

2. Driess, M.; Aust, J.; Merz, K., P−H Activation By Zirconium Amido Complexes: From New Phosphanidozirconium Complexes to the First Zr_2P_6 Cluster with the $[RP{-}P{-}PR]^{3-}$ Ligand [R = $Me_2(^iPrMe_2C)Si$]. *Eur. J. Inorg. Chem.* **2002**, *2002*, 2961-2964.

3. Mena, I.; Casado, M. A.; Polo, V.; García-Orduña, P.; Lahoz, F. J.; Oro, L. A., P–H activation of secondary phosphanes on a parent amido diiridium complex. *Dalton Trans.* **2014**, *43*, 1609-1619.

4. Shaver, M. P.; Fryzuk, M. D., Addition of Primary and Secondary Phosphines to Dinuclear Tantalum Hydrides: Synthesis of Phosphides and Phosphinidenes via P−H Bond Activation. *Organometallics* **2005**, *24*, 1419-1427.

5. García, M. E.; Riera, V.; Ruiz, M. A.; Rueda, M. T.; Sáez, D., Dimolybdenum and Ditungsten Cyclopentadienyl Carbonyls with Electron-Rich Phosphido Bridges. Synthesis of the Hydrido Phosphido Complexes $[M_2Cp_2(\mu\text{-}H)(\mu\text{-}PRR')(CO)_4]$ and Unsaturated Bis(phosphido) Complexes $[M_2Cp_2(\mu\text{-}PR_2)(\mu\text{-}PR'R'')(CO)_x]$ (x = 1, 2; R, R', R'' = Et, Cy, tBu). *Organometallics* **2002**, *21*, 5515-5525.

6. Alvarez, M. A.; Anaya, Y.; García, M. E.; Riera, V.; Ruiz, M. A., Chemistry of Highly Electrophilic Binuclear Cations. 3. Reactivity of $[W_2(\eta^5\text{-}C_5H_5)_2(\mu\text{-}CO)(CO)_2(\mu\text{-}Ph_2PCH_2PPh_2)][B\{3,5\text{-}C_6H_3(CF_3)_2\}_4]_2$ toward Small Donor Molecules. *Organometallics* **2004**, *23*, 433-440.

7. Varela-Izquierdo, V.; Geer, A. M.; de Bruin, B.; López, J. A.; Ciriano, M. A.; Tejel, C., Rhodium Complexes in P−H Bond Activation Reactions. *Chem. Eur. J.* **2019**, *25*, 15915-15928.

8. Mercy, M.; Maron, L., Can 1,3-butadiene be catalytically hydrophosphinated in the presence of Cp_2EuH? A DFT investigation. *Dalton Trans.* **2009**, 3014-3025.

9. Waterman, R., Selective Dehydrocoupling of Phosphines by Triamidoamine Zirconium Catalysts. *Organometallics* **2007**, *26*, 2492-2494.

10. Li, J.; Lamsfus, C. A.; Song, C.; Liu, J.; Fan, G.; Maron, L.; Cui, C., Samarium-Catalyzed Diastereoselective Double Addition of Phenylphosphine to Imines and Mechanistic Studies by DFT Calculations. *ChemCatChem* **2017**, *9*, 1368-1372.

11. Han, L.-B.; Tilley, T. D., Selective Homo- and Heterodehydrocouplings of Phosphines Catalyzed by Rhodium Phosphido Complexes. *J. Am. Chem. Soc.* **2006**, *128*, 13698-13699.

12. Feichtner, K.-S.; Gessner, V. H., Cooperative bond activation reactions with carbene complexes. *Chem. Commun.* **2018**, *54*, 6540-6553.

13. Rosenberg, L., Mechanisms of Metal-Catalyzed Hydrophosphination of Alkenes and Alkynes. *ACS Catalysis* **2013**, *3*, 2845-2855.

14. Bange, C. A.; Waterman, R., Challenges in Catalytic Hydrophosphination. *Chem. Eur. J.* **2016**, *22*, 12598-12605.

15. Ghebreab, M. B.; Bange, C. A.; Waterman, R., Intermolecular Zirconium-Catalyzed Hydrophosphination of Alkenes and Dienes with Primary Phosphines. *J. Am. Chem. Soc.* **2014**, *136*, 9240-9243.

16. Selikhov, A. N.; Mahrova, T. V.; Cherkasov, A. V.; Fukin, G. K.; Kirillov, E.; Alvarez Lamsfus, C.; Maron, L.; Trifonov, A. A., Yb(II) Triple-Decker Complex with the μ-Bridging Naphthalene Dianion $[CpBn_5Yb(DME)]_2(\mu\text{-}\eta^4{:}\eta^4\text{-}C_{10}H_8)$. Oxidative Substitution of $[C_{10}H_8]^{2-}$ by 1,4-Diphenylbuta-1,3-diene and P_4 and Protonolysis of the Yb–$C_{10}H_8$ Bond by $PhPH_2$. *Organometallics* **2016**, *35*, 2401-2409.

17. Ma, W.; Xu, L.; Zhang, W.-X.; Xi, Z., Half-sandwich rare-earth metal tris(alkyl) ate complexes catalyzed phosphaguanylation reaction of phosphines with carbodiimides: an efficient synthesis of phosphaguanidines. *New J. Chem.* **2015**, *39*, 7649-7655.

18. Behrle, A. C.; Schmidt, J. A. R., Insertion Reactions and Catalytic Hydrophosphination of Heterocumulenes using α-Metalated N,N-Dimethylbenzylamine Rare-Earth-Metal Complexes. *Organometallics* **2013**, *32*, 1141-1149.

19. Zhang, W.-X.; Nishiura, M.; Mashiko, T.; Hou, Z., Half-Sandwich o-N,N-Dimethylaminobenzyl Complexes over the Full Size Range of Group 3 and Lanthanide Metals. Synthesis, Structural Characterization, and Catalysis of Phosphine P-H Bond Addition to Carbodiimides. *Chem. Eur. J.* **2008**, *14*, 2167-2179.

20. Douglass, M. R.; Marks, T. J., Organolanthanide-Catalyzed Intramolecular Hydrophosphination/Cyclization of Phosphinoalkenes and Phosphinoalkynes. *J. Am. Chem. Soc.* **2000**, *122*, 1824-1825.

21. Behrle, A. C.; Castro, L.; Maron, L.; Walensky, J. R., Formation of a Bridging Phosphinidene Thorium Complex. *J. Am. Chem. Soc.* **2015**, *137*, 14846-14849.

22. Yuan, J.; Hu, H.; Cui, C., N-Heterocyclic Carbene–Ytterbium Amide as a Recyclable Homogeneous Precatalyst for Hydrophosphination of Alkenes and Alkynes. *Chem. Eur. J.* **2016**, *22*, 5778-5785.

23. Gu, X.; Zhang, L.; Zhu, X.; Wang, S.; Zhou, S.; Wei, Y.; Zhang, G.; Mu, X.; Huang, Z.; Hong, D.; Zhang, F., Synthesis of Bis(NHC)-Based CNC-Pincer Rare-Earth-Metal Amido Complexes and Their Application for the Hydrophosphination of Heterocumulenes. *Organometallics* **2015**, *34*, 4553-4559.

24. Basalov, I. V.; Yurova, O. S.; Cherkasov, A. V.; Fukin, G. K.; Trifonov, A. A., Amido Ln(II) Complexes Coordinated by Bi- and Tridentate Amidinate Ligands: Nonconventional Coordination Modes of Amidinate Ligands and Catalytic Activity in Intermolecular Hydrophosphination of Styrenes and Tolane. *Inorg. Chem.* **2016**, *55*, 1236-1244.

25. Basalov, I. V.; Liu, B.; Roisnel, T.; Cherkasov, A. V.; Fukin, G. K.; Carpentier, J.-F.; Sarazin, Y.; Trifonov, A. A., Amino Ether–Phenolato Precatalysts of Divalent Rare Earths and Alkaline Earths for the Single and Double Hydrophosphination of Activated Alkenes. *Organometallics* **2016**, *35*, 3261-3271.

26. Garner, M. E.; Parker, B. F.; Hohloch, S.; Bergman, R. G.; Arnold, J., Thorium Metallacycle Facilitates Catalytic Alkyne Hydrophosphination. *J. Am. Chem. Soc.* **2017**, *139*, 12935-12938.

27. Luo, G.; Luo, Y.; Hou, Z., E–H (E = N and P) Bond Activation of $PhEH_2$ by a Trinuclear Yttrium Methylidene Complex: Theoretical Insights into Mechanism and Multimetal Cooperation Behavior. *Organometallics* **2017**, *36*, 4611-4619.

28. Lapshin, I. V.; Basalov, I. V.; Lyssenko, K. A.; Cherkasov, A. V.; Trifonov, A. A., CaII, YbII and SmII Bis(Amido) Complexes Coordinated by NHC Ligands: Efficient Catalysts for Highly Regio- and Chemoselective Consecutive Hydrophosphinations with PH_3. *Chem. Eur. J.* **2019**, *25*, 459-463.

29. Selikhov, A. N.; Plankin, G. S.; Cherkasov, A. V.; Shavyrin, A. S.; Louyriac, E.; Maron, L.; Trifonov, A. A., Thermally Stable Ln(II) and Ca(II) Bis(benzhydryl) Complexes: Excellent Precatalysts for Intermolecular Hydrophosphination of C–C Multiple Bonds. *Inorg. Chem.* **2019**, *58*, 5325-5334.

30. Lapshin, I. V.; Cherkasov, A. V.; Asachenko, A. F.; Trifonov, A. A., Ln(II) amido complexes coordinated by ring-expanded N-heterocyclic carbenes – promising catalysts for olefin hydrophosphination. *Chemical Commun.* **2020**, *56*, 12913-12916.

Chapter 3: A Systematic Investigation of the Molecular and Electronic Structure of Thorium and Uranium Phosphorus and Arsenic Complexes

Michael L. Tarlton,[1] O. Jonathan Fajen,[1] Steven P. Kelley,[1] Andrew Kerridge,[2]* Thomas Malcomson,[2] Thomas L. Morrison,[3] Matthew P. Shores,[3]* Xhensila Xhani,[1] and Justin R. Walensky[1]*

[1] Department of Chemistry, University of Missouri, 601 S. College Avenue, Columbia, MO 65211, United States

[2] Department of Chemistry, Lancaster University, Lancaster LA1 4YB, U.K.

[3] Department of Chemistry, Colorado State University, Fort Collins, Colorado 80523, United States

ABSTRACT. Reaction of $(C_5Me_5)_2An(CH_3)_2$, An = Th, U, with two equivalents of H_2AsMes, Mes = 2,4,6-$Me_3C_6H_2$ forms the primary bis(arsenido) complexes, $(C_5Me_5)_2An[As(H)Mes]_2$. Both exhibit thermal instability at room temperature, leading to the elimination of H_2, and the formation of the diarsenido species, $(C_5Me_5)_2An(\eta^2\text{-}As_2Mes_2)$. The analogous diphosphido complexes, $(C_5Me_5)_2An(\eta^2\text{-}P_2Mes_2)$ could not be synthesized via the same route, even upon heating the bis(phosphido) species to 100 °C in toluene. However, they were accessed via reaction of dimesityldiphosphane, MesP(H)P(H)Mes, with $(C_5Me_5)_2AnMe_2$ at 70 ºC in toluene. When $(C_5Me_5)_2AnMe_2$ is reacted with one equivalent of H_2AsMes, the bridging μ_2-arsinidiide complexes $[(C_5Me_5)_2An]_2(\mu_2\text{-}AsMes)_2$ are formed. The reaction of $(C_5Me_5)_2UMe_2$ is reacted with one equivalent of H_2PMes, the phosphinidiide, $[(C_5Me_5)_2U(\mu_2\text{-}PMes)]_2$, is isolated. However, the analogous thorium reaction leads to a phosphido and C-H bond activation of the methyl on the mesityl group forming, $\{(C_5Me_5)_2Th[P(H)(2,4\text{-}Me_2C_6H_2\text{-}6\text{-}CH_2)]\}_2$. The reactivity

of $[(C_5Me_5)_2An(\mu_2\text{-}EMes)]_2$ was investigated with $OPPh_3$ to attempt to form the terminal phosphinidene or arsinidene. When E = As, An = U, a cation-anion pair, $[(C_5Me_5)_2U(\eta^2\text{-}As_2Mes_2)][(C_5Me_5)_2U(OPPh_3)_2]$, was isolated with each complex consisting of a U(III) center. Reaction of $[(C_5Me_5)_2Th)(\mu_2\text{-}AsMes)]_2$ with $OPPh_3$ does not result in a terminal arsinidene, but in elimination of PPh_3 to yield a bridging arsinidiide/oxo complex, $[(C_5Me_5)_2Th]_2(\mu_2\text{-}AsMes)(\mu_2\text{-}O)$**.** Finally, $[((C_5Me_5)_2U)(\mu_2\text{-}PMes)]_2$ with $OPPh_3$, results in a terminal phosphinidene, $(C_5Me_5)_2U(=PMes)(OPPh_3)$, with a short U-P bond distance of 2.502(2) Å. Electrochemical measurements on the uranium pnictinidiide complexes demonstrate only a small anodic shift in the U(V/IV) redox couple for the phosphinidiide. Finally, QTAIM analysis shows highly polarized actinide-pnictogen bonds with only slight covalent character with the exception of the phosphinidene.

INTRODUCTION.

The structural characteristics and fundamental chemical behavior of actinide complexes bearing soft donor ligands have become increasingly relevant to the design of radionuclide remediation processes, as these complexes serve a role as extractants.[1-6] Such ligands are employed to more efficiently separate the chemically similar lanthanides from the actinides, owing to the actinides' greater selectivity for them over the more common N- and O-donors. Greater covalent character of actinide soft-donor bonds has been suggested as the reason for this selectivity, but the paucity of such complexes in the literature precludes elucidation of the origin, which hinders further progress of potential applications as few studies have investigated differences in structure, bonding, and reactivity of heavier main group elements.[7-17] This is especially true of phosphorus and arsenic since arsenic is poorly represented in the organoactinide literature.[17-26]

One of the developments that has emerged in understanding this phenomenon is the energy-driven-covalency concept in which the energy difference between the 5f orbitals and the *n*p orbitals decreases with increasing *n*. To probe this concept, our laboratory, along with others, have been examining the structure, bonding, and reactivity of actinide-phosphorus and actinide-arsenic bonds. There are a number of phosphido complexes of thorium and uranium,[27] but there are few examples of arsenido,[17-23, 25-26] diphosphido,[28-30] diarsenido,[19, 26] phosphinidiide,[21, 31] arsinidiide,[19, 21] phosphinidene,[28, 32-37] and only one arsinidene,[18] Scheme 1. However, the design of structurally characterized compounds for direct comparison is limited, especially between two Th and U as well as two different elements in the same group. Herein, we describe the synthesis and characterization of a series of new actinide complexes with phosphorus and arsenic bonds, the molecular and electronic structure of these complexes, and reactivity with $OPPh_3$ to achieve actinide-ligand multiple-bonding. Magnetic and electrochemical measurements on the uranium complexes were also undertaken, and all complexes were studied using QTAIM analysis (DFT) to examine the energy-driven-covalency concept.

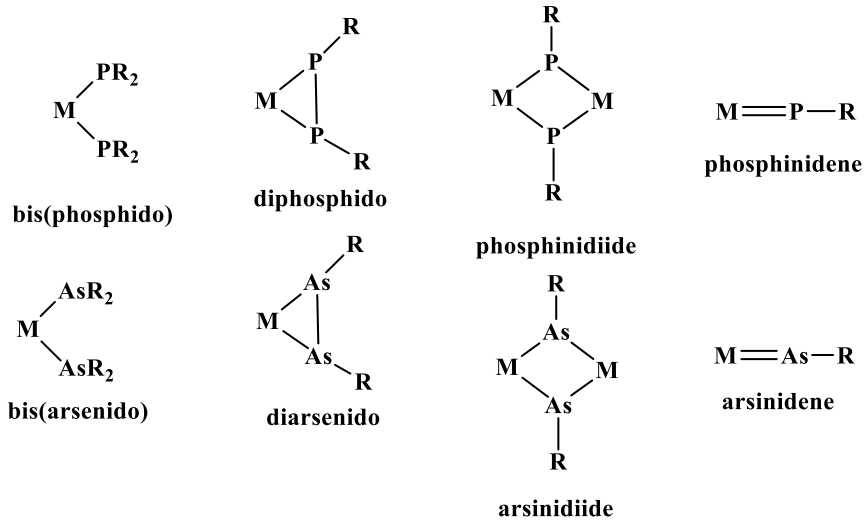

Scheme 1. Functional groups of phosphorus and arsenic involved in this work.

EXPERIMENTAL.

General considerations. All reactions were performed under an inert atmosphere of dry N_2 inside of a glovebox. $MesAsH_2$, MesP(H)P(H)Mes, and $(C_5Me_5)_2AnMe_2$ (An = Th, U) were prepared according to literature procedures.[38-39] Solvents were dried via activated alumina, and dispensed through a solvent-purification system, MBRAUN, USA. C_6D_6 (Cambridge Isotope Laboratories) was subjected to three freeze-pump-thaw cycles and dried over activated 4 Å molecular sieves for 72 h prior to use. All ^1H and $^{13}C\{^1H\}$ NMR experiments were performed on a 500 or 600 MHz Bruker NMR spectrometer. Spectra were referenced to residual C_6D_5H at 7.16 ppm (^1H) and 128.06 ppm ($^{13}C\{^1H\}$), respectively. IR spectra were collected from samples prepared as KBr plates with a Nicolet Summit PRO FTIR Spectrometer. Elemental analyses were performed by the Microanalytical Facility, University of California, Berkeley, USA.

Synthesis of $(C_5Me_5)_2Th[As(H)Mes]_2$, 1. A colorless, 5 mL pentane solution of H_2AsMes (757 mg, 3.86 mmol) was added dropwise to a stirring, 5 mL, pentane slurry of $(C_5Me_5)_2ThMe_2$ (822 mg, 1.54 mmol) at -30 ºC. The mixture was allowed to warm to ambient temperature and stirred for 2 h, during which time the color of the reaction mixture progressed from colorless to yellow, to yellow/orange, then to deep orange with precipitation of a large amount of a fine orange solid. The mixture was then filtered over a M-porosity, fritted glass funnel, and washed with 2 x 4 mL cold (-30 ºC) pentane, leaving a bright orange solid on the filter. The solid was stripped of volatiles under vacuum, leaving **1** as an analytically pure, bright-orange powder, 1.09 g, 79%. Crystals of **1** suitable for X-ray crystallography were grown from a concentrated diethyl ether solution at -30 ºC. ^1H

NMR (C_6D_6, 600 MHz, 25 ^oC): δ 6.98 (s, 4H, *m*-H), 2.63 (s, 12 H, *o*-CH_3), 2.51 (s, 2H, As-H), 2.34 (s, 6H, *p*-CH_3) 1.92 (s, 30H, C_5Me_5). $^{13}C\{^1H\}$ NMR (C_6D_6, 600 MHz): δ 143.1 (s, *p*-C_{aryl}), 140.0 (s, *o*-C_{aryl}), 134.24 (s, *i*-C_{aryl}), 127.5 (s, C_5Me_5), 26.68 (s, *o*-CH_3), 20.93 (s, *p*-CH_3), 11.73 (s, C_5Me_5), resonance for *m*-C(H) overlaps with signal from residual C_6D_5H. IR (cm^{-1}): 2953 (s), 2900 (s), 2855 (s), 2725 (w), 2090 (m), 1712 (w), 1600 (w), 1550 (w), 1456 (s), 1375 (m), 1261 (m), 1091 (m), 1022 (s), 845 (s), 802 (m), 705 (w), 684 (w), 611 (w), 543 (w). Elemental analysis calculated for $C_{38}H_{54}As_2Th$ (892.71 g/mol): C, 51.13%; H, 6.10%. Found: C, 50.77%; 5.84%.

Synthesis of $(C_5Me_5)_2U[As(H)Mes]_2$, 2. A 6 mL, deep orange, Et_2O solution of $(C_5Me_5)_2UMe_2$ (252 mg, 0.468 mmol) was added dropwise to a stirring, colorless, 5 mL Et_2O solution of the H_2As-Mes (200 mg, 1.02 mmol) at room temperature. The color became darker within 5 min, and the mixture was left to stir for 2.5 h. After filtration through Celite®, the mixture was concentrated to a black solid, then dissolved in 2 mL pentane and cooled to -30 ^oC in a glovebox freezer to facilitate crystallization. The solution grew a crop of black crystals that were collected by filtration over a medium-porosity glass frit and washed with another portion of room-temperature pentane (8 mL). A black, microcrystalline powder remained, 335 mg, 80%. Crystals of **2** suitable for X-ray crystallography were grown from a concentrated pentane solution at -30 ^oC. ^1H NMR (600 MHz, C_6D_6, 25 ^oC): δ 15.43 (s, 30H, C_5Me_5), 5.04 (s, 6H, *p*-CH_3), 2.95 (s, 4H, *m*-H), -24.3 (s, 12H, *o*-CH_3), -153.6 (s, br, 2H, As-H). IR (cm^{-1}): 2935 (m), 2896 (s), 2853 (m), 2723 (s), 2093 (m), 1599 (w), 1549 (w), 1456 (s), 1375 (s), 1261 (w), 1173 (w), 1046 (w), 1021(s), 845 (s), 804 (w), 704 (w), 602 (w), 543 (w). The thermal instability of **2** at room temperature made elemental analysis not possible.

Synthesis of $(C_5Me_5)_2Th(\eta^2\text{-}As_2Mes_2)$, 3. A 5 mL, colorless toluene solution of H_2AsMes (225 mg, 1.2 mmol) was added dropwise to a stirring, white slurry of $(C_5Me_5)_2ThMe_2$ (300 mg, 0.563 mmol) in 5 mL toluene. The mixture was heated to 75 ^oC overnight, causing a color change from from yellow to orange-red over the first 2 hours, and finally a dark green after stirring for 12 hours. The solution was filtered through Celite®, then stripped of volatiles under vacuum, triturated in pentane, then collected over a F-porosity fritted glass funnel, leaving a green powder 351 mg, 70%. Crystals suitable for X-ray diffraction were grown from an Et_2O solution at -30 ^oC. ^1H NMR (C_6D_6, 600 MHz, 25 ^oC): δ 6.94 (s, 4H, *m*-H), 2.57 (s, 12H, *o*-CH_3), 2.35 (s, 6H, *p*-CH_3), 1.92 (s, 30H, C_5Me_5). $^{13}C\{^1H\}$ NMR (C_6D_6, 600 MHz): δ 144.06 (s, *o*-C_{aryl}), 133.04 (s, *p*-C_{aryl}), 128.16 (s, *m*-C_{aryl}), 127.98 (s, *i*-C_{aryl}), 126.59 (s, C_5Me_5), 26.86 (s, *o*-CH_3), 20.51 (s, *p*-CH_3), 10.94 (s, C_5Me_5). IR (cm^{-1}): 2959 (s), 2919 (s), 2853 (s), 2724 (w), 2107 (w), 1644 (w), 1598 (w), 1451 (m), 1376 (m), 1261 (m), 1095 (s), 1044 (s), 1022 (s), 848 (w), 803 (m). Elemental analysis calculated for $C_{38}H_{52}As_2Th$ (890.70 g/mol): C, 51.24%; H, 5.88%. Found: C, 50.91%; 5.74%.

Synthesis of $(C_5Me_5)_2U(\eta^2\text{-}As_2Mes_2)$, 4. A 100 mL Strauss flask was charged with $(C_5Me_5)_2UMe_2$ (143 mg, 0.266 mmol) and 20 mL toluene. To this stirring red solution was added H_2AsMes (111 mg, 0.566 mmol). The resulting dark red solution was then heated at 80 ^oC overnight. The dark-red solution was allowed to cool to room temperature and volatiles were removed *in vacuo*, leaving a dark red solid, which was triturated with ~3 mL of pentane and dried again, leaving a dark red powder, 122 mg, 51%. Crystals of **4** suitable for X-ray diffraction were grown from a concentrated Et_2O solution at -30 °C. ^1H NMR (C_6D_6, 600 MHz, 25 °C): δ 7.57 (s, 30H, C_5Me_5), 1.41 (s, 6H, *p*-CH_3). The *o*-CH_3 and aryl-H resonances in **4** were not observable at room-temperature or with variable-temperature

NMR spectroscopy. IR (cm^{-1}): 2961 (s), 2910 (s), 2855 (s), 2723 (w), 2105 (w), 1627 (w), 1599 (w), 1558 (w), 1450 (s), 1375 (m), 1269 (w), 1261 (m), 1082 (m), 1021 (s), 846 (m), 800 (m). Elemental analysis calculated for $C_{38}H_{52}As_2U$ (896.69 g/mol): C, 50.90%; H, 5.84%. Found: C, 50.67%; 5.92%.

Synthesis of $(C_5Me_5)_2Th(\eta^2\text{-}P_2Mes_2)$, 5. In a glovebox, a 5 mL toluene solution of MesP(H)P(H)Mes (247 mg, 0.817 mmol) was added to a 50 mL Strauss flask containing a 15 mL toluene solution of $(C_5Me_5)_2ThMe_2$ (435 mg, 0.817 mmol), sealed, brought out of a glovebox, and heated with stirring to 70 ^oC for 24 h. The color became dark green, then brown over the course of the reaction. The flask was brought back into a glovebox, stripped of volatiles under vacuum, and the residue extracted in 2 x 3 mL Et_2O, filtered through Celite® and concentrated to ~2 mL. Cooling to -40 ^oC in a glovebox freezer facilitated growth of dark-green crystals over ~ 16 h, which were isolated, rinsed with 2 x 2 mL cold pentane, and stripped of volatiles under vacuum, 430 mg, 67%. ^1H NMR (600 MHz, C_6D_6, 25 ^oC): δ 6.89 (s, 4H, *m*-H), 2.64 (s, 12H, *o*-CH_3), 2.32 (s, 6H, *p*-CH_3), 1.90 (s, 30H, (C_5Me_5). $^{13}C\{^1H\}$ NMR (C_6D_6, 600 MHz): δ 143.56 (t, $^1J_{C\text{-}P}$ = 114 Hz), 140.98 (s, *o*-C_{aryl}), 132.36 (s, *p*-C_{aryl}), 129.22 (s, *m*-C_{aryl}), 126.77 (s, C_5Me_5), 126.12 (t, $^3J_{C\text{-}P}$ = 36 Hz, *o*-CH_3), 20.83 (s, *p*-CH_3), 11.37 (s, C_5Me_5). $^{31}P\{^1H\}$ NMR (C_6D_6, 101 MHz, 25 ^oC): δ 58.92 (s). IR (cm^{-1}): 2956 (s), 2897 (s), 2856 (s), 2725 (w), 1601 (w), 1453 (s), 1376 (s), 1262 (m), 1173 (w), 1096 (m), 1042 (s), 1022 (s), 949 (w), 849 (m), 712 (w), 616 (w), 547 (w). Elemental analysis calculated for $C_{38}H_{52}P_2Th$ (802.80 g/mol): C, 56.85%; H, 6.53%. Found: C, 57.00%; 6.36%.

Synthesis of $(C_5Me_5)_2U(\eta^2\text{-}P_2Mes_2)$, 6. In a glovebox, a 10 mL toluene solution of $(C_5Me_5)_2UMe_2$ (267 mg, 0.496 mmol) was added to a 50 mL round-bottom Strauss flask

followed by a 5 mL toluene solution of MesP(H)P(H)Mes (150 mg, 0.496 mmol). The flask was sealed and heated to 70 ^{o}C with stirring. The mixture darkened to a dark brown/black within 5 min, then after 1 h of total stirring, the volatiles were removed under vacuum, leaving a black/brown solid. The flask was brought back into a glovebox, the crude product extracted in 2 x 15 mL Et_2O, filtered through celite, and concentrated to a black solid. The solid was triturated in 5 mL pentane, and collected over a M-porosity glass frit, followed by washing with 5 mL more pentane, leaving a microcrystalline, black solid which was collected and stripped of volatiles under vacuum again, 195 mg, 49%. ^{1}H NMR (600 MHz, C_6D_6, 25 ^{o}C): δ 5.05 (s, 30H, C_5Me_5), 3.73 (s, 6H, *p*-CH_3), 1.23 (s, 4H, *m*-H), -22.26 (s, br, 12H, *o*-CH_3). IR (cm^{-1}): 2960 (s), 2907 (s), 2856 (s), 2723 (w), 2329 (w), 1719 (w), 1632 (w), 1602 (m), 1452 (s), 1376 (s), 1290 (w), 1261 (m), 1095 (s), 1022 (s), 849 (m), 804 (m), 712 (w), 603 (w), 548 (w), 497 (w). Elemental analysis calculated for $C_{38}H_{52}P_2U$ (808.79 g/mol): C, 56.43%; H, 6.48%. Found: C, 56.12%; 6.36%.

Synthesis of [$(C_5Me_5)_2Th]_2(\mu^2$-AsMes)$_2$, 7. A 5 mL, colorless, Et_2O solution of H_2AsMes (102 mg, 0.520 mmol) was added dropwise to a stirring, 4 mL, colorless solution of $(C_5Me_5)_2ThMe_2$ (277 mg, 0.520 mmol) at room temperature. The mixture became golden-yellow over the course of the addition, then orange, then orange-red over the following 20 min. The mixture was then left to stir for the night, and by the morning it had become dark orange/red. The mixture was filtered through Celite®, and concentrated to ~2 mL, then cooled to -30 ^{o}C to facilitate crystallization. By 30 min, large dark orange-red crystals had formed which were isolated, triturated in ~3 mL pentane then isolated and dried again, leaving a dark orange-brown powder, 145 mg, 40%. Crystals suitable for X-ray diffraction were grown from a concentrated Et_2O solution at -30 ^{o}C. ^{1}H NMR (C_6D_6, 600 MHz, 25

°C): δ 7.18 (s, 4H, *m*-H), 2.67 (s, 12 H, *o*-CH_3), 2.46 (s, 6H, *p*-CH_3), 2.21 (s, 30H, C_5Me_5). $^{13}C\{^1H\}$ NMR (C_6D_6, 600 MHz, 25 °C): δ 155.93 (s, *i*-C_{aryl}), 140.78 (s, *o*-CH_3), 132.84 (s, *p*-CH_3), 127.84 (s, C_5Me_5) 127.36 (*m*-C_{aryl}), 30.87 (s, *o*-CH_3), 20.92 (s, *p*-CH_3), 14.27 (s, (C_5Me_5). IR (cm^{-1}): 2958 (s), 2909 (s), 2857 (s), 2722 (w), 2369 (w), 2308 (w), 2090 (w), 1627 (w), 1599 (w), 1447 (m), 1377 (m), 1261 (m), 1085 (m), 1018 (s), 846 (w), 803 (w), 803 (w), 617 (w). Elemental analysis calculated for $C_{58}H_{82}As_2Th_2$ (1393.19 g/mol): C, 50.00%; H, 5.93%. Found: C, 50.25%; 5.67%.

Synthesis of $[(C_5Me_5)_2U]_2(\mu^2$-AsMes$)_2$, 8. A 20 mL scintillation vial was charged with $(C_5Me_5)_2UMe_2$ (130 mg, 0.241 mmol), and 6 mL toluene. The dark-orange solution was cooled to -30 °C in a glovebox freezer, the H_2AsMes (47 mg, 0.240 mmol) was added dropwise as a 3 mL, colorless toluene solution. The mixture was allowed to warm to ambient temperature, and in ~30 min, it had noticeably darkened. By the morning, the mixture had become dark brown/black, and was filtered through Celite®, then concentrated to a black solid under vacuum. The residue was triturated in 3 mL pentane, then isolated and dried under vacuum, leaving a black, analytically pure, microcrystalline solid, 109 mg, 64%. Crystals suitable for X-ray diffraction were grown from a concentrated Et_2O solution at -30 °C. ^1H NMR (C_6D_6, 600 MHz, 25 °C): δ 10.17 (s, 60 H, (C_5Me_5), 5.15 (s, 6 H, *p*-CH_3), -4.59 (s, 4 H, *m*-H), -65.7 (s, 12H, *o*-CH_3). IR (cm^{-1}): 2954 (s), 2883 (s), 2856 (s), 2719 (w), 2091 (w), 1626 (w), 1598 (w), 1449 (s), 1377 (m), 1267 (w), 1261 (w), 1174 (w), 1095 (w), 1017 (m), 945 (w), 846 (m), 803 (w), 706 (w), 602 (w). Elemental Analysis calculated for $C_{58}H_{82}As_2U_2$ (1405.17 g/mol): C, 49.58%; H, 5.88%; Found: C, 49.94%; 5.72%.

Synthesis of {(C_5Me_5)$_2$Th[μ^2-P(H)(2,4-$Me_2C_6H_2$-6-CH_2)]}$_2$, 9, Method A. A 10 mL toluene solution of (C_5Me_5)$_2$ThMe_2 and H_2PMes were heated with stirring in a sealed flask to 60 ^{o}C for 1 h. The mixture became yellow-orange. The mixture was cooled to room temperature and stripped of volatiles inside a glovebox. The yellow/orange residue was extracted in 2 x 4 mL Et_2O, filtered through Celite, reduced to ~ 2 mL under vacuum, and then cooled to -40 ^{o}C to facilitate crystallization. After a second recrystallization from Et_2O, a crop of yellow crystals was recovered, 161 mg, 66%. The ^{1}H NMR spectrum of **9** exhibited a resonance consistent with 4 equivalent (C_5Me_5)$^-$ ligands at 1.89 ppm, as well as resonances indicative of methyl and methylene groups integrating to 6 and 4H, respectively, at -0.12 and -0.19, a doublet for the P-H bonds ($^1J_{P\text{-}H}$ = 235 Hz), and a single resonance corresponding to 4 aryl protons at 6.94, but additional resonances indicative of a mixture of products were also visible. ^{31}P{^{1}H} NMR (C_6D_6, 101 MHz, 25 ^{o}C): δ (ppm) -33.54 (s). ^{31}P NMR (C_6D_6, 101 MHz, 25 ^{o}C): δ (ppm) -32.54 (d, $^1J_{P\text{-}H}$ = 192 Hz).

Method B. A 2 mL C_6D_6 solution of (C_5Me_5)$_2$ThMe(I) (50 mg, 0.078 mmol) was added to KP(H)Mes (15 mg, 0.079 mmol), resulting in a cloudy mixture that immediately turned orange. The mixture was transferred to a J-young tube and shaken vigorously for 5 min. The ^{1}H, ^{31}P{^{1}H}, and ^{31}P NMR spectra were collected at 10 min total reaction time, indicating conversion to a mixture of the previously published (C_5Me_5)$_2$Th[P(H)Mes]$_2$, and **9** in an approximate 1:5 ratio.

Synthesis of [(C_5Me_5)$_2$U(μ^2-PMes)]$_2$, 10. A 3 mL toluene solution of H_2PMes (332 mg, 2.18 mmol), was added dropwise to a stirring, 5 mL toluene solution of (C_5Me_5)$_2$UMe_2 (1.174 g, 2.18 mmol). The mixture was allowed to stir for 18 h, then filtered through Celite and the volatiles removed under vacuum. The resulting black solid was triturated in

pentane, resulting in a microcrystalline suspension which was collected over a medium-porosity fritted glass funnel. The resulting black solid was washed with 2 x 4 mL cold (-40 ^{o}C) pentane, leaving a microcrystalline black solid, 1.07 g, 74%. ^{1}H NMR (C_6D_6, 600 MHz, 25 ^{o}C): δ 10.65 (s, 30H, C_5Me_5), 5.63 (s, 6H, *p*-CH_3), -4.80 (s, 4H, *m*-H), -74.3 (s, 12H, *o*-H). IR (cm^{-1}): 2955 (s), 2909 (s), 2884 (s), 2854 (s), 2718 (w), 2299 (w), 1475 (w), 1449 (s), 1376 (m), 1260 (w), 1173 (w), 1081 (w), 1034 (m), 1020 (m), 947 (w), 847 (m), 803 (w), 711 (w), 605 (w). Elemental Analysis calculated for $C_{58}H_{82}P_2U_2$ (1317.27 g/mol): C, 52.88%; H, 6.27%. Found: C, 52.54%; 6.09%.

Synthesis of [(C_5Me_5)$_2$Th]$_2$(μ_2-AsMes)(μ_2-O), 11. A 100 mL Strauss-flask was charged with a 10 mL toluene solution of **7** (175 mg, 0.126 mmol) and the $OPPh_3$ (70 mg, 0.252 mmol) was added dropwise, as a 5 mL solution in toluene. The flask was sealed, and the mixture was heated to 70 ^{o}C for 2 h, during which the color changed from dark orange/brown to dark red-orange/red). The flask was allowed to cool to room-temperature, and brought into a glovebox, and the solution filtered through Celite, then concentrated to a dark red-brown solid. The solid residue was recrystallized twice from Et_2O, affording red crystals, 115 mg, 75%. Crystals suitable for X-ray diffraction were grown at -40 ^{o}C from a concentrated solution in THF. ^{1}H NMR (C_6D_6, 600 MHz, 25 ^{o}C): δ (ppm) 7.22 (s, 2H, *m*-H), 2.80 (s, 6H, *o*-CH_3), 2.39 (s, 3H, *p*-CH_3), 2.13 (s, 60H, (C_5Me_5). ^{13}C{^{1}H} NMR (C_6D_6, 600 MHz): δ (ppm) 153.96 (s, *o*-C), 140.89 (s, *i*-C), 133.02 (s, *p*-C), 128.34 (s, *m*-C), 126.54-125.54 (m, C_5Me_5) 28.55 (s, *o*-CH_3), 21.09 (s, *p*-CH_3), 13.17 (s, (C_5Me_5)) IR (cm^{-1}): 2962 (s), 2907 (s), 2858 (s), 2723 (w), 2279 (w), 2903 (w), 1627 (w), 1599 (w), 1439 (m), 1384 (m), 1261 (m), 1092 (m), 1020 (s), 846 (m), 617 (m), 519 (m). Elemental

Analysis calculated for $C_{49}H_{71}OAsTh_2$ (1215.08 g/mol): C, 48.44%; H, 5.89%. Found: C, 48.79%; 6.07%.

Synthesis of $[(C_5Me_5)_2U(\eta^2\text{-}As_2Mes_2)][(C_5Me_5)_2U(OPPh_3)_2]$, 12. A 4 mL toluene solution of $OPPh_3$ (60 mg, 0.216 mmol) was added dropwise to a stirring, 3 mL, toluene solution of **8** (151 mg, 0.107 mmol) at room temperature. The mixture was allowed to stir for 18 h, then filtered through Celite and stripped of volatiles under vacuum, leaving 180 mg of a brown/black solid. Attempts were made to crystallize the resulting black residue from a wide range of organic solvents, but the product would nearly always precipitate as an oil. A small number of black crystals were grown from Et_2O at -40 ^oC, only once, which were suitable for X-ray diffraction. $^{31}P\{^1H\}$ (C_6D_6, 121 MHz, 25 ^oC): δ 86.97 (s, $OPPh_3$).

Synthesis of $(C_5Me_5)_2U(=PMes)OPPh_3$, 13. Solid $OPPh_3$ (253 mg, 0.909 mmol) was added portion wise to a stirring, 8 mL toluene solution of **10** (600 mg, 0.455 mmol) at room-temperature. The mixture was allowed to stir for 45 h at room temperature, then filtered through Celite and stripped of volatiles under vacuum, leaving a dark red/brown solid. The solid was recrystallized twice from Et_2O at -40 ^oC, 399 mg, 47%. ^1H NMR (C_6D_6, 600 MHz, 25 ^oC): δ 22.89 (s, 2H, Mes-H), 22.71 (s, 3H, *p*-CH_3), 15.62 (s, 6H, *o*-CH_3), 4.20 (t, 3H, $^3J_{H\text{-}H}$ = 7.80 Hz, $OPPh_3$ *p*-H), 2.52 (s, 6H, $OPPh_3$ *m*-H), 1.957 (s, 30H, C_5Me_5), -13.22 (s, br, 6H, $OPPh_3$ *o*-H). $^{31}P\{^1H\}$ NMR (C_6D_6, 110 MHz, 25 ^oC): δ 12.56. IR (cm^{-1}): 3055 (s), 2964 (s), 2898 (s), 2854 (s), 2715 (w), 2329 (w), 1590 (w), 1468 (w), 1454 (w), 1438 (s), 1373 (w), 1160 (w), 1124 (s), 1122 (s), 1078 (s), 1047 (w), 1025 (w), 997 (w), 750 (m), 720 (m), 695 (m), 626 (w), 541 (s). Elemental Analysis calculated for $C_{47}H_{56}OP_2U$ (936.92 g/mol): C, 60.25%; H, 6.02%; Found: C, 60.48%; 6.15%.

Electrochemistry. Cyclic voltammetry (CV) experiments were conducted using a CH Instruments (CHI) model 700D series workstation and the data was analyzed using CHI software version 12.05. All experiments were conducted inside a N_2 atmosphere glovebox with an electrochemical cell consisting of a 10 mL vial, Pt disc electrode (3 mm diameter), a platinum wire counter electrode, and a silver wire plated with AgCl as a quasi-reference electrode. The working electrode surfaces were polished prior to each set of experiments and were periodically replaced to prevent buildup of oxidized or reduced products on the electrode surfaces. Solutions employed during CV studies were between 1.0–1.5 mM in analyte and 100 mM in tetrabutylammonium tetrakis(pentafluorophenylborate as the supporting electrolyte. Potentials were reported versus decamethylferrocene, which was added as an internal standard for calibration at the end of each experiment. Decamethylferrocene was separately referenced to ferrocene (0 V), under the same conditions. The peak-to-peak voltage in decamethylferrocene was found to be 0.573 V, which is attributed to the resistivity of the system. The initial scan polarity was negative for all measurements. Scan rate dependence experiments were performed at 500, 250, 100, and 50 mV/s. All data were collected in a positive-feedback IR compensation mode to minimize uncompensated resistance in the solution cells. The THF solution cell resistances were measured prior to each run to ensure resistances were approximately 1600 Ω or less.

Computational Details. Structural optimizations where carried out on phosphido, arsenido, diphosphido, diarsenido, phosphinidene, phosphinidiide and arsinidiide complexes of U(IV) and Th(IV) utilizing the PBE0[40,41] density functional along with the def-TZVP basis set;[42] a 60-electron effective core potential was applied to both thorium and uranium centers.[43-45] Apart from the dinuclear open-shell U(IV) arsinidiide and

phosphinidiide complexes, energetic minima were verified by harmonic frequency analysis. In the case of outstanding complexes, frequency analysis revealed imaginary frequencies of approximately $i20$ cm^{-1} which could not be eliminated despite repeated attempts. Inspection of the corresponding mode revealed them to be associated with rotation of peripheral methyl groups, indicating that the non-optimal structures were suitable for use in the investigation of metal-ligand bond characterization. All DFT calculations were conducted utilizing the Turbomole V6.6 software package;[46] orbital analysis was conducted utilizing NBO6,[47] and schematic production was carried out using the GaussView 5.0 visualization package[48] and QTAIM analysis was carried out within the AIMAll V19.02.13 software suite.[49]

Crystallographic Data Collection and Structure Determination. The selected single crystal of each complex was coated with viscous hydrocarbon oil inside a glove box before being mounted on a nylon cryoloop using Parabar® hydrocarbon oil. The X-ray data were collected on a Bruker D8 Phaser diffractometer equipped with a Photon 100 CMOS area detector using Mo-Kα radiation (λ = 0.71073 Å) from a microfocus source, or on a Bruker Apex SMART diffractometer equipped with a Bruker APEX II area detector using Mo-Kα radiation (λ = 0.71073 Å) from a sealed Source Mo with TRIUMPH optics. The data collection and processing utilized Bruker Apex3 suite of programs.[50] The structures were solved using an iterative dual space method as implemented in SHELXT and refined by full-matrix least-squares methods on F*2* using Bruker SHELX-2017/1 program.[51] Full-occupancy non-hydrogen atoms were refined anisotropically. Disorder, when present, could be detected and modeled by locating all conformations from the difference map. Partial occupany atoms were refined at fixed occupancies, and in most cases the minor

conformation could only be refined isotropically. Hydrogen atoms were placed at calculated positions and included in the refinement using a riding model, except for those bound to P and As atoms in **1**, **2**, and **9**, where difference map peaks in chemically reasonable positions were modeled as H atoms and their coordinates were allowed to freely refine. Thermal ellipsoid plots were prepared by using Olex2[52] with 50% of probability displacements for non-hydrogen atoms. In **11**, after the assignment of all chemically reasonable atoms, several large difference map peaks continued to appear next to full-occupancy carbon atoms. The unmodeled electron density in these regions had the effect of causing C atom coordinates to shift from their realistic positions and ADPs to refine to non-positive definite values. The indexing program CELL_NOW found that 3105 out of 3226 reflections with I/sigma > 4, or 96.24%, were consistent with a single domain of the unit cell, which indicated an absence of twinning. It was possible to index the data to a larger unit cell with triple volume (related by expansion of the *a* and *c* axes but with an identical *b* axis), but no improvement to the difference map was made using this unit cell. Examination of the coordinates of the difference map peaks revealed that they tended to have similar *x* and nearly identical *z* coordinates to Th and As atoms. Furthermore they appeared in traingular groups with very similar distances to the triangle formed between the Th and As atoms. In the crystal packing it can be seen that the molecules are arranged in columns parallel to the *b* axis, so taken together this suggested a form of disorder analogous to a stacking fault in which entire columns of molecules are shifted along *b* with respect to the rest of the structure. Three peaks were assigned as alternate positions for Th atoms and two peaks were assigned as alternate positions for As atoms and refined isotropically. The occupancies were refined with constraints so that the sum of all Th atoms

would equal 2 and all As atoms would equal 1. The final refinement indicates that 91.7% of the molecules are in the main position, and the remaining 8.3 % are shifted in either the positive or negative *b* direction in equal probability. The occupancies of the partial atoms are too low to allow location and refinement of the light atoms, so all carbon and oxygen atoms were left at full occupancy, and the minor metal atoms were completely excluded from the connectivity table. Inclusion of the minor metal atoms allowed all carbon atoms to be refined anisotropically without restraint. In structures **1** and **2** the partial occupancy carbon atoms which were refined anisotropically have very prolate ellipsoids; this is common when partial occupancy light atoms are refined anisotropically against a heavy atom data set. In structures **7** and **10**, the molecules appear to be disordered by very slight rotation about an axis passing through the center of the molecule; this causes the carbon atoms farthest from the center, on the mesityl groups, to have prolate ellipsoids. Structure **8** has a false B-level alert due to the unusually large difference in thermal motion of the As and Th atoms along the bond axis; the As atoms are expected to have larger motion in this direction because it is perpindicular to the rigid C-As bond. Structure **9** has a several large residual different map peaks which cannot be assigned to chemically reasonable atoms; this is likely caused by contributions to F_{obs} from other crystal domains. There were a significant number of intense reflections from the crystal of **9** that did not fit the unit cell. These could be fit to a second domain related by very slight rotation about an arbitrary axis, indicating the crystal may have cracked. Correcting for twinning using this matrix as a SHELXL TWIN instruction did not significantly improve the model.

Table 3-1. Crystallographic Details for Complexes **1** to **6**.

CSD Deposition mumbers	1998117	1996293	1996917	1996892	2056215	2056207
Complex	**1**	**2**	**3**	**4**	**5**	**6**
Molecular Formula	$C_{38}H_{54}As_2Th$	$C_{38}H_{54}As_2U$	$C_{38}H_{52}As_2Th$	$C_{38}H_{52}As_2U$	$C_{38}H_{52}P_2Th$	$C_{38}H_{52}P_2U$
Formula weight (g/mol)	892.71	898.71	890.70	896.69	802.80	808.79
Crystal habit/color	Orange Prism	Black Prism	Dark Green Prism	Black Prism	Dark Green Prism	Black Prism
Temperature (K)	100	100	100	100	150	150
Space group	*Pbcn*	*Pbcn*	*P2₁/n*	*P2₁/n*	*P2₁/n*	*P2₁/n*
Crystal system	Orthorhombic	Orthorhombic	Monoclinic	Monoclinic	Monoclinic	Monoclinic
Volume ($Å^3$)	3643.7(3)	3597.44(19)	3549.4(3)	3524.9(3)	3458.9(6)	3410.1(14)
a (Å)	10.7977(5)	10.8517(3)	12.3115(5)	12.26197)	12.2999(12)	12.222(3)
b (Å)	15.7582(7)	15.6491(5)	19.0955(16)	18.9207(11)	19.1890(18)	18.804(4)
c (Å)	21.4141(9)	21.1839(7)	15.1279(6)	15.2189(8)	14.6779(14)	14.856(4)
α (º)	90	90	90	90	90	90
β (º)	90	90	93.6162(16)	93.316(2)	93.202(2)	92.814(4)
γ (º)	90	90	90	90	90	90
Z	4	4	4	4	1	1
Calculated density (g/cm^3)	1.624	1.648	1.667	1.690	1.542	1.575
Absorption coefficient (mm^{-1})	5.918	5.994	6.075	6.492	4.428	4.878

Final *R* indices [$I > 2\sigma(I)$]	*R* = 0.0518 *Rw* = 0.1600	*R* = 0.0326 *Rw* = 0.0783	*R* = 0.0395 *Rw* = 0.0715	*R* = 0.0288 *Rw* = 0.0746	*R = 0.0220* *Rw = 0.0503*	*R = 0.0301* *Rw = 0.0680*

Table 3-2. Crystallographic Details for Complexes **7** to **10**.

CSD Deposition numbers	1998880	1998572	2061431	2056283
Complex	**7**	**8**	**9**	**10**
Molecular Formula	$C_{58}H_{82}As_2Th$	$C_{58}H_{82}As_2U$	$C_{58}H_{82}P_2Th_2$	$C_{58}H_{82}P_2U_2$
Formula weight (g/mol)	1393.16	1405.17	1305.29	1317.27
Crystal habit/color	Dark Orange/Red Prism	Black Prism	Yellow Prism	Black Prism
Temperature (K)	150	150	100	100
Space group	*Fddd*	*Fddd*	$P2_1/c$	*Fddd*
Crystal system	Orthorhombic	Orthorhombic	Monoclinic	Orthorhombic
Volume ($Å^3$)	15119.6(11)	14738.3(12)	6310.3(10)	14606(4)
a (Å)	19.3992(8)	19.1333(9)	12.3619(11)	19.272(3)
b (Å)	20.6778(8)	20.1994(10)	23.682(2)	19.838(3)
c (Å)	37.6922(16)	38.1347(19)	21.556(2)	38.203(5)
α (°)	90	90	90	90
β (°)	90	90	90.711(3)	90
γ (°)	90	90	90	90

Z	8	8	4	8
Calculated density (g/cm^3)	1.224	1.267	1.530	1.198
Absorption coefficient (mm^{-1})	4.823	5.306	4.799	4.499
Final *R* indices [$I > 2\sigma(I)$]	R = 0.0397 Rw = 0.1203	R = 0.0283 Rw = 0.0795	R = 0.0337 Rw = 0.0.0806	R = 0.993 Rw = 0.0337

Table 3-3. Crystallographic Details for Complexes **11** to **13**.

2062035	2056521	2056520
11	**12**	**13**
$C_{49}H_{71}AsOTh$	$C_{94}H_{112}As_2P_2O_2U_2$	$C_{58}H_{82}As_2U$
983.04	1961.74	1405.17
Dark Orange/Red Prism	Black Prism	Black Prism
100	100	100
$P2_1/c$	*P-1*	*Fddd*
Monoclinic	Orthorhombic	Orthorhombic
4884.7(13)	14738.3(12)	14738.3(12)
17.084(3)	19.1333(9)	9.5838(8)
17.783(3)	20.1994(10)	20.0944(18)
16.628(2)	38.1347(19)	21.3079(19)
90	90	90
104.770(3)	90	91.450(2)

90	90	90
4	8	4
1.753	1.267	1.517
6.798	5.306	4.069
R = 0.0478	R = 0.0283	R = 0.0495
Rw = 0.1030	Rw = 0.0795	Rw = 0.0495

RESULTS AND DISCUSSION.

Complexes **1**, $(C_5Me_5)_2Th[As(H)Mes]_2$, and **2**, $(C_5Me_5)_2U[As(H)Mes]_2$, were prepared via protonolysis reactions between $(C_5Me_5)_2AnMe_2$ and two equivalents of H_2AsMes, and isolated in yields of 79% and 80% for **1** and **2**, respectively, eq 1. The resonances of **1** in the ^1H NMR spectrum spans the typical diamagnetic range, with the As-H resonance at 2.51 ppm, slightly upfield than that of $(C_5Me_5)_2Th[As(H)Tipp]_2$[20] at 2.61 ppm. Complex **2** exhibits the broadened and paramagnetically shifted resonances in the ^1H NMR spectrum characteristic of a U(IV) species. The chemical shift of the As-H resonance in **2** at -153.6 ppm is upfield compared to that reported for $[U(Tren^{TIPS})(AsH_2)]$[18] at -131.4 ppm as well as the -122.9 ppm for the P-H in $(C_5Me_5)_2U[P(H)Mes]_2$. Both **1** and **2** have absorptions at 2090 and 2093 cm^{-1}, respectively, which are attributed to the As-H bond stretch.[18]

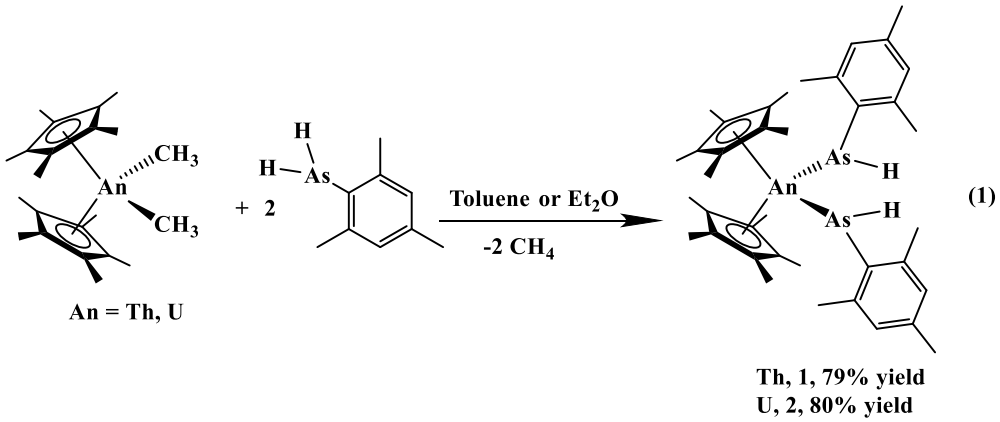

The solid-state structures of **1** and **2** were determined using X-ray crystallographic analysis, Figure 1. The Th-As bond distance of 2.9942(7) Å is very close to that of $(C_5Me_5)_2Th[As(H)Tipp]_2$[20] at 3.0028(6) Å, and the arsenido-moiety in $[\{(C_5Me_5)_2Th[\mu_2\text{-}As(H)Tip](\mu_2\text{-}AsTipp)\}K]_2$ at 3.0860(4) Å.[25] The structural characteristics of **1** are similar to the previously reported Th-arsenido complexes[22] bearing ancillary triamidosilylamine (Tren) ligands, $[Th(Tren^{TIPS})(AsH_2)]$, $[Th(Tren^{TIPS})\{As(SiMe_3)_2\}]$, $[Th(Tren^{DMBS})\{As(SiMe_3)_2\}]$, at 3.065(3) Å, 2.956(9) Å, and 3.0456(9) Å, respectively. Complex **1** also bears some similarity to the arsenido-cluster-bridged $[Cp'_2Th(\mu\text{-}\eta^{2:1:2:1}\text{-}As_6)ThCp'_2]$ (Cp′ = 1,3-*di*(tert-butyl)cyclopentadienyl) complex reported by the Wolmerhauser group,[26] with the Th-As bond distances at 2.930(3) Å, 3.018(2) Å, 3.040(2) Å, 3.044(2) Å, 3.005 Å, and 2.913(2) Å. Complex **2**, exhibiting a U-As bond length of 2.9087(5) Å is shorter than that in $[U(Tren^{TIPS})(AsH_2)]$,[18] with a U-As bond distance of 3.004(4) Å, and within the range of the asymmetric bond distances of $[\{U(Tren^{TIPS})\}_2(\mu\text{-}As)]$[53] at 2.943(4) Å and 2.889(4) Å. The structural characteristics of **2** are also similar to the previously reported U-arsenido complexes[22] of 2.942(9) Å and 2.9062(7) Å for the cases of $Tren^{DMBS}$, and $Tren^{TIPS}$, respectively.

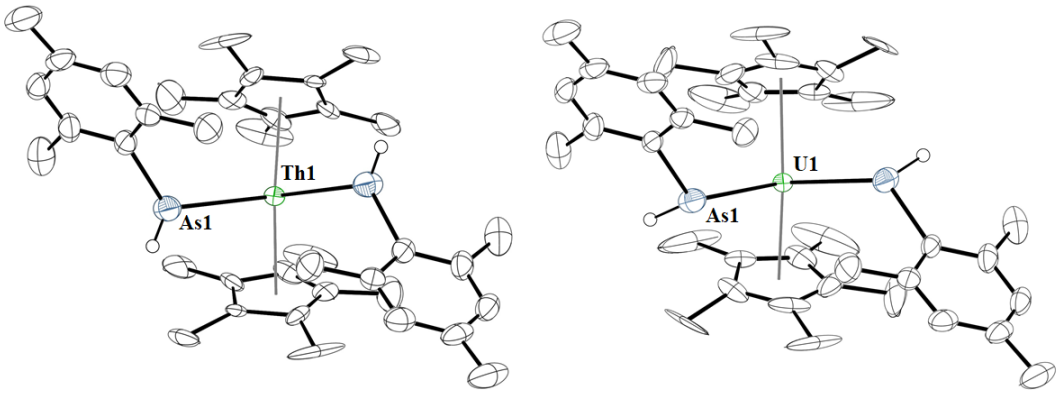

Figure 3-1. Thermal ellipsoid plot of **1** (left) and **2** (right) are shown at the 50% probability level. Hydrogen atoms have been omitted for clarity, with the exception of those bound to the arsenic atoms. Pertinent structural information is as follows: Th1-As1, 2.9942(7) Å; As1-Th1-As1, 103.48(3)°; U1-As1, 2.9087(5) Å; As1-U1-As1, 100.61(2)°.

Both **1** and **2** exhibit thermal instability at room temperature, gradually eliminating one equivalent of H_2 (as observed by ^{1}H NMR spectroscopy) and coupling the arsenido moieties, forming the diarsenido species, $(C_5Me_5)_2An(\eta^2\text{-}As_2Mes_2)$, An = Th, **3**; U, **4**, eq 2. Likely as a consequence of the steric bulk at the *ortho*-positions on the aryl rings, $(C_5Me_5)Th[As(H)Tip]_2$[4] did not exhibit thermal decomposition to a diarsenido complex even after stirring for extended periods of time at room temperature. Beginning with **1**, conversion to **3** is completed over 12-16 h when stirring in either Et_2O or toluene with an accompanying color change of deep orange to dark green. The ^{1}H NMR spectrum of **3** showed the $(C_5Me_5)^{1-}$ methyl resonances for both **1** and **3** are nearly identical, and that the resonances for the ring-protons and *ortho*/*para* methyl groups in **3** deviate only slightly from those of **1**. The $(C_5Me_5)^{1-}$ methyl resonance for **4** exhibited a large shift to 7.47 ppm, from that of **2** at 15.57 ppm. Apart from that for the *para*-methyl groups in **4**, the resonances

for the aryl protons and methyl groups on the rings in **4** are unobservable across the range of temperatures examined.

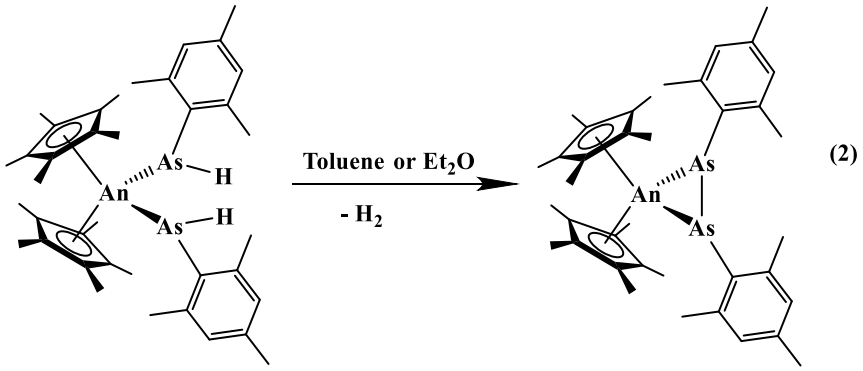

The structures of **3** and **4** were determined by X-ray crystallography analysis. This, and similar moieties[11, 54] often take the form of anionic clusters containing As-As bonds, and more commonly encountered in transition-metal chemistry.[55-61] Several carborane-type anionic ligands incorporating diarsenido-type fragments have also been reported.[62-67] The Th-As bond distances of 2.923(2) and 2.971(3) Å, and U-As bond lengths of 2.9231(9) and 2.8994(7) Å are slightly shorter than those observed in **1** and **2**, respectively. The As-As bond lengths of 2.4454(7) Å in **3** and 2.4320(3) Å in **4**, are consistent with As-As bond distances of 2.472(3) Å in Mes2AsAsMes2[68] as well as the 2.4572(3) Å in $(C_5H_5)_2Ti(\eta^2\text{-}As_2Tip_2)$.[69] Complexes **3** and **4** bear similarity to the Liddle group's bridging $(HAsAsH)^{2-}$ complex, $[U(Tren^{TIPS})]_2(\mu_2{:}\eta^2\text{-}As_2H_2)$,[19] with U-As bond distances at 3.1203(7) Å, and 3.1273(7) Å, a significant increase in bond length due to the steric demand of $Tren^{TIPS}$ ligand. We note that the As-As bond distance is 2.1402(13) Å in $[U(Tren^{TIPS})]_2(\mu_2{:}\eta^2\text{-}As_2H_2)$. The An-As1-C(ipso) bond angles are 99.18(14)° and 111.53(14)° for **3**, and 96.70(7)° and 111.13(7)° for **4**. Complex **4** exhibits anagostic interactions[70] from the *o*-CH_3

groups on one of the mesityl rings in each case, with a U-H36C distance of ~2.55 Å. This is contrast to the thorium analog, **3**, whose closest Th-H contact is 2.798 Å.

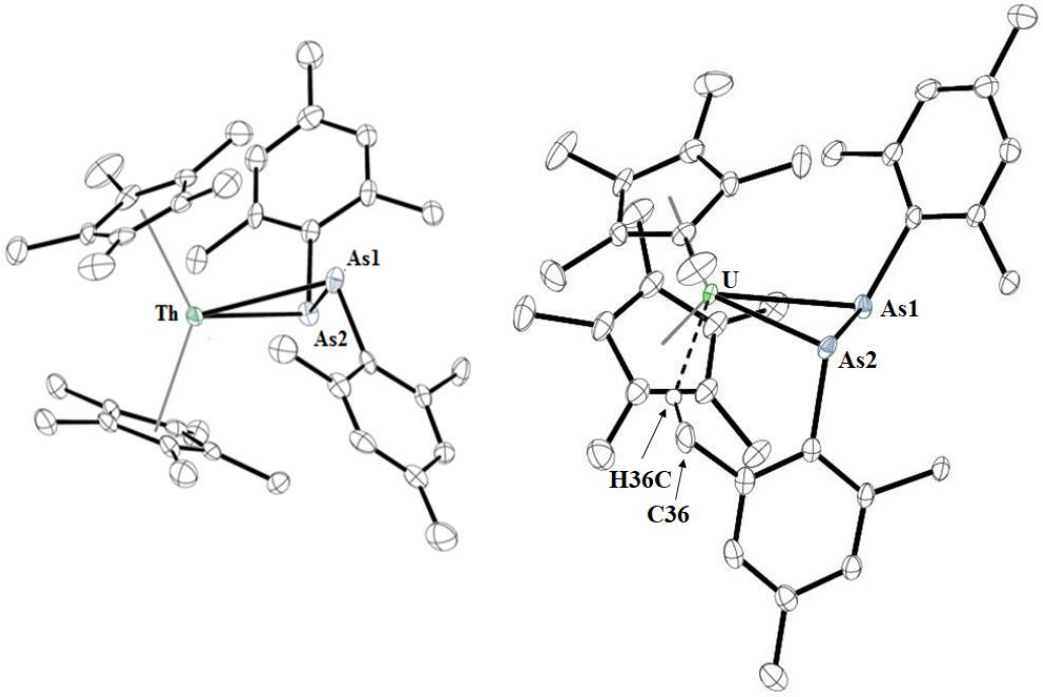

Figure 3-2. Thermal ellipsoid plot of **3** (left) and **4** (right) are shown at the 50% probability level. Hydrogen atoms have been omitted for clarity. Pertinent bond distances and angles are as follows: Th1-As1, 2.923(2) Å; Th1-As2, 2.971(3) Å; As1-As2, 2.4454(7) Å; As1-Th-As2, 49.01(4)°; U1-As1, 2.9231(9) Å; U1-As2, 2.8914(11) Å; As1-As2, 2.4320(3) Å; As1-U-As2, 49.326(18)°.

In contrast to the bis(arsenido) complexes, the bis(phosphido) complexes are more thermally stable. Heating $(C_5Me_5)_2An[P(H)Mes]_2$ to 100 °C in toluene does not form the diphosphido complexes or lead to decomposition, hence an alternate method was employed. The reaction of $(C_5Me_5)_2An(CH_3)_2$ with dimesityldiphosphane, MesP(H)P(H)Mes,[71] was conducted, eq 3. At room temperature, no reaction takes place,

but heating to 70 °C afforded the desired diphosphido complexes, $(C_5Me_5)_2An(\eta^2\text{-}P_2Mes_2)$, An = Th, **5**; U, **6**. We note that the uranium complex reacted immediately with the diphosphane at elevated temperature, while the reaction with thorium took several hours to reach completion. This is presumably due to the higher effective nuclear charge of uranium, giving more basicity to the methyl groups coordinated to uranium versus thorium. Complex **5** is dark green while **6** is black in color, similar to their diarsenido counterparts. The ^{31}P NMR spectrum of **5** exhibits a resonance at 58.92 ppm, somewhat downfield from that of the Holoch group's recently reported[72] $(PN)_2La(\eta^2\text{-}P_2Mes_2)$ (PN = *N*-(2-(diisopropyl-phosphanyl)-4-

methylphenyl)-2,4,6-trimethylanilide) complex, at 30.5 ppm, but similar to the resonance at 55.3 ppm in $(C_5Me_5)_2Th(\kappa^2\text{-}P_3Ph_3)$,[73] and in between those of 81.9 and 14.4 ppm for $(1,3\text{-}^tBu_2C_6H_3)_2Th(\eta^2\text{-}P_2Tip_2)$ and $(1,3\text{-}^tBu_2C_6H_3)_2Th(\eta^2\text{-}P_2Tip_2)(DMAP)$,[30] respectively.

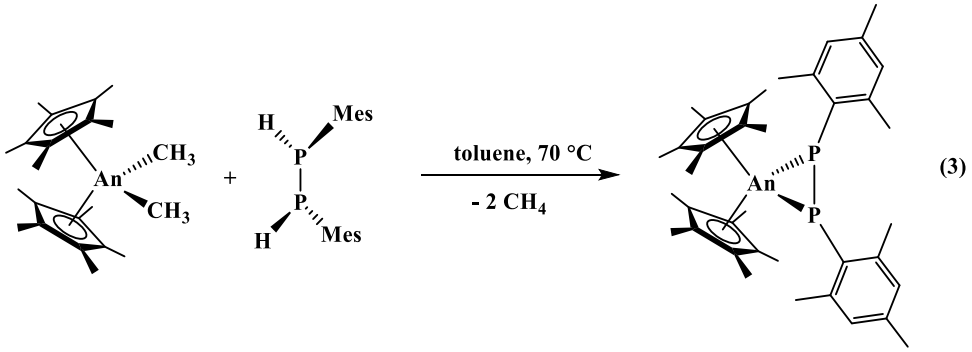

The An-P bond distances are 2.8463(7) and 2.8322(6) Å in **5**, and 2.7799(10) and 2.7903(10) Å in **6**. These can be compared to $(1,3\text{-}^tBu_2C_6H_3)_2Th(\eta^2\text{-}P_2Tip_2)(DMAP)$ which has a P-Th-P bond angle of 44.5(1)°,[30] smaller than the P-An-P angles of 45.486(18) and 46.13(3)° in **5** and **6**, respectively. The identical Zr(IV) structure, $(C_5Me_5)_2Zr(\eta^2\text{-}P_2Mes_2)$, has a P-Zr-P angle of 48.65(9)°.[74] The P-P bond distance in **5** and **6** of 2.1953(8) Å and

2.1825(13) Å, respectively, is consistent with the 2.1826(7), Ar = Tip, and 2.1699(5), Ar = 2,6-$^{i}Pr_2C_6H_3$, Å in $(C_5H_5)_2Ti(\eta^2\text{-}P_2Ar_2)$ complexes.[75] As observed in the uranium diarsenido, **4**, the uranium diphosphido, **6**, also displays anagostic interactions. The U1-H36C distance is 2.545 Å with a U-H36C-C36 angle of 147.9°. In contrast to the diarsenido complexes, the **5** does contain a Th-H29A contact of 2.672 Å. We note that in all cases, the hydrogen atoms were modeled.

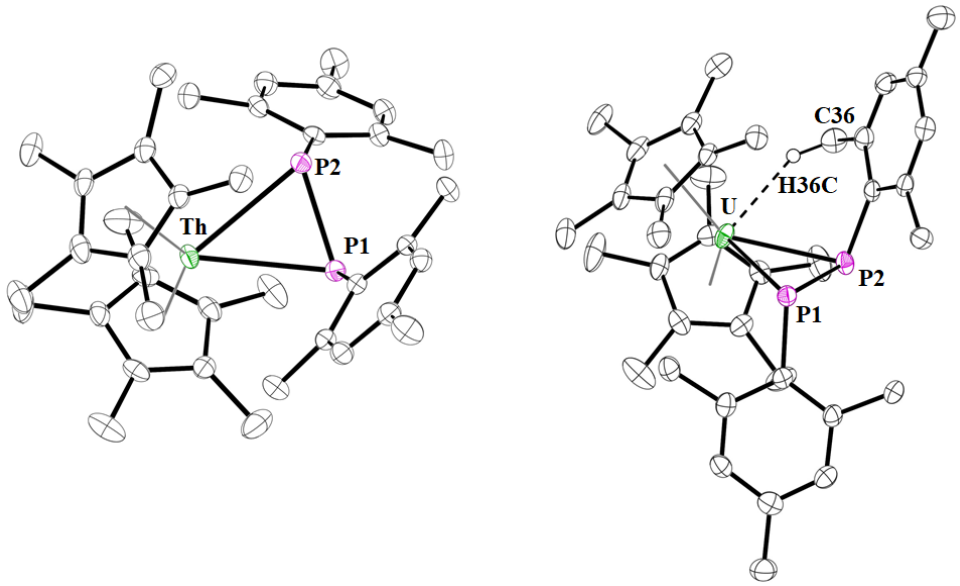

Figure 3-3. Thermal ellipsoid plot of **5** (left) and **6** (right) are shown at the 50% probability level. Hydrogen atoms have been omitted for clarity, with the exception of the methyl group participating in the anagostic interaction in **6**. Pertinent bond distances and angles are as follows: Th1-P1, 2.8463(7) Å; Th1-P2, 2.8322(6) Å; P1-P2, 2.1953(8) Å; P1-Th-P2, 45.486(18)°; U1-P1, 2.7799(10) Å; U1-P2, 2.7903(10) Å; U1-H36C, 2.545 Å; P1-P2, 2.1825(13) Å; P1-U-P2, 46.13(3)°.

Reaction of one equivalent of H_2AsMes with $(C_5Me_5)_2AnMe_2$ (An = Th, U) in diethyl ether or toluene, and stirring the reaction for ~12-16 h at room temperature. Complexes **7** and **8** are isolable in average yields of approximately 40, and 64%, respectively, eq 4. The

chemical shifts for **7** in the ^{1}H NMR spectrum are similar to those of **1** except for the lack of an As-H resonance. The ^{1}H NMR spectrum of **8** shows expected paramagnetic character, with the resonance for the *o*-CH_3 groups appearing at -65.7 ppm, a stark contrast from that of **2** at -24.30 ppm. The $(C_5Me_5)^{1-}$ resonances for **2** and **8** appear at 15.43, and 10.17 ppm, respectively, reflecting a similar upfield shift.

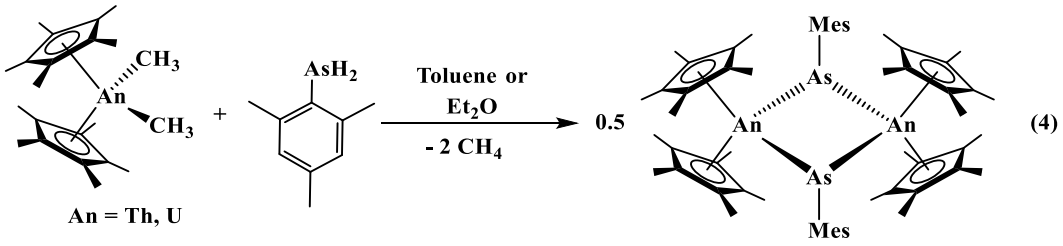

An = Th, 7, 40% yield
U, 8, 64% yield

The structures of **7** and **8** were also determined by X-ray crystallography analysis, Figure 4. The Th-As bond distance of 2.8787(6) Å in **7** is longer than the arsinidiide bond distance of 2.7994(4) Å in $[\{(C_5Me_5)_2Th[\mu_2\text{-}As(H)Tipp](\mu_2\text{-}AsTipp)\}K]_2$, 2.8565(7) Å in $Th(Tren^{TIPS})(\mu_2\text{-}AsH)K(15C5)$, 15C5 = 15-crown-5, and $\{Th(Tren^{TIPS})\}_2(\mu\text{-}As)][K(15C5)_2$[22] at 2.8063(14) and 2.8060(14) Å. The U-As bond length of 2.8310(4) Å is much longer than the terminal arsinidene $[U(Tren^{TIPS})(AsH)]^{1-}$ bond distance of 2.7159(13) Å as well as the 2.74(1) Å in the arsinidiide $[U(Tren^{TIPS})(AsH)K(2.2.2\text{-cryptand})]$.[18] However, these distances are significantly shorter than the corresponding An-As distances in **1**, 2.9953(7) Å, and **2**, 2.9087(5) Å.

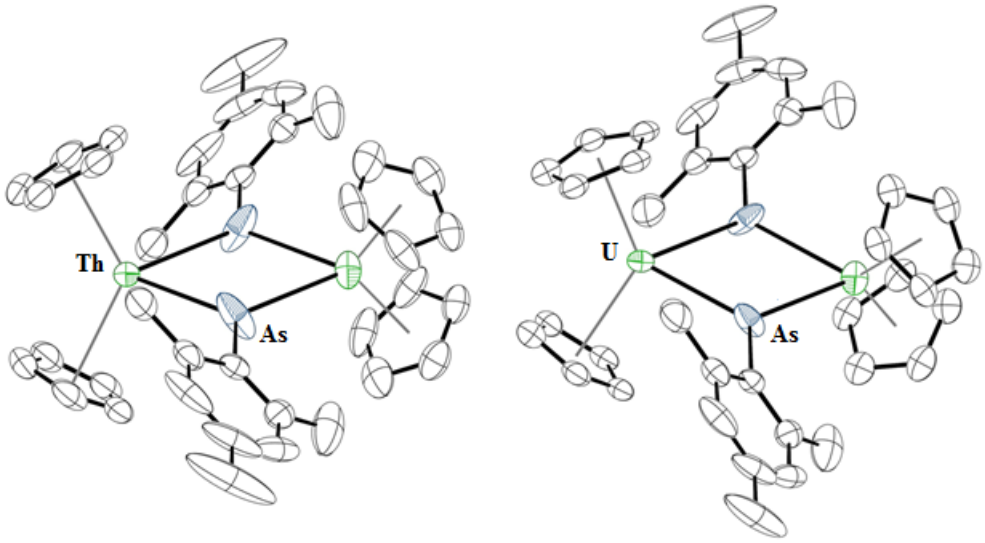

Figure 3-4. Thermal ellipsoid plot of **7** (left) and **8** (right) are shown at the 50% probability level. Hydrogen atoms and cyclopentadienyl methyl groups have been omitted for clarity. Pertinent bond distances and angles are as follows: Th-As, 2.8787(6) Å; As-Th-As, 71.516(4)°; U-As, 2.8310(4) Å; As-U-As, 69.808(19)°.

To make a comparison with phosphorus, the analogous reactions with $(C_5Me_5)_2ThMe_2$ and one equivalent of H_2PMes was attempted, eq 5. Heating the reaction to 60 °C was necessary to observe a color change from colorless to yellow. However, it was apparent from the $^{31}P\{^1H\}$ NMR spectrum that the phosphinidiide did not form, as a doublet at -33.54 ppm in the ^{31}P NMR spectrum was observed, while other thorium phosphinidiide complexes show $^{31}P\{^1H\}$ NMR resonances >100 ppm. Additionally, the ^{31}P NMR spectrum showed a doublet ($^1J_{P\text{-}H}$ = 192 Hz) as well as a $\nu_{P\text{-}H}$ stretch at 2305 cm^{-1}, indicative of a primary phosphido ligand.[76] Spectroscopic characterization of **9** is consistent with the proposed structure, however the ^1H NMR spectrum exhibited signals indicative of two products, which persisted through multiple recrystallizations. While **9** seems to be the major product, the presence of the other byproduct indicates the reactivity of

$(C_5Me_5)_2ThMe_2$ with H_2PMes is more complicated. Efforts to understand this reaction in more detail are currently underway.

Reaction of $(C_5Me_5)_2UMe_2$ with one equivalent of H_2PMes at room temperature afforded a black solid in good yield (74%). The ^1H NMR spectrum showed a resonance at 10.65 ppm for the $(C_5Me_5)^{1-}$, similar to the 10.03 ppm for $(C_5Me_5)_2U[P(H)Mes]_2$.[77] With no resonance for the P-H bond observed in the ^{31}P NMR or IR spectra, the X-ray crystallography showed the expected phosphinidiide product, $[(C_5Me_5)_2U(\mu_2\text{-}PMes)]_2$, **10**. The difference between thorium and uranium is striking. Whether this is due to the 5f orbitals participating in bonding uranium to form the multiply-bonded phosphinidiide is not understood at present time. However, we note that in a previous report, the reaction of $(C_5Me_5)_2U[P(H)Mes]_2$ with two equivalents of ^{t}BuCN formed $(C_5Me_5)_2U[\kappa^2\text{-}(N=C^tBu)_2P(Mes)]$,[77] which we attributed to the formation of a transient phosphinidene or phosphinidiide. Reaction of **10** with ^{t}BuCN also forms $(C_5Me_5)_2U[\kappa^2\text{-}(N=C^tBu)_2P(Mes)]$, which provides evidence of this intermediate, as is the case for zirconium.[78]

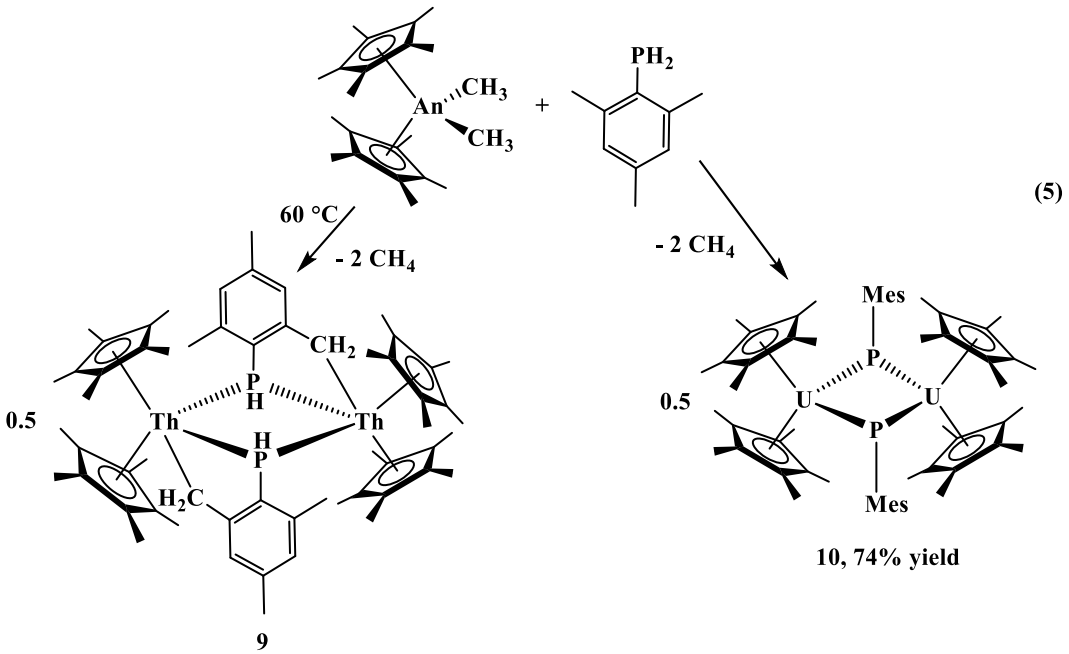

The structure was determined by X-ray crystallography to be a dimeric alkyl-phosphido complex, $\{(C_5Me_5)_2Th[\mu_2\text{-}P(H)(2,4\text{-}Me_2C_6H_2\text{-}6\text{-}CH_2)]\}_2$, **9**, the result of C-H bond activation at the *o*-CH_3 of the mesityl ring on the phosphido moiety. This result may be due to insufficient steric saturation of the available coordination site of the $(C_5Me_5)_2Th^{2+}$ moiety, given that the smaller U(IV) center does form a bridging phosphinidiide complex. An alternate synthetic route was employed in an effort to obtain $[(C_5Me_5)_2Th(\mu_2\text{-}PMes)]_2$, involving reaction of $(C_5Me_5)_2ThMe(I)$ with KP(H)Mes. The result was again a mixture, this time of **9** as well as the previously reported bis(phosphido) complex, $(C_5Me_5)_2Th[P(H)Mes]_2$, in an approximate 5:1 ratio. This metalation is reminiscent of the proposed mechanism for the formation of the bridging phosphinidiide from reaction of two equivalents of $(C_5Me_5)_2ThMe_2$ with $H_2P(2,4,6\text{-}^iPr_3C_6H_2)$.[31] In that reaction, transition state calculations described a P-H, followed by a C-H bond activation, similar to the formation of **9**.

Complex **9** has Th1-P bond distances of 3.020(1) and 3.085(1) Å and Th2-P bond lengths of 3.080(1) and 3.036(1) Å. These distances are much longer than the 2.872(5) Å in $(C_5Me_5)_2Th[P(H)Mes]_2$[20] and 2.888(4) Å in $(C_5Me_5)_2Th(Cl)[P(SiMe_3)_2]$.[79] The Th1-C1 and Th2-C10 bond distances are 2.542(5) and 2.533(5) Å, respectively. These Th-C bond lengths are significant longer than other phosphido-methyl complexes reported which range from 2.429(5) to 2.473(4) Å.[80-81] Complex **10** is a symmetric dimer in the solid-state with a U-P bond distance of 2.742(3) Å. This is only slightly shorter than the 2.7768(12) Å in $(C_5Me_5)_2U[P(H)Mes]_2$,[77] but identical to the 2.743(1) Å for the bridging phosphinidiide, $[(C_5Me_5)_2U(OMe)]_2(\mu_2\text{-}PH)$.[82]

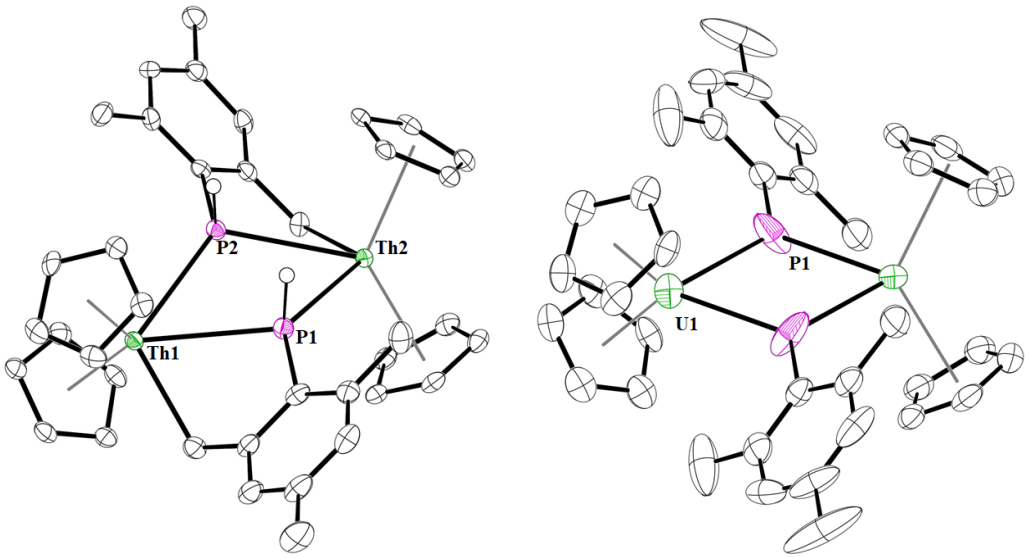

Figure 3-5. Thermal ellipsoid plot of **9** and **10** shown at the 50% probability level. All hydrogens apart from the phosphido (in **9**) and the methyl groups on the $(C_5Me_5)^{1-}$ ligands have been omitted for clarity. Selected bond distances and angles: Th1-P1: 3.0202(14) Å; Th1-C1: 2.541(6) Å; Th1-P2: 3.0849(14) Å; Th2-P1: 3.0806(14) Å; Th2-P2: 3.0364(14) Å; Th2-C10: 2.534(5) Å; P1-Th1-P2: 58.96(4)°; P1-Th2-P2: 58.84(4)°; U1-P1: 2.742(3) Å; U1-P1-U1*: 109.72(3)°; P1-U1-P1*: 70.28(2)°.

Computational Analysis. Complexes **1**-**10** were analyzed using density functional analysis incorporating the PBE0 exchange-correlation functional to compare the amount of covalent bonding in the pnictido, dipnictido, and pnictinidiide complexes. The thorium phosphinidiide, which is not observed experimentally, was modeled after the analogous uranium phosphinidiide, **10**, to make a direct comparison. All bond distances and angles showed excellent agreement (within 0.03 Å and 2°) with the experimentally determined values, Table 3-4. As would be expected, bond covalency is more pronounced in the U

Complex	Calculated M-E (avg) (Å)		Experimental M-E (avg) (Å)	
	Th	U	Th	U
Phosphido	2.888	2.774	2.888(4)[20]	2.7768(12)[77]
Arsenido	3.013	2.935	2.9942(7)	2.9087(5)
Diphosphido	2.840	2.786	2.839(1)	2.785(1)
Diarsinido	2.962	2.933	2.947(3)	2.907(1)
Phosphinidiide	2.835	2.784	---	2.742(3)
Arsinidiide	2.922	2.873	2.8787(6)	2.8310(4)
Phosphinidene	2.548	2.499	---	2.502(1)

Table 3-4. Calculated and experimental bond distances. Values are averaged over M-E bonds (E = P, As).

complexes than the Th analogues. This is more pronounced in U-P than U-As bonds but is supressed from the pnictido → dipnictido → pnictinidene → pnictidiide complex. ρ_{BCP} is small in all cases, indicative of predominantly ionic interactions, Table 3-5. These densities compare well with previously reported thorium and uranium phosphido and arsenido complexes.[22, 76, 83] Bond ellipticities were typically found to be larger in the U complexes, indicative of higher multiple bond character, with the exception of the pnictidiide complexes, for which the Th-E bonds had notably high ellipticity. The ellipticity of the U-E bond in the arsenido complex appears to be anomalous. The delocalization indices (DI), quantifying electron sharing between bonded atoms, are typically larger in the U complexes and, in contrast to the ρ_{BCP} values, increases in the order pnictido < dipnictido < pnictidiide. It is worth noting that ρ_{BCP} will only measure σ-type bond character whereas DI measures electron sharing through all bonding interactions.

Complex	ρ_{BCP} (a.u.)		$\nabla^2\rho_{BCP}$ (a.u.)		ε (a.u.)		H (a.u)		DI (a.u)	
	Th	U	Th	U	Th	U	Th	U	Th	U
Phosphido	0.056	0.062	0.035	0.050.	0.228	0.327	-0.015	-0.018	0.594	0.691
Arsenido	0.050	0.054	0.021	0.027	0.129	0.076	-0.013	-0.015	0.584	0.655
Diphosphido*	0.062	0.067	0.032	0.027	0.149	0.186	-0.019	-0.022	0.604	0.667
Diarsinido*	0.055	0.057	0.022	0.015	0.149	0.161	-0.016	-0.017	0.625	0.671
Phosphinidene	0.077	0.082	0.105	0.116	0.297	0.553	-0.027	-0.030	1.195	1.345
(M-O bond)	(0.060	0.057	0.210	0.225	0.046	0.215	-0.009	-0.007	0.365	0.354)
Phosphinidiide*	0.060	0.062	0.040	0.047	0.332	0.206	-0.017	-0.018	0.657	0.731
Arsinidiide*	0.055	0.056	0.034	0.040	0.336	0.215	-0.015	-0.016	0.662	0.734

Table 3-5. QTAIM-derived bond metric for M-X bonds (M = Th, U; X = P, As). ε = bond ellipticity, H = energy density, DI = Delocalization index.

In comparison, ρ_{BCP} is consistently larger in M-P than M-As bonds, with the difference being more pronounced in the U complexes. Bond ellipticities are noticeably larger in the phosphido complexes when compared to the arsenide analogues, whereas values are comparable in the dipnictido and pnictidiide. Delocalization indices indicate that M-E electron sharing is comparable, irrespective of the chemical nature of E, although the general trend is for M-As bonds to exhibit slightly greater electron sharing than M-P bonds. This is suggestive of greater overlap-driven covalency in M-P bonds, and greater energy degeneracy-driven covalency in M-As bonds.

Electrochemistry of 8 and 10. To experimentally compare the donating properties of phosphorus and arsenic ligands, electrochemical measurements were performed on the

uranium(IV) arsinidiide, **8**, and phosphinidiide, **10**. While several irreversible features are observed in each cyclic voltammagram, one quasi-reversible wave is also observed, with $E_{1/2}$ values of -2.316 V, and -2.385 V, for **8** and **10**, respectively, corresponding to the $U^{IV/III}$ couple, Fig. 3-6 and 3-7. This is consistent with the calculations in which the LUMO of **8** and **10** are both uranium-based. While a direct comparison cannot be made, it is noteworthy that the reduction potentials of **8** and **10** are far more negative than those of the imido complexes reported by Kiplinger, $(C_5Me_5)_2U{=}N(2,4,6\text{-}^tBu_3C_6H_2)$[84] and $(C_5Me_5)_2U(THF)[{=}N(2,6\text{-}^iPr_2C_6H_3)]$,[85] which have more cathodic potentials. This is a consequence of the large change in electronegativity from N to P, and the nearly identical electronegativity of P and As,[86] but also supports the computational results that the differences in bonding between P and As are small, and not as good a donor as nitrogen.

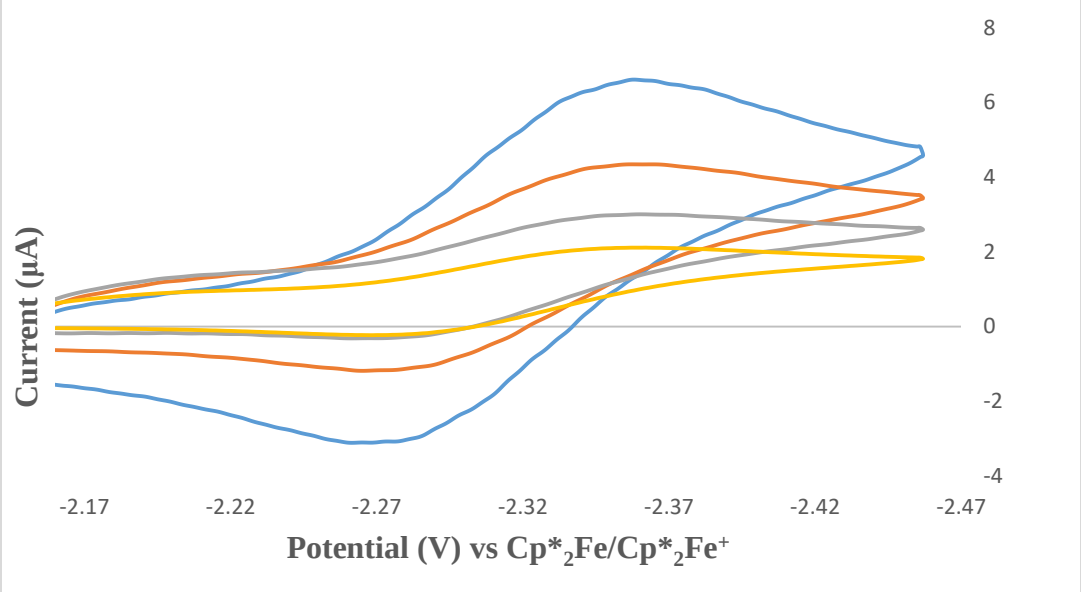

Figure 3-6. Overlaid cyclic voltammograms of **8** for the quasireversible region at scan rates (V/s) of 0.5 (blue), 0.25 (orange), 0.125 (grey), and 0.05 (yellow). $E_{1/2}$ = -2.316 V.

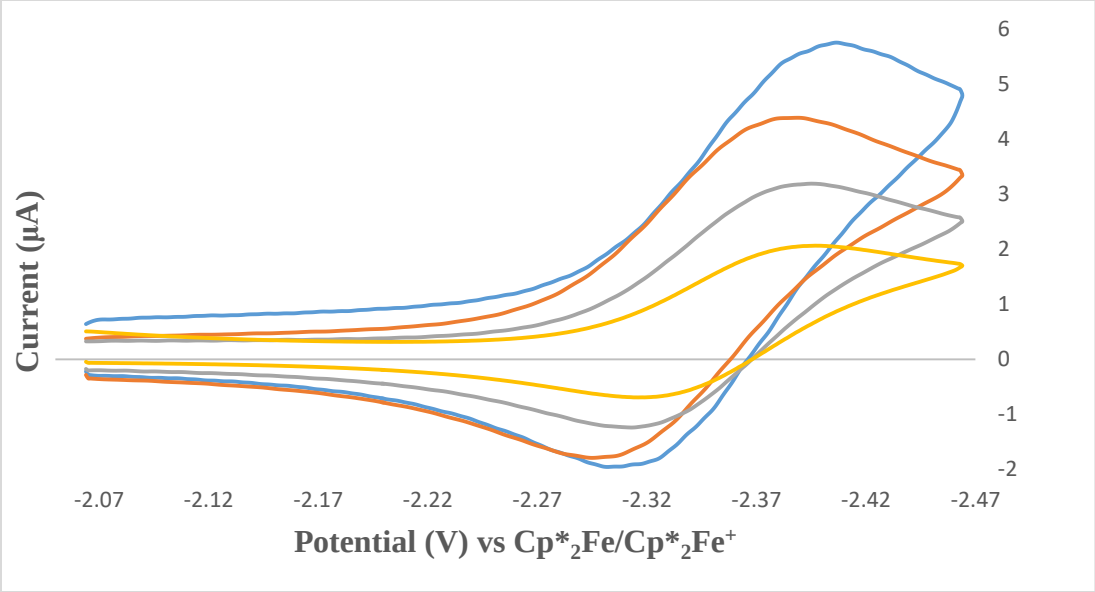

Figure 3-7. Overlaid cyclic voltammograms of **10** for the quasireversible region at scan rates (V/s) of 0.5 (blue), 0.25 (orange), 0.125 (grey), and 0.05 (yellow). $E_{1/2}$ = -2.385 V.

Reactivity with $OPPh_3$. Next, we endeavored to separate the dimeric phosphinidiide and arsinidiide complexes of **7**, **8**, and **10** with triphenylphosphine oxide, $OPPh_3$, to prepare the corresponding thorium and uranium arsinidene as well as the uranium phosphinidene. The reaction of **7** with $OPPh_3$, eq 6, exhibited no reaction at room temperature, but upon heating to 70 °C, a color change from dark orange-brown to dark red-brown. The $(C_5Me_5)^{1-}$ resonance shifted from 2.21 ppm from **7**, to 2.13 ppm in the ^1H NMR spectrum. Surprisingly, a single resonance in the $^{31}P\{^1H\}$ spectrum at -6 ppm, indicative of free PPh_3 was observed. Indeed, structural characterization showed the product, $[(C_5Me_5)_2Th]_2(\mu_2\text{-AsMes})(\mu_2\text{-O})$, **11**, an arsinidiide, oxo bridged dimer, Figure 3-8. We note that the presumed byproduct, MesAs=AsMes, has not been reported.

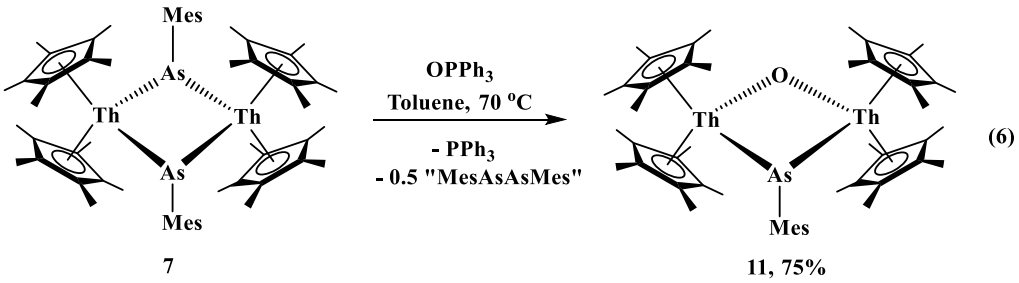

7 **11, 75%** (6)

This use of $OPPh_3$ as an oxo-delivering agent is rare with f elements. Even Sm(II) and U(III) complexes, known for their reductive chemistry,[87] typically only coordinate $OPPh_3$[88-89] due to the P-O bond strength. For this reason, the conversion of $OPPh_3$ to PPh_3 is rare,[90] and has been recently done electrochemically.[91-93] The formation of **11** demonstrates the tremendous electronic unsaturation and oxophilicity of thorium in **7**. Since the oxo and arsinidiide are quite different in electronegativity and ionic radii, the Th-E-Th bond angles differ significantly with a Th-O-Th angle of 132.0(3)°, and Th-As-Th angle of 85.94(3)°. The Th-O bond distances of 2.146(5) and 2.151(5) Å are similar to $[(C_5H_2{}^tBu_3)_2Th(\mu_2\text{-}O)]_2$ which has average Th-O bond lengths of 2.179(2) Å.[94] The Th-As bond distances of 2.8733(10) and 2.8850(10) Å are very similar to the 2.8787(6) Å in the parent arsinidiide, **7**.

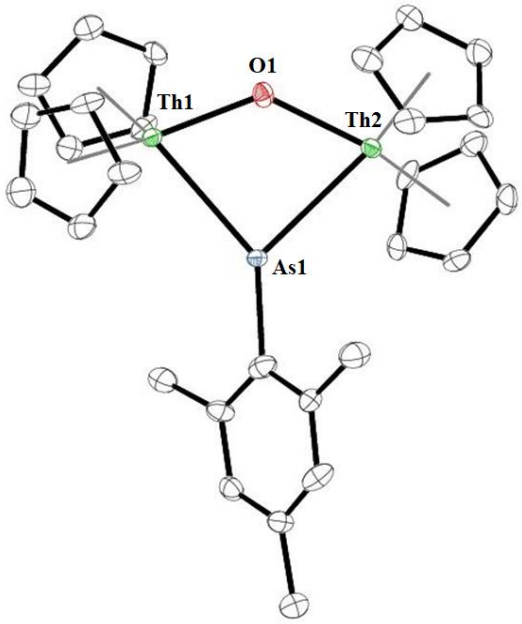

Figure 3-8. Thermal ellipsoid plot of **11,** shown at the 50% probability level. All hydrogens in the structure, and methyl groups on the $(C_5Me_5)^{-1}$ ligands, have been omitted for clarity. Pertinent bond lengths and angles are as follows: Th1-As1, 2.8733(10) Å; Th2-As1, 2.8850(10); Th1-O1, 2.146(5) Å; Th2-O1, 2.151(5) Å; Th1-As1-Th2, 85.94(3)°; Th1-O1-Th2, 132.0(3)°.

The reaction of **8** with $OPPh_3$ was attempted to form the corresponding terminal uranium arsinidene, eq 7, resulted in a black solution. The ^{31}P NMR spectrum of the product shows only a single singlet resonance at 86.97 ppm. The oily nature hampered characterization, and while the purity and yield are questionable, a small number of black crystals suitable for X-ray crystallography were isolated only once. The structure was identified via X-ray crystallography to be $[(C_5Me_5)_2U(\eta^2\text{-}As_2Mes_2)][(C_5Me_5)_2U(OPPh_3)_2]$, **12**. We note that a related product, $[(C_5H_3{}^tBu_2)_2U(OPMe_3)_2][C_5H_3{}^tBu_2]$, was recently reported in low yield from the reduction of U(IV) with KPHMes*, Mes* = 2,4,6-$^tBu_3C_6H_2$.[34]

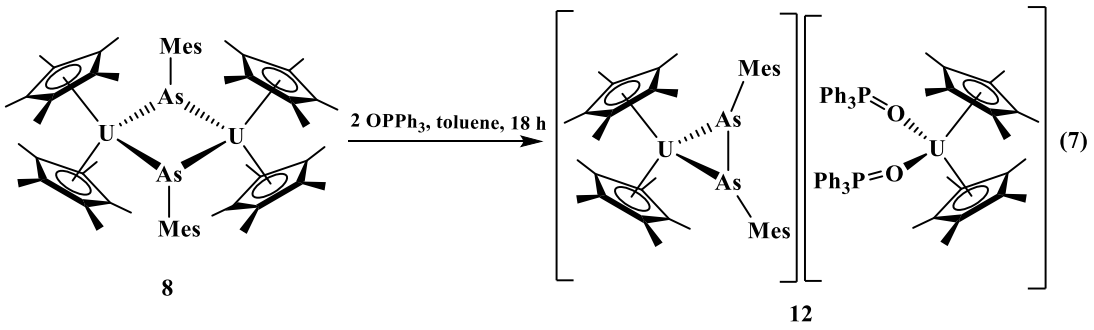

8 12

Based on charge balance, **12** is a cation-anion pair of two U(III) complexes with the anion consisting of two $(C_5Me_5)^{1-}$ and one $(MesAsAsMes)^{2-}$ ligands, while the cation has two $(C_5Me_5)^{1-}$ and two neutral $OPPh_3$ ligands. The U-As bond distances in **12** are 2.9757(8) and 2.9814(8) Å, which are longer than the 2.9231(9) and 2.8994(7) Å in **4**, indicating that **12** contains more reduced metal center than **4**. The only other U(III)-As bonds, with distances of 2.895(4) and 2.923(4) Å are in the mixed-valence complex, $[U(TrenTIPS)_2(\mu\text{-}\eta^2\text{-}(OAs):\eta^2\text{-}(CAs)\text{-}OCAs]^{1-}$.[53] The U-O distances of 2.361(4) and 2.359(3) Å in **12** are similar compared to those in $[(C_5H_3{}^tBu_2)_2U(OPMe_3)_2][C_5{}^tBu_2H_3]$ of 2.331(5) and 2.348(5) Å.

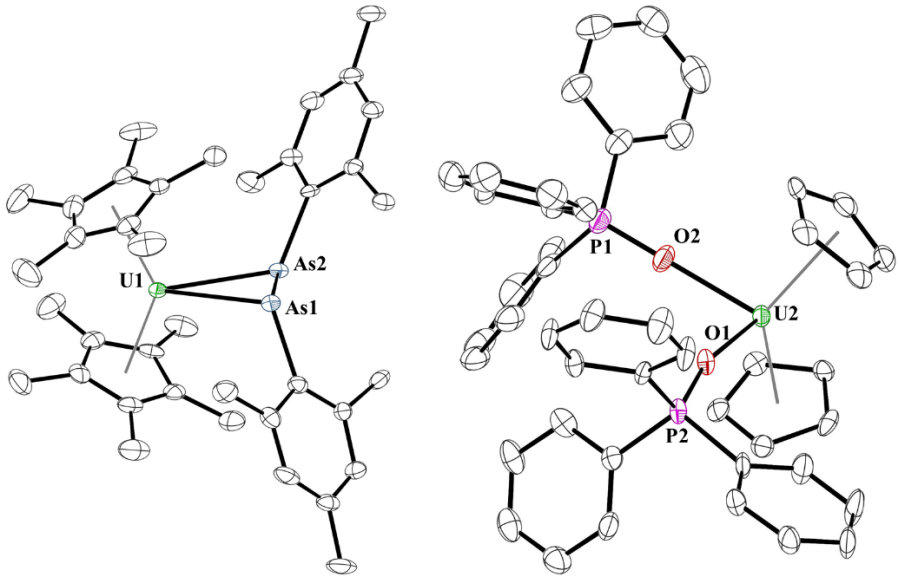

Figure 3-9. Thermal ellipsoid plot of **12** shown at the 50% probability level. All hydrogens and the methyl groups on the $(C_5Me_5)^{1-}$ ligands on the cationic complex have been omitted for clarity. Pertinent bond distances and angles are as follows: U1-As1, 2.9813(6) Å; U1-As2, 2.9756(6) Å; As1-As2, 2.4671(8) Å; U2-O1, 2.361(4) Å; U2-O2, 2.359(3) Å.

Reaction of **10** with $OPPh_3$ takes place slowly over time as monitored by ^1H and ^{31}P NMR spectroscopy, eq 8. Finally, after 45 hours, the reaction was complete during which time the color changed from black to red-brown. One resonance in the ^{31}P NMR spectrum at 12.56 ppm, which was attributed to the $OPPh_3$ coordinating to the uranium center in $(C_5Me_5)_2U(=PMes)(OPPh_3)$, **13**. Crystals suitable for X-ray crystallographic analysis were grown from a saturated diethyl ether solution at -40 °C, Figure 3-10.

Complex **13** is nearly identical to the first uranium phosphinidene isolated, $(C_5Me_5)_2U(=PMes^*)(OPMe_3)$, Mes* = 2,4,6-$^tBu_3C_6H_2$, which has a U-P bond distance of 2.562(3) Å and U-P-C(ipso) angle of 143.7(3)°, while the U-P and U-P-C(ipso) in **9** is 2.502(2) Å and 156.8(2)°, respectively. In addition, these metrics can be compared to

three recent metallocene uranium phosphinidene complexes, $(C_5H_2{}^tBu_3)_2U$=PMes* with U-P length of 2.495(1) Å, and U-P-C(*ipso*) angle of 177.4(1)°,[34] and $(C_5H_3{}^tBu_2)_2U$(=PMes*)($OPMe_3$) with U-P bond distance of 2.508(1) Å and U-P-C(*ipso*) angle of 162.8(1)°.[34]

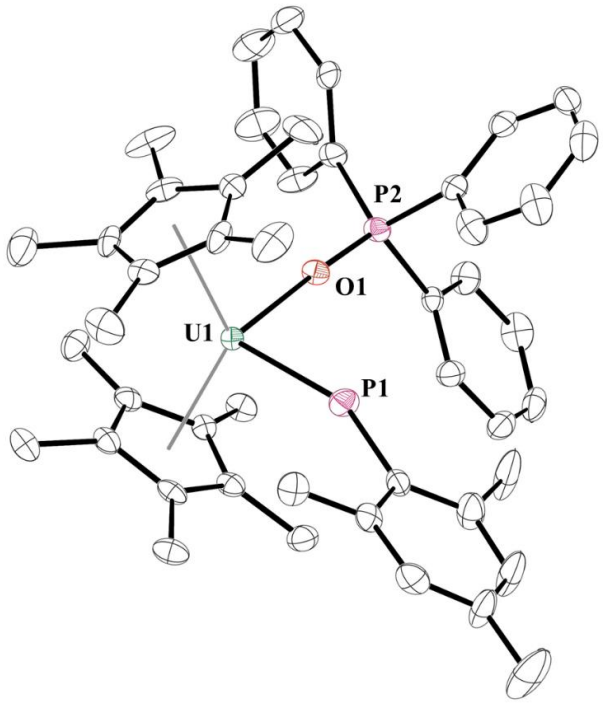

Figure 3-10. Thermal ellipsoid plot of **13** shown at the 50% probability level. The hydrogen atoms have been omitted for clarity. Pertinent bond distances are angles are as follows: U1-P1, 2.5022(18) Å; U1-O1, 2.364(4) Å; U-P1-C(ipso): 156.8(2)°.

Complex **13** was also analyzed by QTAIM analysis. The bond ellipticity, ε, is an indicator of multiple bond character, measuring the deviation from cylindrical symmetry of a bond. For a single or triple bond, ε should be close to zero, whereas for a double bond, deviations are substantial. All complexes considered here show deviations larger than would be expected for a single bond, however this is most pronounced in **13**, which might be expected to have more developed multiple bond character. To further

investigate potential multiple bond character, NBO analysis was performed. Qualitative analysis of the phosphinidene complexes revealed a single M-E σ-bond, as well as two well-defined NBOs representing M-E π-bonding interactions, Figure 3-11. The delocalization index for **13** is 1.345, which can be compared to both the calculated thorium analog of 1.19, as well as our previously reported thorium phosphinidene, $\{(C_5Me_5)_2Th(=PTrip)[P(H)Trip]\}^{1-}$, which also has a DI of 1.19.[21]

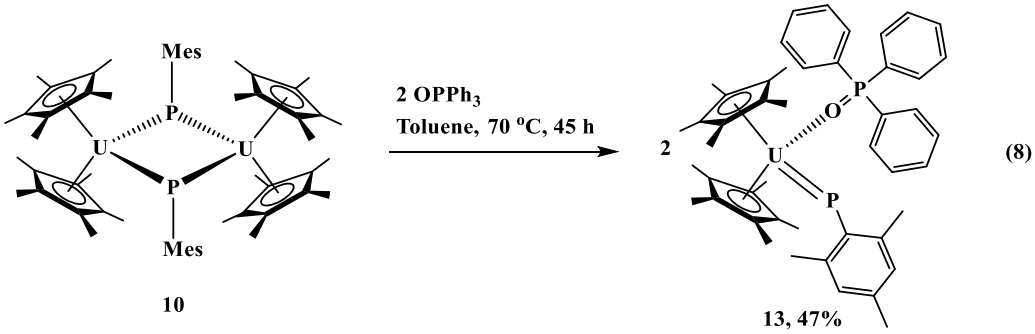

(8)

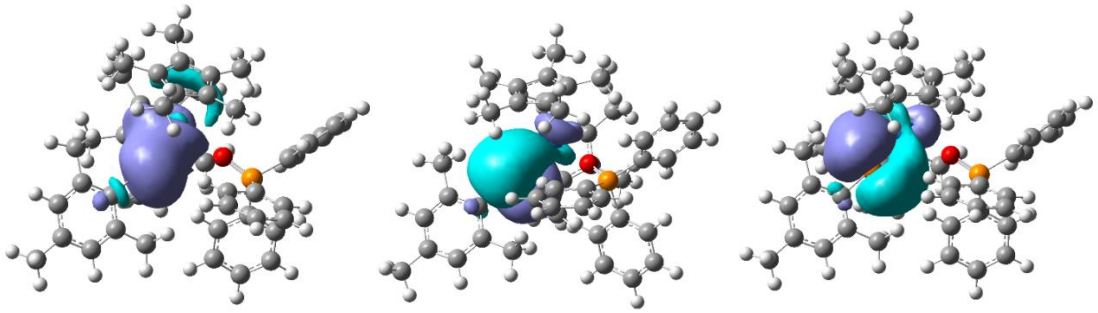

Figure 3-11. Uranium-phosphorus σ-bond (left) and two π-bonds (middle and right), derived from NBO analysis.

CONCLUSION.

The investigation of the structure, bonding, and reactivity of primary phosphine and arsine, H_2EMes, has been conducted with thorium and uranium complexes. Differences in thermal stability are observed for not only the phosphido and arsenido complexes, but also between thorium and uranium. Computational methods, in tandem with electrochemical measurements, demonstrate that these are highly polarized, thus the electronegativity of phosphorus and arsenic drive their donating properties, which are nearly identical. Computational analysis also suggests that there is greater overlap-driven covalency in An-P bonds, and greater energy degeneracy-driven covalency in An-As bonds.[95] However, all of these complexes indicate that the energy-driven covalency concept does not have any effect on stability or reactivity, and the electronegativity of the ligands drives their overall chemistry.

FUTURE WORK.

Future work will include extension of the aforementioned chemistry to the preparation of Sb analogs. Similar analysis of the structural characteristics, stability, and reactivity of such Sb complexes would provide an even more complete trend that would yield more information regarding the interplay of overlap and energy-degeneracy driven

covalency, in that the chemistry should still be driven primarily by the ionic character of the An-Sb bonds. However, the An-Sb bonds should exhibit even greater covalent character than those of the arsenido complexes, so the increased degree of covalent character may lead to divergent characteristics and reactivity.

A wider range of Lewis bases could be reacted with phosphinidiide and arsinidiide complexes, **7** and **10**, in an attempt to generate stable, terminal arsinidenes. No such neutral arsinidenes stable at room temperature have been reported, likely due to the poor orbital overlap of the arsinidene moiety with An-centers. Although reduction of U(IV) centers will likely occur for **10**, complex **7** may yield s terminal arsinidene if it is reacted a suitable Lewis base with a donor atom that is not amenable to abstraction, such as fluoroorgnanic phoshine oxides such as $O=P(C_6F_5)_3$.

Given the wide range of oxidation states readily accessible to U (typically III to VI), reaction of the aforementioned U-complexes with suitable oxidants and reductants could yield U(III), U(V), and potentially U(VI) complexes, which would provide a valuable comparison for bonding characteristics. Reduction of the U-centers by the ligands may occur, but the high stability of the diphosphido and diarsenido ligands may allow for stabilization of U-dipnictido complexes of varying oxidation states. Suitable oxidants could include Ag(L) salts (L = OTf^-, BPh_4^-, PF_6^-, SbF_6^-), CuI, $CuPF_6^-$, and KC_8-/Cryptand-222.

REFERENCES.

1. Xu, L.; Pu, N.; Li, Y.; Wei, P.; Sun, T.; Xiao, C.; Chen, J.; Xu, C., Selective Separation and Complexation of Trivalent Actinide and Lanthanide by a Tetradentate Soft–Hard Donor Ligand: Solvent Extraction, Spectroscopy, and DFT Calculations. *Inorg. Chem.* **2019**, *58*, 4420-4430.

2. Lehman-Andino, I.; Su, J.; Papathanasiou, K. E.; Eaton, T. M.; Jian, J.; Dan, D.; Albrecht-Schmitt, T. E.; Dares, C. J.; Batista, E. R.; Yang, P.; Gibson, J. K.; Kavallieratos, K., Soft-donor dipicolinamide derivatives for selective actinide(III)/lanthanide(III) separation: the role of S- vs. O-donor sites. *Chem. Commun.* **2019**, *55*, 2441-2444.

3. Grimes, T. S.; Heathman, C. R.; Jansone-Popova, S.; Ivanov, A. S.; Bryantsev, V. S.; Zalupski, P. R., Exploring Soft Donor Character of the N-2-Pyrazinylmethyl Group by Coordinating Trivalent Actinides and Lanthanides Using Aminopolycarboxylates. *Inorg. Chem.* **2019**, 59, 138-150.

4. Behrle, A. C.; Barnes, C. L.; Kaltsoyannis, N.; Walensky, J. R., Systematic Investigation of Thorium(IV)– and Uranium(IV)–Ligand Bonding in Dithiophosphonate, Thioselenophosphinate, and Diselenophosphonate Complexes. *Inorg. Chem.* **2013**, *52*, 10623-10631.

5. Street, K.; Seaborg, G. T., The Separation of Americium and Curium from the Rare Earth Elements. *J. Am. Chem. Soc.* **1950**, *72*, 2790-2792.

6. Diamond, R. M.; Street, K.; Seaborg, G. T., An Ion-exchange Study of Possible Hybridized 5f Bonding in the Actinides1. *J. Am. Chem. Soc.* **1954**, *76*, 1461-1469.

7. Gaunt, A. J.; Reilly, S. D.; Enriquez, A. E.; Scott, B. L.; Ibers, J. A.; Sekar, P.; Ingram, K. I. M.; Kaltsoyannis, N.; Neu, M. P., Experimental and Theoretical Comparison

of Actinide and Lanthanide Bonding in $M[N(EPR_2)_2]_3$ Complexes (M = U, Pu, La, Ce; E = S, Se, Te; R = Ph, iPr, H). *Inorg. Chem.* **2008**, *47*, 29-41.

8. Brown, J. L.; Fortier, S.; Lewis, R. A.; Wu, G.; Hayton, T. W., A Complete Family of Terminal Uranium Chalcogenides, $[U(E)(N\{SiMe_3\}_2)_3]^-$ (E = O, S, Se, Te). *J. Am. Chem. Soc.* **2012**, *134*, 15468-15475.

9. Brown, J. L.; Fortier, S.; Wu, G.; Kaltsoyannis, N.; Hayton, T. W., Synthesis and Spectroscopic and Computational Characterization of the Chalcogenido-Substituted Analogues of the Uranyl Ion, $[OUE]^{2+}$ (E = S, Se). *J. Am. Chem. Soc.* **2013**, *135*, 5352-5355.

10. Behrle, A. C.; Kerridge, A.; Walensky, J. R., Dithio- and Diselenophosphinate Thorium(IV) and Uranium(IV) Complexes: Molecular and Electronic Structures, Spectroscopy, and Transmetalation Reactivity. *Inorg. Chem.* **2015**, *54*, 11625-11636.

11. Matson, E. M.; Goshert, M. D.; Kiernicki, J. J.; Newell, B. S.; Fanwick, P. E.; Shores, M. P.; Walensky, J. R.; Bart, S. C., Synthesis of Terminal Uranium(IV) Disulfido and Diselenido Compounds by Activation of Elemental Sulfur and Selenium. *Chem. Eur. J.* **2013**, *19*, 16176-16180.

12. Jones, M. B.; Gaunt, A. J.; Gordon, J. C.; Kaltsoyannis, N.; Neu, M. P.; Scott, B. L., Uncovering f-element bonding differences and electronic structure in a series of 1 : 3 and 1 : 4 complexes with a diselenophosphinate ligand. *Chem. Sci.* **2013**, *4*, 1189-1203.

13. Matson, E. M.; Breshears, A. T.; Kiernicki, J. J.; Newell, B. S.; Fanwick, P. E.; Shores, M. P.; Walensky, J. R.; Bart, S. C., Trivalent Uranium Phenylchalcogenide Complexes: Exploring the Bonding and Reactivity with CS_2 in the Tp^*_2UEPh Series (E = O, S, Se, Te). *Inorg. Chem.* **2014**, *53*, 12977-12985.

14. Smiles, D. E.; Wu, G.; Hrobárik, P.; Hayton, T. W., Use of ^{77}Se and ^{125}Te NMR Spectroscopy to Probe Covalency of the Actinide-Chalcogen Bonding in $[Th(En)\{N(SiMe_3)_2\}_3]^-$ (E = Se, Te; n = 1, 2) and Their Oxo-Uranium(VI) Congeners. *J. Am. Chem. Soc.* **2016**, *138*, 814-825.

15. Wu, W.; Rehe, D.; Hrobárik, P.; Kornienko, A. Y.; Emge, T. J.; Brennan, J. G., Molecular Thorium Compounds with Dichalcogenide Ligands: Synthesis, Structure, ^{77}Se NMR Study, and Thermolysis. *Inorg. Chem.* **2018**, *57*, 14821-14833.

16. Ringgold, M.; Rehe, D.; Hrobárik, P.; Kornienko, A. Y.; Emge, T. J.; Brennan, J. G., Thorium Cubanes–Synthesis, Solid-State and Solution Structures, Thermolysis, and Chalcogen Exchange Reactions. *Inorg. Chem.* **2018**, *57*, 7129-7141.

17. Rookes, T. M.; Wildman, E. P.; Balázs, G.; Gardner, B. M.; Wooles, A. J.; Gregson, M.; Tuna, F.; Scheer, M.; Liddle, S. T., Actinide–Pnictide (An−Pn) Bonds Spanning Non-Metal, Metalloid, and Metal Combinations (An=U, Th; Pn=P, As, Sb, Bi). *Angew. Chem. Int. Ed.* **2018**, *57*, 1332-1336.

18. Gardner, B. M.; Balázs, G.; Scheer, M.; Tuna, F.; McInnes, E. J. L.; McMaster, J.; Lewis, W.; Blake, A. J.; Liddle, S. T., Triamidoamine uranium(IV)–arsenic complexes containing one-, two- and threefold U–As bonding interactions. *Nat. Chem.* **2015**, *7*, 582.

19. Gardner, B. M.; Balázs, G.; Scheer, M.; Wooles, A. J.; Tuna, F.; McInnes, E. J. L.; McMaster, J.; Lewis, W.; Blake, A. J.; Liddle, S. T., Isolation of Elusive HAsAsH in a Crystalline Diuranium(IV) Complex. *Angew. Chem. Int. Ed.* **2015**, *54*, 15250-15254.

20. Behrle, A. C.; Walensky, J. R., Insertion of tBuNC into thorium–phosphorus and thorium–arsenic bonds: phosphaazaallene and arsaazaallene moieties in f element chemistry. *Dalton Trans.* **2016**, *45*, 10042-10049.

21. Vilanova, S. P.; Alayoglu, P.; Heidarian, M.; Huang, P.; Walensky, J. R., Metal–Ligand Multiple Bonding in Thorium Phosphorus and Thorium Arsenic Complexes. *Chem. Eur J.* **2017**, *23*, 16748-16752.

22. Wildman, E. P.; Balázs, G.; Wooles, A. J.; Scheer, M.; Liddle, S. T., Triamidoamine thorium-arsenic complexes with parent arsenide, arsinidiide and arsenido structural motifs. *Nat. Commun.* **2017**, *8*, 14769.

23. Hoerger, C. J.; Heinemann, F. W.; Louyriac, E.; Rigo, M.; Maron, L.; Grützmacher, H.; Driess, M.; Meyer, K., Cyaarside (CAs^-) and 1,3-Diarsaallendiide ($AsCAs^{2-}$) Ligands Coordinated to Uranium and Generated via Activation of the Arsaethynolate Ligand ($OCAs^-$). *Angew. Chem. Int. Ed. Engl.* **2019**, *58*, 1679-1683.

24. Andrews, L.; Wang, X.; Roos, B. O., As≡UF_3 Molecule with a Weak Triple Bond to Uranium. *Inorg. Chem.* **2009**, *48*, 6594-6598.

25. Rozenel, S. S.; Edwards, P. G.; Petrie, M. A.; Andersen, R. A., Eight coordinate 1,2-bis(dimethylarsino) and 1,2-bis(dimethylphosphino)-benzene complexes of uranium tetrachloride, $UCl_4[(1,2\text{-}Me_2E)_2C_6H_4]_2$ where E is As or P. *Polyhedron* **2016**, *116*, 122-126.

26. Scherer, O. J.; Schulze, J.; Wolmershäuser, G., Bicyclisches As6 als komplexligand. *J. Organomet. Chem.* **1994**, *484*, c5-c7.

27. Actinides: Pnictogen Complexes. In *Encyclopedia of Inorganic and Bioinorganic Chemistry*, pp 1-17.

28. Zhang, C.; Hou, G.; Zi, G.; Walter, M. D., A base-free terminal thorium phosphinidene metallocene and its reactivity toward selected organic molecules. *Dalton Trans.* **2019**, *48*, 2377-2387.

29. Scherer, O. J.; Werner, B.; Heckmann, G.; Wolmershäuser, G., Bicyclic P_6 as Complex Ligand. *Angew. Chem. Int. Ed. Engl* **1991**, *30*, 553-555.

30. Zhang, C.; Wang, Y.; Hou, G.; Ding, W.; Zi, G.; Walter, M. D., Experimental and computational studies on a three-membered diphosphido thorium metallaheterocycle [η^5-1,3-$(Me_3C)_2C_5H_3]_2$Th[η^2-P_2(2,4,6-$^i Pr_3C_6H_2)_2$]. *Dalton Trans.* **2019,** *48* (20), 6921-6930.

31. Behrle, A. C.; Castro, L.; Maron, L.; Walensky, J. R., Formation of a Bridging Phosphinidene Thorium Complex. *J. Am. Chem. Soc.* **2015**, *137*, 14846-14849.

32. Arney, D. S. J.; Schnabel, R. C.; Scott, B. C.; Burns, C. J., Preparation of Actinide Phosphinidene Complexes: Steric Control of Reactivity. *J. Am. Chem. Soc.* **1996**, *118*, 6780-6781.

33. Zhang, C.; Hou, G.; Zi, G.; Ding, W.; Walter, M. D., A Base-Free Terminal Actinide Phosphinidene Metallocene: Synthesis, Structure, Reactivity, and Computational Studies. *J. Am. Chem. Soc.* **2018**, *140*, 14511-14525.

34. Wang, D.; Wang, S.; Hou, G.; Zi, G.; Walter, M. D., A Lewis Base Supported Terminal Uranium Phosphinidene Metallocene. *Inorg. Chem.* **2020**, *59*, 14549-14563.

35. Wang, D.; Hou, G.; Zi, G.; Walter, M. D., (η^5-$C_5Me_5)_2$U(=P-2,4,6-$^t Bu_3C_6H_2$)($OPMe_3$) Revisited—Its Intrinsic Reactivity toward Small Organic Molecules. *Organometallics* **2020**, *39*, 4085-4101.

36. Wang, D.; Hou, G.; Zi, G.; Walter, M. D., Influence of the Lewis Base Ph_3PO on the Reactivity of the Uranium Phosphinidene (η^5-$C_5Me_5)_2$U(═P-2,4,6-$^i Pr_3C_6H_2$)($OPPh_3$). *Organometallics* **2021**, 40, 383-396.

37. Wang, D.; Ding, W.; Hou, G.; Zi, G.; Walter, M. D., Experimental and Computational Studies on a Base-Free Terminal Uranium Phosphinidene Metallocene. *Chem. Eur. J.* **2020**, *26*, 16888-16899.

38. Pagano, J. K.; Dorhout, J. M.; Waterman, R.; Czerwinski, K. R.; Kiplinger, J. L., Phenylsilane as a safe, versatile alternative to hydrogen for the synthesis of actinide hydrides. *Chem. Commun.* **2015**, *51*, 17379-17381.

39. Pugh, T.; Kerridge, A.; Layfield, R. A., Yttrium Complexes of Arsine, Arsenide, and Arsinidene Ligands. *Angew. Chem. Int. Ed.* **2015**, *54*, 4255-4258.

40. Adamo, C.; Barone, V., Toward reliable density functional methods without adjustable parameters: The PBE0 model. *J. Chem. Phys.* **1999**, *110*, 6158-6170.

41. Ernzerhof, M.; Scuseria, G. E., Assessment of the Perdew–Burke–Ernzerhof exchange-correlation functional. *J. Chem. Phys.* **1999**, *110*, 5029-5036.

42. Weigend, F.; Ahlrichs, R., Balanced basis sets of split valence, triple zeta valence and quadruple zeta valence quality for H to Rn: Design and assessment of accuracy. *Phys. Chem. Chem. Phys.* **2005**, *7*, 3297-3305.

43. Cao, X.; Dolg, M.; Stoll, H., Valence basis sets for relativistic energy-consistent small-core actinide pseudopotentials. *J. Chem. Phys.* **2003**, *118*, 487-496.

44. Cao, X.; Dolg, M., Segmented contraction scheme for small-core actinide pseudopotential basis sets. *Comp. Theor. Chem.* **2004**, *673*, 203-209.

45. Küchle, W.; Dolg, M.; Stoll, H.; Preuss, H., Energy-adjusted pseudopotentials for the actinides. Parameter sets and test calculations for thorium and thorium monoxide. *J. Chem. Phys.* **1994**, *100*, 7535-7542.

46. Balasubramani, S. G.; Chen, G. P.; Coriani, S.; Diedenhofen, M.; Frank, M. S.; Franzke, Y. J.; Furche, F.; Grotjahn, R.; Harding, M. E.; Hättig, C.; Hellweg, A.; Helmich-Paris, B.; Holzer, C.; Huniar, U.; Kaupp, M.; Khah, A. M.; Khani, S. K.; Müller, T.; Mack, F.; Nguyen, B. D.; Parker, S. M.; Perlt, E.; Rappoport, D.; Reiter, K.; Roy, S.; Rückert, M.; Schmitz, G.; Sierka, M.; Tapavicza, E.; Tew, D. P.; Wüllen, C. v.; Voora, V. K.; Weigend, F.; Wodyński, A.; Yu, J. M., TURBOMOLE: Modular program suite for ab initio quantum-chemical and condensed-matter simulations. *J. Chem. Phys.* **2020**, *152*, 184107.

47. E. D. Glendening, J. K. B., A. E. Reed, J. E. Carpenter, J. A. Bohmann, C. M. Morales, C. R. Landis, and F. Weinhold (Theoretical Chemistry Institute, University of Wisconsin, Madison, WI, 2013); http://nbo6.chem.wisc.edu/.

48. R. Denningto, T. A. K. a. J. M. M., GaussView V5.0, Semichem Inc. Shawnee Mission KS, 2009.

49. T. A. Keith, A. V. T. G. S., Overland Park KS, USA, 2019.

50. APEX3 Suite, M., WI, 2016.

51. Sheldrick, G., Crystal structure refinement with SHELXL. *Acta Crystallographica Section C* **2015,** *71* (1), 3-8.

52. Dolomanov, O. V.; Bourhis, L. J.; Gildea, R. J.; Howard, J. A. K.; Puschmann, H., OLEX2: a complete structure solution, refinement and analysis program. *J. of Appl. Crystallogr.* **2009**, *42*, 339-341.

53. Magnall, R.; Balázs, G.; Lu, E.; Kern, M.; van Slageren, J.; Tuna, F.; Wooles, A. J.; Scheer, M.; Liddle, S. T., Photolytic and Reductive Activations of 2-Arsaethynolate in a Uranium–Triamidoamine Complex: Decarbonylative Arsenic-Group Transfer Reactions and Trapping of a Highly Bent and Reduced Form. *Chem. Eur. J.* **2019**, *25*, 14246-14252.

54. Bugaris, D. E.; Ibers, J. A., Syntheses and characterization of some solid-state actinide (Th, U, Np) compounds. *Dalton Trans.* **2010**, *39*, 5949-5964.

55. Elmes, P. S.; Leverett, P.; West, B. O., X-Ray determination of the structure of $Fe(CO)_4(AsC_6F_5)_2$, a complex containing "decafluoro-arsenobenzene". *J. Chem. Soc., Chem. Commun.* **1971**, 747b-748.

56. Schmidt, M.; Konieczny, D.; Peresypkina, E. V.; Virovets, A. V.; Balázs, G.; Bodensteiner, M.; Riedlberger, F.; Krauss, H.; Scheer, M., Arsenic-Rich Polyarsenides Stabilized by Cp*Fe Fragments. *Angew. Chem. Int. Ed.* **2017**, *56*, 7307-7311.

57. Spitzer, F.; Sierka, M.; Latronico, M.; Mastrorilli, P.; Virovets, A. V.; Scheer, M., Fixation and Release of Intact E4 Tetrahedra (E=P, As). *Angew. Chem. Int. Ed. Engl.* **2015**, *54*, 4392-4396.

58. Arleth, N.; Gamer, M. T.; Köppe, R.; Konchenko, S. N.; Fleischmann, M.; Scheer, M.; Roesky, P. W., Molecular Polyarsenides of the Rare-Earth Elements. *Angew. Chem. Int. Ed. Engl.* **2016**, *54*, 1557-1560.

59. Dütsch, L.; Fleischmann, M.; Welsch, S.; Balázs, G.; Kremer, W.; Scheer, M., Dicationic E_4 Chains (E=P, As, Sb, Bi) Embedded in the Coordination Sphere of Transition Metals. *Angew. Chem. Int. Ed. Engl.* **2018**, *57*, 3256-3261.

60. Hierlmeier, G.; Hinz, A.; Wolf, R.; Goicoechea, J. M., Synthesis and Reactivity of Nickel-Stabilised μ^2:η^2,η^2-P_2, As_2 and PAs Units. *Angew. Chem. Int. Ed. Engl.* **2018**, *57*, 431-436.

61. Blacque, O.; Brunner, H.; M. Kubicki, M.; Leis, F.; Lucas, D.; Mugnier, Y.; Nuber, B.; Wachter, J., Structural Rearrangements in Triple-Decker-Like Complexes with Mixed

Group 15/16 Ligands: Synthesis and Characterization of the Redox Couple $[Cp^*_2Fe_2As_2Se_2]/[Cp^*_2Fe_2As_2Se_2]^+$ ($Cp^*=C_5Me_5$). *Chem. Eur. J.* **2001**, *7*, 1342-1349.

62. McGrath, M.; Spalding, T. R.; Fontaine, X. L. R.; Kennedy, J. D.; Thornton-Pett, M., Metallaheteroborane chemistry. Part 9. Syntheses and spectroscopy of platinum and palladium phosphine complexes containing η^5-{As_2B_9}-based cluster ligands. Crystal structures of [3,3-L2-closo-3,1,2-$PtAs_2B_9H_9$](L = PPh_3 or PMe_2Ph) and [3-Cl-3,8-$(PPh_3)_2$-closo-3,1,2-$PdAs_2B_9H_8$]. *J. Chem. Soc., Dalton Trans.* **1991**, 3223-3233.

63. McLellan, R.; Boag, N. M.; Dodds, K.; Ellis, D.; Macgregor, S. A.; McKay, D.; Masters, S. L.; Noble-Eddy, R.; Platt, N. P.; Rankin, D. W. H.; Robertson, H. E.; Rosair, G. M.; Welch, A. J., New chemistry of 1,2-closo-$P_2B_{10}H_{10}$ and 1,2-closo-$As_2B_{10}H_{10}$; in silico and gas electron diffraction structures, and new metalladiphospha- and metalladiarsaboranes. *Dalton Trans.* **2011**, *40*, 7181-7192.

64. Ferguson, G.; Gallagher, J. F.; Kennedy, J. D.; Kelleher, A.-M.; Spalding, T. R., Pentahapto-bonded gold heteroborane clusters [3-(R_3P)-closo-2,1-$AuTeB_{10}H_{10}]^-$ and [3-(R_3P)-closo-3,1,2-$AuAs_2B_9H_9]^-$. *Dalton Trans.* **2006**, 2133-2139.

65. O'Connell, D.; Patterson, J. C.; Spalding, T. R.; Ferguson, G.; Gallagher, J. F.; Li, Y.; Kennedy, J. D.; Macías, R.; Thornton-Pett, M.; Holub, J., Conformational polymorphism and fluxional behaviour of $M(PR_3)_2$ units in closo-twelve-atom metallaheteroboranes with MX_2B_9(X = C or As) and MZB_{10} cages (Z = S, Se or Te). *J. Chem. Soc., Dalton Trans.* **1996**, 3323-3333.

66. Jasper, S. A.; Roach, S.; Stipp, J. N.; Huffman, J. C.; Todd, L. J., The synthesis and chemistry of icosahedral bis(phosphine)metalladiarsaboranes and -distibaboranes containing nickel and palladium. Crystal and molecular structures of closo-1,1-$(Me_2PPh)_2$-

1,2,3-$PdAs_2B_9H_9$, closo-1,6-Cl_2-1,5-$(Me_2PPh)^{2-}$1,2,3-$PdAs_2B_9H_7CH_2Cl_2$, and closo-1,1-$(Me_2PPh)^{2-}$1,2,3-$PdSb_2B_9H_9$. *Inorg. Chem.* **1993**, *32*, 3072-3080.

67. Ferguson, G.; Li, Y.; Spalding, T. R.; Patterson, J. C., (3-tert-Butyl isocyanide)-3,8-bis(dimethylphenylphosphine)octahydro-1,2-diarsa-3-pallada-closo-dodecaboron(1+) Hexafluoroantimonate. *Acta Crystallogr. C.* **1995**, *51*, 1498-1500.

68. Chen, H.; Olmstead, M. M.; Pestana, D. C.; Power, P. P., Reactions of low-coordinate transition-metal amides with secondary phosphanes and arsanes: synthesis, structural, and spectroscopic studies of $[M\{N(SiMe_3)_2\}(\mu\text{-}PMes_2)]_2$ (M = manganese, iron), $[Mn\{N(SiMe_3)_2\}\ \mu\text{-}AsMes_2)]_2$ and $Mes_2AsAsMes_2$. *Inorg. Chem.* **1991**, *30*, 1783-1787.

69. Schumann, A.; Bresien, J.; Fischer, M.; Hering-Junghans, C., Aryl-substituted triarsiranes: synthesis and reactivity. *Chem. Commun.* **2021**, 1014-1017.

70. Brookhart, M.; Green, M. L. H.; Parkin, G., Agostic interactions in transition metal compounds. *Proc. Natl. Acad. Sci. U.S.A.* **2007**, *104*, 6908-6914.

71. Kurz, S.; Oesen, H.; Sieler, J.; Hey-hawkins, E., Synthesis and Molecular Structure of Mes(H)P-P(H)Mes (Mes = 2,4,6-$Me_3C_6H_2$). *Phosphorus Sulfure* **1996**, *117*, 189-196.

72. Watt, F. A.; McCabe, K. N.; Schoch, R.; Maron, L.; Hohloch, S., A transient lanthanum phosphinidene complex. *Chem. Commun.* **2020**, *56*, 15410-15413.

73. Vilanova, S. P.; Tarlton, M. L.; Barnes, C. L.; Walensky, J. R., Double insertion of benzophenone into thorium-phosphorus bonds. *J. Org. Chem.* **2018**, *857*, 159-163.

74. Hou, Z.; Breen, T. L.; Stephan, D. W., Formation and reactivity of the early metal phosphides and phosphinidenes $Cp^*_2Zr{:}PR$, $Cp^*_2Zr(PR)_2$, and $Cp^*_2Zr(PR)_3$. *Organometallics* **1993**, *12*, 3158-3167.

75. Schumann, A.; Reiß, F.; Jiao, H.; Rabeah, J.; Siewert, J.-E.; Krummenacher, I.; Braunschweig, H.; Hering-Junghans, C., A selective route to aryl-triphosphiranes and their titanocene-induced fragmentation. *Chem. Sci.* **2019**, *10*, 7859-7867.

76. Gardner, B. M.; Balázs, G.; Scheer, M.; Tuna, F.; McInnes, E. J. L.; McMaster, J.; Lewis, W.; Blake, A. J.; Liddle, S. T., Triamidoamine–Uranium(IV)-Stabilized Terminal Parent Phosphide and Phosphinidene Complexes. *Angew. Chem. Int. Ed. Engl.* **2014**, *53*, 4484-4488.

77. Tarlton, M. L.; Del Rosal, I.; Vilanova, S. P.; Kelley, S. P.; Maron, L.; Walensky, J. R., Comparative Insertion Reactivity of CO, CO_2, ^{t}BuCN, and ^{t}BuNC into Thorium– and Uranium–Phosphorus Bonds. *Organometallics* **2020**, *39*, 2152-2161.

78. Leszczynski, J.; Kwiatkowski, J. S.; Leszczynska, D., Is the structure of selenoformamide similar to those of formamide and thioformamide? *J. Am. Chem. Soc.* **1992**, *114*, 10089-10091.

79. Hall, S. W.; Huffman, J. C.; Miller, M. M.; Avens, L. R.; Burns, C. J.; Sattelberger, A. P.; Arney, D. S. J.; England, A. F., Synthesis and characterization of bis(pentamethylcyclopentadienyl)uranium(IV) and -thorium(IV) compounds containing the bis(trimethylsilyl)phosphide ligand. *Organometallics* **1993**, *12*, 752-758.

80. Rungthanaphatsophon, P.; Duignan, T. J.; Myers, A. J.; Vilanova, S. P.; Barnes, C. L.; Autschbach, J.; Batista, E. R.; Yang, P.; Walensky, J. R., Influence of Substituents on the Electronic Structure of Mono- and Bis(phosphido) Thorium(IV) Complexes. *Inorg. Chem.* **2018,** *57*, 7270-7278.

81. Rungthanaphatsophon, P.; Rosal, I. d.; Ward, R. J.; Vilanova, S. P.; Kelley, S. P.; Maron, L.; Walensky, J. R., Formation of an α-Diimine from Isocyanide Coupling Using

Thorium(IV) and Uranium(IV) Phosphido–Methyl Complexes. *Organometallics* **2019**, *38*, 1733-1740.

82. Duttera, M. R.; Day, V. W.; Marks, T. J., Organoactinide phosphine/phosphite coordination chemistry. Facile hydride-induced dealkoxylation and the formation of actinide phosphinidene complexes. *J. Am. Chem. Soc.* **1984**, *106*, 2907-2912.

83. Wildman, E. P.; Balázs, G.; Wooles, A. J.; Scheer, M.; Liddle, S. T., Thorium–phosphorus triamidoamine complexes containing Th–P single- and multiple-bond interactions. *Nat. Commun.* **2016**, *7*, 12884.

84. Morris, D. E.; Da Re, R. E.; Jantunen, K. C.; Castro-Rodriguez, I.; Kiplinger, J. L., Trends in Electronic Structure and Redox Energetics for Early-Actinide Pentamethylcyclopentadienyl Complexes. *Organometallics* **2004**, *23*, 5142-5153.

85. Graves, C. R.; Scott, B. L.; Morris, D. E.; Kiplinger, J. L., Facile Access to Pentavalent Uranium Organometallics: One-Electron Oxidation of Uranium(IV) Imido Complexes with Copper(I) Salts. *J. Am. Chem. Soc.* **2007**, *129*, 11914-11915.

86. Pauling, L., The Nature of The Chemical Bond. *Cornell University Press* **1961**.

87. Tatebe, C. J.; Tong, Z.; Kiernicki, J. J.; Coughlin, E. J.; Zeller, M.; Bart, S. C., Activation of Triphenylphosphine Oxide Mediated by Trivalent Organouranium Species. *Organometallics* **2018**, *37*, 934-940.

88. Evans, W. J.; Grate, J. W.; Bloom, I.; Hunter, W. E.; Atwood, J. L., Synthesis and x-ray crystallographic characterization of an oxo-bridged bimetallic organosamarium complex, $[(C_5Me_5)_2Sm]_2(\mu\text{-O})$. *J. Am. Chem. Soc.* **1985**, *107*, 405-409.

89. Brennan, J. G.; Andersen, R. A.; Zalkin, A., Chemistry of trivalent uranium metallocenes: electron-transfer reactions. Synthesis and characterization of

[$(MeC_5H_4)_3U]_2E$ (E = S, Se, Te) and the crystal structures of hexakis(methylcyclopentadienyl)sulfidodiuranium and tris(methylcyclopentadienyl)(triphenylphosphine oxide)uranium. *Inorg. Chem.* **1986**, *25*, 1761-1765.

90. Podyacheva, E.; Kuchuk, E.; Chusov, D., Reduction of phosphine oxides to phosphines. *Tet. Lett.* **2019**, *60*, 575-582.

91. Manabe, S.; Wong, C. M.; Sevov, C. S., Direct and Scalable Electroreduction of Triphenylphosphine Oxide to Triphenylphosphine. *J. Am. Chem. Soc.* **2020**, *142*, 3024-3031.

92. Chakraborty, B.; Menezes, P. W.; Driess, M., Beyond CO_2 Reduction: Vistas on Electrochemical Reduction of Heavy Non-metal Oxides with Very Strong E—O Bonds (E = Si, P, S). *J. Am. Chem. Soc.* **2020**, *142*, 14772-14788.

93. Elias, J. S.; Costentin, C.; Nocera, D. G., Direct Electrochemical P(V) to P(III) Reduction of Phosphine Oxide Facilitated by Triaryl Borates. *J. Am. Chem. Soc.* **2018**, *140*, 13711-13718.

94. Ren, W.; Zi, G.; Fang, D.-C.; Walter, M. D., Thorium Oxo and Sulfido Metallocenes: Synthesis, Structure, Reactivity, and Computational Studies. *J. Am. Chem. Soc.* **2011**, *133*, 13183-13196.

95. Cooper, S.; Kaltsoyannis, N., Covalency in $AnCl_3$ (An = Th–No). *Dalton Trans.* **2021**, 1478-1485.

Appendix A: Synthesis and Characterization of the First U(IV)-Carbonyl complex, $(C_5Me_5)_2U(\eta^2\text{-}As_2Mes_2)(CO)$

Michael L. Tarlton,[1] Steven P. Kelley,[1] and Justin R. Walensky[1]*

[1] Department of Chemistry, University of Missouri, 601 S. College Avenue, Columbia, MO 65211, United States

ABSTRACT. Reactivity of (C5Me5)2U(η^2-As_2Mes_2) with with ^{t}BuNC, and CO was conducted, leading to the formation of $(C_5Me_5)_2U(\eta^2\text{-}As_2Mes_2)(L)$, is observed, with L = tBuNC and CO. The latter compound is the first characterized U(IV) carbonyl complex. Both $(C_5Me_5)_2U(\eta^2\text{-}As_2Mes_2)(CO)$ and $(C_5Me_5)_2U(\eta^2\text{-}As_2Mes_2)(^{13}CO)$ were prepared, demonstrating a shift in CO stretching frequency , further supporting the proposed structure. The CO ligand sufficiently labile that loss was observed at room temperature when the atmosphere was removed or substituted with N_2, precluding X-ray crystallographic characterization.

INTRODUCTION.

The influence of steric and electronic properties on the ability to control metal complexes cannot be overstated. This can be readily observed throughout the periodic table when sterically unsaturated compounds show higher reactivity towards small molecules. The alternative scenario, when sterically saturated, readily isolable complexes are electronically unsaturated. Our group has previously investigated the reactivity of such substrates by reacting tert-butylnitrile, tert-butylisocyanide, and isoelectronic CO with Th- and U-phosphido complexes.[1-3] The products of which were largely the result of insertion reactions, usually concomitant with elimination of H_2EMes (E = P, As; Mes = 2,4,6-trimethylphenyl) via proton migration. We endeavored to investigate the reactivity

of such unsaturated small molecules In contrast to the ubiquity of metal carbonyl chemistry in the transition block, the inherently poor ability of the f-orbitals to participate in backbonding interactions makes coordination of CO to f-elements rare. The first example was reported by Slater and Sheline in 1971,[4] which entailed the use of matrix-isolation techniques to prepare a series of $U(CO)_n$ species, and similar techniques were employed to prepare lanthanide-carbonyl complexes with Ce.[5] The first molecular f-element CO complex, $(Me_3SiC_5H_4)_3U(CO)$, was reported by Andersen in 1986,[6] in which the lability of the CO led to immediate dissociation under vacuum. Following this, $(C_5Me_4H)_3U(CO)$ was prepared by Parry and coworkers,[7] which exhibited significantly greater stability owing to the more donating C_5Me_4H ligands, enabling solid-state characterization including single crystal X-ray diffraction (U-CO, 2.383(6) Å, ν(CO): 1880 cm^{-1}). Similarly, the Evans' group reported preparation of the pentamethyl analog, $(C_5Me_5)_3U(CO)$[8]. The only known Th-CO complex, $[(C_5Me_5)_3Th(CO)][BPh_4]$ was also isolated using this ligand framework, with a CO stretching frequency of 2131cm^{-1}, near that of free CO at 2143 cm^{-1}.[9] Our group recently reported the synthesis of $(C_5Me_5)_2U(\eta^2\text{-}As_2Mes_2)$ via elimination of H_2 through thermolysis of $(C_5Me_5)_2U[As(H)Mes]_2$ (Mes = 2,4,6-trimethylphenyl), the crystal structure of which exhibits an anagostic interaction between the U(IV) center and the *ortho*-CH_3 group on one of the mesityl rings. Such a feature implies that the ligand environment affords insufficient electron density to the U making for the potential to favorably bind small ligands to the U(IV) center such as CO. Therefore, the resulting adduct could be stable enough to characterize despite the lower electron density hence less ability to backbond of the f^2 system in U(IV) when compared

to the f^3 configuration of U(III). We have undertaken the efforts reported herein, to prepare adducts of $(C_5Me_5)_2U(\eta^2\text{-}As_2Mes_2)$ with CO, and it's analogs ^{t}BuCN and ^{t}BuNC.

EXPERIMENTAL.

General Considerations. All reactions were performed under an inert atmosphere of dry N_2 inside of a glovebox. The previously reported Th- and U-diarsenido complexes $(C_5Me_5)_2Th(\eta^2\text{-}As_2Mes_2)$ and $(C_5Me_5)_2U(\eta^2\text{-}As_2Mes_2)$ were prepared according to literature procedures.[10] Solvents were dried via activated alumina, and dispensed through a solvent-purification system, MBRAUN, USA. C_6D_6 (Cambridge Isotope Laboratories) was subjected to three freeze-pump-thaw cycles and dried over activated 4 Å molecular sieves for 72 h prior to use. All ^{1}H and $^{13}C\{^1H\}$ NMR experiments were performed on a 500 or 600 MHz Bruker NMR spectrometer. Spectra were referenced to residual C_6D_5H at 7.16 ppm (^{1}H) and 128.06 ppm ($^{13}C\{^1H\}$), respectively. IR spectra were collected from samples prepared as KBr plates with a Nicolet Summit PRO FTIR Spectrometer. Elemental analyses were performed by the Microanalytical Facility, University of California, Berkeley, USA.

Synthesis of $(C_5Me_5)_2Th(\eta^2\text{-}As_2Mes_2)(CN^tBu)$, 2. A toluene solution of ^{t}BuNC (1 molar equivalent, 0.5 M) was added to a stirring, dark green, Et_2O slurry of **1**. The color progressed quickly from dark green, to dark red, to light red orange, with concomitant precipitation of a bright orange powder. The mixture was stirred for 30 min at room temperature, then filtered over a M-porosity fritted glass funnel to collect the precipitate. The precipitate was rinsed with ~2 mL Et_2O, then stripped of volatiles under vacuum, 103 mg, 78%. ^{1}H NMR (C_6D_6, 600 MHz, 25 ^{o}C): δ 6.99-6.91 (m, 4H, *m*-H), 2.97 (s, 12H *o*-CH_3), 2.29 (s, 6 H, *p*-CH_3), 2.04 (s, 30H, $C_5\mathbf{Me}_5$), 0.787 (s, 9H, ^{t}Bu). $^{13}C\{^1H\}$ NMR

(C_6D_6, 600 MHz, 25 °C): δ 145.84 (s, *o*-C_{aryl}), 143.80 (s, *p*-C_{aryl}), 132.6-132.4 (m, **C**N^{t}Bu), 128.34 (s, *m*-H), 123.21 (s, **C**$_5$Me$_5$), 50.72 (s, CN-**C**$(CH_3)_3$), 29.27 (s, *o*-CH_3), CNC(**C**$H_3)_3$), 20.9 (s, *p*-CH_3), 12.29 (s, C_5**Me**$_5$). IR (cm^{-1}): 2976 (m), 2947 (m), 2907 (s), 2858 (m), 2722 (w), 2152 (s), 1597 (w), 1452 (s), 1425 (m), 1371 (m), 1261 (w), 1234 (w), 1187 (m), 1086 (m), 1022 (m), 1009 (m), 948 (w), 845 (m), 801 (w), 706 (w), 543 (w), 463 (w). The $^{13}C\{^1H\}$ resonance corresponding to the *ipso*-C in the mesityl rings overlapped with the C_6D_6 peaks. Elemental analysis calculated for ($C_{43}H_{61}NAs_2Th$) (973.83 g/mol): C, 53.03%; H, 6.31%; N, 1.44%. Found: C, 53.15%; H, 6.44%; N, 1.53%.

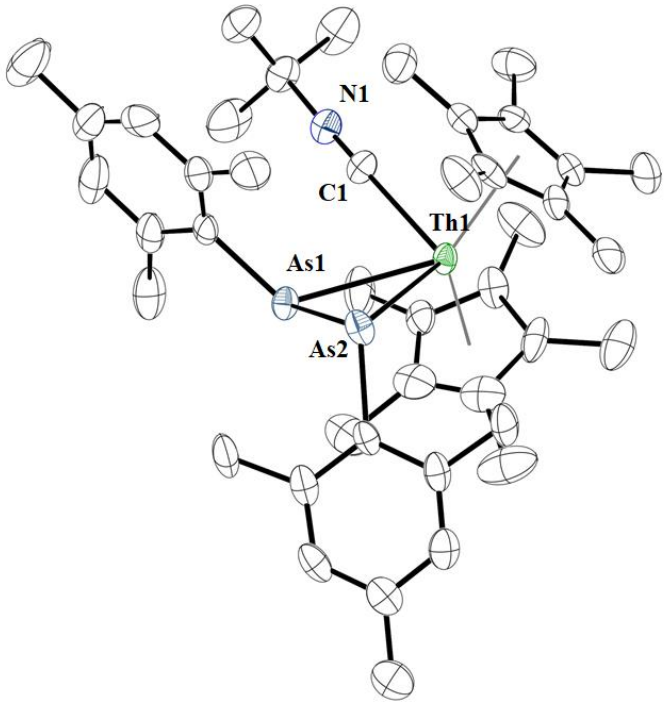

Figure 4-1. Thermal ellipsoid plot of **3** shown at the 50% probability level. The hydrogen atoms have been omitted for clarity. Pertinent bond distances are angles are as follows: U1-C21, 2.46(2) Å; U1-As1, 2.960(2) Å; U1-As1, 2.912(2) Å; As1-U1-As2: 48.02(6)°.

Synthesis of $(C_5Me_5)_2U(\eta^2\text{-}As_2Mes_2)(CN^tBu)$, 3. To a stirring, 5 mL toluene solution of $(C_5Me_5)_2U(\eta^2\text{-}As_2Mes_2)$ (75 mg, 0.084 mmol), ^{t}BuNC (0.167 mL, 1 equivalent of a 0.5 M solution in toluene) was added dropwise with stirring, at room temperature. The color of the mixture immediately changed from dark brown to dark orange, and stirring was continued for 1 h. The volatiles were then removed from the solution under vacuum, and the resulting dark orange/black residue was triturated in pentane and filtered over a fritted glass funnel to isolate a black solid, which was washed with an additional 2 mL volume of pentane and isolated and evacuated to remove residual solvent, leaving a black, microcrystalline solid, 81 mg, 99%. ^{1}H NMR (C_6D_6, 600 MHz, 25 ^{o}C): δ 6.39 (s, 30H, $C_5\textit{Me}_5$), 4.44 (s, 3H, *p*-CH_3), 3.75 (s, 3H, *p*-CH_3). ^{1}H NMR resonances for the *meta*-H and *o*-CH_3 signals were unobservable. IR (cm^{-1}): 2977 (s), 2948 (s), 2906 (s), 2860 (s), 2721 (w), 2131 (s), 1713 (w), 1597 (w), 1452 (s), 1370 (s), 1184 (s), 1085 (s), 1024 (s), 948 (w), 846 (s), 799 (w). Elemental analysis calculated for $C_{43}H_{61}NAs_2U$ (979.82 g/mol): C, 52.71%; H, 6.27%; N, 1.43%. Found: C, 52.35%; H, 6.49%; N, 1.05%.

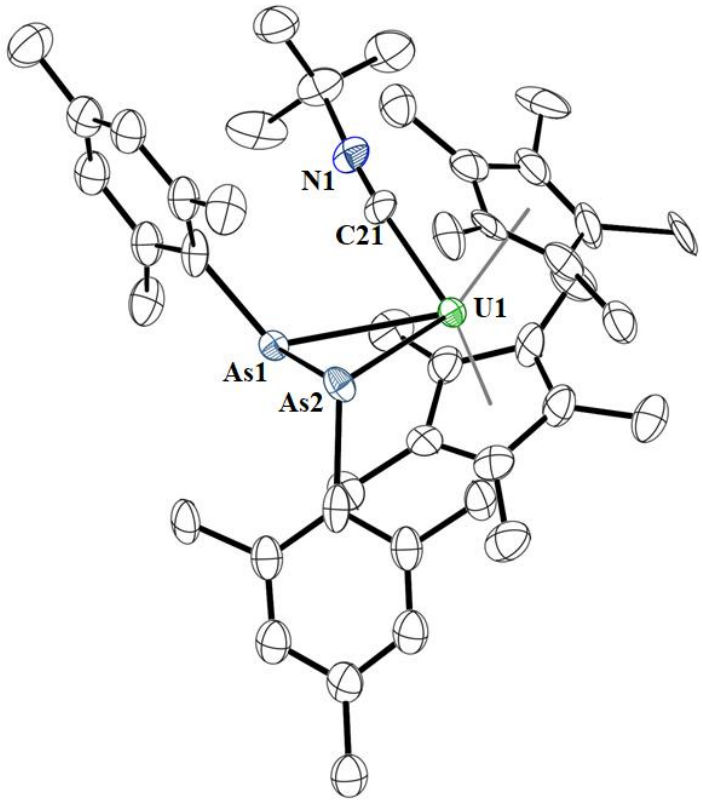

Figure 4-2. Thermal ellipsoid plot of **3** shown at the 50% probability level. The hydrogen atoms have been omitted for clarity. Pertinent bond distances are angles are as follows: U1-C21, 2.46(2) Å; U1-As1, 2.960(2) Å; U1-As1, 2.912(2) Å; As1-U1-As2: 48.02(6)°.

Synthesis of $(C_5Me_5)_2U(\eta^2\text{-}As_2Mes_2)(CO)$, 4. A J-young tube was charged with a ~1.5 mL C6D6 solution of 25 mg $(C_5Me_5)_2U(\eta^2\text{-}As_2Mes_2)$, the solution frozen with liquid N_2, and the N_2 atmosphere in the headspace replaced with 1 atm CO. The color of the solution immediately changed from dark brown to dark red, and was complete (by ^1H NMR spectroscopy) by 10 min at room temperature. The CO ligand is labile enough to disassociate quickly upon removal of the CO atmosphere, so solid-state characterization methods could not be performed. An IR spectrum was collected by quickly transferring a toluene solution to a liquid-IR cell, where the compound was stable enough for the

spectrum to be collected. ^{1}H NMR (C_6D_6, 600 MHz, 25 ^{o}C): δ 5.73 (s, 30H, $C_5\mathit{Me}_5$), 3.49 (s, 6H, *p*-CH_3). ^{1}H NMR resonances for the *meta*-H and *o*-CH_3 signals were unobservable. IR (cm^{-1}, solution-state): 2965 (w), 2987 (w), 1939 (s), 1434 (w), 1374 (w), 1020 (w), 847 (w), 727 (s), 470 (m).

Synthesis of $(C_5Me_5)_2U(\eta^2\text{-}As_2Mes_2)(^{13}CO)$, 5. A preparative procedure identical to that of **4** was performed, using ^{13}CO instead. IR spectra was identical with the exception of the IR absorption corresponding to the CO stretching mode, at 1898 cm^{-1}.

REFERENCES.

1. Tarlton, M. L.; Del Rosal, I.; Vilanova, S. P.; Kelley, S. P.; Maron, L.; Walensky, J. R., Comparative Insertion Reactivity of CO, CO2, tBuCN, and tBuNC into Thorium– and Uranium–Phosphorus Bonds. *Organometallics* **2020**, *39*, 2152-2161.

2. Vilanova, S. P.; Tarlton, M. L.; Barnes, C. L.; Walensky, J. R., Double insertion of benzophenone into thorium-phosphorus bonds. *J. Organomet. Chem.* **2018**, *857*, 159-163.

3. Behrle, A. C.; Walensky, J. R., Insertion of tBuNC into thorium–phosphorus and thorium–arsenic bonds: phosphaazaallene and arsaazaallene moieties in f element chemistry. *Dalton Trans.* **2016**, *45*, 10042-10049.

4. Slater, J. L.; Sheline, R. K.; Lin, K. C.; Jr., W. W., Synthesis of Uranium Carbonyls Using Matrix Isolation. *J. Chem. Phys.* **1971**, *55*, 5129-5130.

5. Zhou, M.; Jin, X.; Li, J., Reactions of Cerium Atoms and Dicerium Molecules with CO: Formation of Cerium Carbonyls and Photoconversion to CO-Activated Insertion Molecules. *J. Phys. Chem. A* **2006**, *110*, 10206-10211.

6. Brennan, J. G.; Andersen, R. A.; Robbins, J. L., Preparation of the first molecular carbon monoxide complex of uranium, $(Me_3SiC_5H_4)_3UCO$. *J. Am. Chem. Soc.* **1986**, *108*, 335-336.

7. Parry, J.; Carmona, E.; Coles, S.; Hursthouse, M., Synthesis and Single Crystal X-ray Diffraction Study on the First Isolable Carbonyl Complex of an Actinide, $(C_5Me_4H)_3U(CO)$. *J. Am. Chem. Soc.* **1995**, *117*, 2649-2650.

8. Evans, W. J.; Kozimor, S. A.; Nyce, G. W.; Ziller, J. W., Comparative Reactivity of Sterically Crowded nf3 (C5Me5)3Nd and (C5Me5)3U Complexes with CO: Formation

of a Nonclassical Carbonium Ion versus an f Element Metal Carbonyl Complex. *J. Am. Chem. Soc.* **2003**, *125*, 13831-13835.

9. Langeslay, R. R.; Chen, G. P.; Windorff, C. J.; Chan, A. K.; Ziller, J. W.; Furche, F.; Evans, W. J., Synthesis, Structure, and Reactivity of the Sterically Crowded Th3+ Complex (C5Me5)3Th Including Formation of the Thorium Carbonyl, $[(C_5Me_5)_3Th(CO)][BPh_4]$. *J. Am. Chem. Soc.* **2017**, *139*, 3387-3398.

10. Michael L. Tarlton, O. J. F., Steven P. Kelley, Andrew Kerridge, Thomas Malcomson, Thomas L. Morrison, Matthew P. Shores, Xhensila Xhani, Justin R. Walensky, *Inorg. Chem.*, Submitted.

Vita

Michael Lloyd Tarlton was born and raised on Bainbridge Island, WA. Prior to earning his PhD in Chemistry from the University of Missouri, Columbia, Michael attended Seattle University for his Bachelor of Science degree in Chemistry where he worked as an undergraduate researcher in Dr. Eric Watson's laboratory. He continued his education in the Master of Science degree program in chemistry at Illinois State University under Dr. Craig C. McLauchlan.

Michael began his graduate research career at the University of Missouri, Columbia in the spring of 2015, in the laboratory of Dr. Justin R. Walensky. Michael successfully defended his dissertation in the spring of 2021.